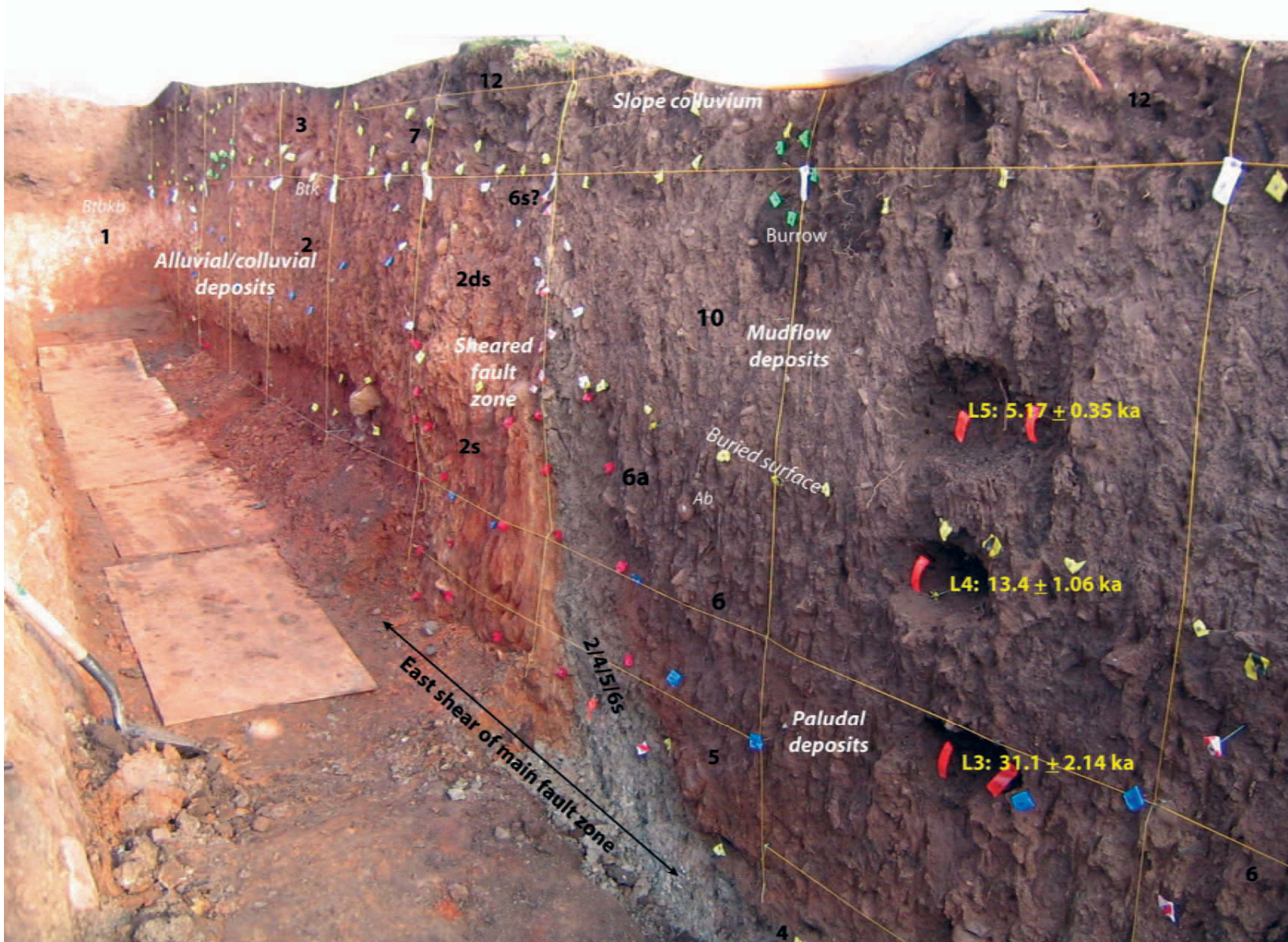


*Paleoseismology of Utah, Volume 19*

# Late Quaternary Faulting in East Canyon Valley, Northern Utah

*by Lucille A. Piety, Larry W. Anderson, and Dean A. Ostenaar*



MISCELLANEOUS PUBLICATION 10-5  
UTAH GEOLOGICAL SURVEY  
*a division of*  
DEPARTMENT OF NATURAL RESOURCES  
2010

*Paleoseismology of Utah, Volume 19*

# Late Quaternary Faulting in East Canyon Valley, Northern Utah

by *Lucille A. Piety<sup>1</sup>, Larry W. Anderson<sup>1</sup>, and Dean A. Ostenaar<sup>2</sup>*

<sup>1</sup>U.S. Bureau of Reclamation, Denver, Colorado

<sup>2</sup>Fugro William Lettis and Associates, Inc., Lakewood, Colorado

*Cover photo: South wall of trench near the northern end of Main Canyon fault on the east side of East Canyon valley in northern Utah.*

ISBN 978-1-55791-841-3



MISCELLANEOUS PUBLICATION 10-5  
UTAH GEOLOGICAL SURVEY  
*A division of*  
UTAH DEPARTMENT OF NATURAL RESOURCES  
2010

**STATE OF UTAH**

Gary R. Herbert, Governor

**DEPARTMENT OF NATURAL RESOURCES**

Michael Styler, Executive Director

**UTAH GEOLOGICAL SURVEY**

Richard G. Allis, Director

**PUBLICATIONS**

contact

Natural Resources Map & Bookstore

1594 W. North Temple

Salt Lake City, UT 84116

telephone: 801-537-3320

toll-free: 1-888-UTAH MAP

Web site: [mapstore.utah.gov](http://mapstore.utah.gov)

email: [geostore@utah.gov](mailto:geostore@utah.gov)

**UTAH GEOLOGICAL SURVEY**

contact

1594 W. North Temple, Suite 3110

Salt Lake City, UT 84116

telephone: 801-537-3300

Web site: [geology.utah.gov](http://geology.utah.gov)

*The Miscellaneous Publication series provides non-UGS authors with a high-quality format for documents concerning Utah geology. Although review comments have been incorporated, this document does not necessarily conform to UGS technical, editorial, or policy standards. The Utah Department of Natural Resources, Utah Geological Survey, makes no warranty, expressed or implied, regarding the suitability of this product for a particular use. The Utah Department of Natural Resources, Utah Geological Survey, shall not be liable under any circumstances for any direct, indirect, special, incidental, or consequential damages with respect to claims by users of this product.*

*This report was originally released as U.S. Bureau of Reclamation Seismotectonic Report 2008-1.*

## CONTENTS

Abstract.....	1
Introduction .....	1
Geology and Tectonic Geomorphology of East Canyon Valley .....	4
East Canyon Fault.....	8
Main Canyon Fault .....	14
Late Quaternary Surface Ruptures .....	20
Trench Across the Main Canyon Fault.....	23
Methods .....	25
Characteristics, Ages, and Tectonic Interpretation of the Stratigraphic Units Exposed in the Trench .....	25
Sequence of Faulting, Deposition, and Erosion .....	33
Conclusions .....	36
Acknowledgments .....	38
References .....	39
Appendices .....	on CD
A. Topographic Profiles Across the Main Canyon Fault in the Vicinity of the Trench .....	on CD
B. Photograph Mosaics and Interpretative Logs of the Trench Across the Main Canyon Fault.....	on CD
C. Complete Descriptions of Stratigraphic Units and Soils Exposed in the Trench Across the Main Canyon Fault .....	on CD
D. Descriptions of Samples Collected From the Trench Across the Main Canyon Fault.....	on CD
E. Informal Memo From USGS Luminescence Dating Laboratory by Shannon Mahan, U.S. Geological Survey, Denver, Colorado .....	on CD
F. Examination of Bulk Soil and AMS Radiocarbon Analysis of Material From the Trench Across the Main Canyon Fault by Kathryn Puseman, Paleo Research Institute, Golden, Colorado .....	on CD
G. Analyses on Asphaltum Samples From the Trench Across the Main Canyon Fault (Geochemical Analysis of an Asphaltum Sample by B.M. Jarvie and D.M. Jarvie, Humble Instruments and Services, Inc., Humble, Texas; FTIR Spectrum Analysis for Asphaltum in Sample ECT-C6 by Paleo Research Institute, Golden, Colorado).....	on CD
H. Review of Trench Across the Main Canyon Fault, Utah, of October 2006 by James P. McCalpin, GEO-HAZ Consulting, Inc., Crestone, Colorado ...	on CD

## FIGURES

Figure 1.	East Canyon valley and Quaternary faults in northeastern Utah.....	3
Figure 2.	Generalized geology of East Canyon valley.....	5
Figure 3.	Explanation of geologic units mapped in East Canyon valley .....	6
Figure 4.	Geomorphic sections and tectonic geomorphic features along the East Canyon and Main Canyon faults in East Canyon valley .....	7
Figure 5.	East-facing escarpment along section ECF1 of the East Canyon fault .....	9
Figure 6.	Enlargement of geology and geomorphic features along the East Canyon fault near East Canyon Dam.....	11
Figure 7.	Sections ECF4 and ECF5 along the East Canyon fault immediately south of East Canyon Dam .....	12
Figure 8.	Sections ECF5 and ECF6 of the East Canyon fault south of East Canyon Dam. ....	13
Figure 9.	Distribution of possible tectonic geomorphic features along the Main Canyon fault. ....	15
Figure 10.	Possible tectonic geomorphic features in the vicinity of the trench excavated near the north end of the Main Canyon fault.....	16
Figure 11.	Topographic profiles in the vicinity of the trench excavated near the north end of the Main Canyon fault.....	17
Figure 12.	Oblique aerial photograph of sections MCF1 and MCF2 of the Main Canyon fault and sections ECFO, ECF1, and ECF2 of the East Canyon fault.....	18
Figure 13.	Facets and bedrock scarp along section MCF2 of the Main Canyon fault.....	19
Figure 14.	Lineaments, facets, bedrock scarps, and disrupted drainage along section MCF2 of the Main Canyon fault .....	19
Figure 15.	Oblique aerial photograph looking south along sections MCF1 and MCF2 of the Main Canyon fault .....	21
Figure 16.	Geomorphic features in the vicinity of the trench excavated near the north end of the Main Canyon fault.....	22
Figure 17.	Sketch map showing the orientation of the trench relative to the west-facing fault scarp and the main shears exposed in the walls of the trench.....	24
Figure 18.	Interpreted log of the trench excavated near the north end of the Main Canyon fault.....	27
Figure 19.	Schematic drawing (looking south) of possible sequence of events interpreted from the trench exposure.....	34
Figure 20.	Stratigraphic units, ages, and tectonic events interpreted from the trench excavated near the north end of the Main Canyon fault.....	37

## TABLES

Table 1.	Quartz blue-light OSL ages from trench across Main Canyon fault.....	29
----------	--	----

## FOREWORD

This Utah Geological Survey Miscellaneous Publication, *Late Quaternary Faulting in East Canyon Valley, Northern Utah*, is the nineteenth report in the Paleoseismology of Utah series. This series makes the results of paleoseismic investigations in Utah available to geoscientists, engineers, planners, public officials, and the general public. These studies provide critical information regarding paleoearthquake parameters such as earthquake timing, recurrence, displacement, slip rate, fault geometry, and segmentation, which can be used to characterize potential seismic sources and evaluate the long-term seismic hazard of Utah's Quaternary faults.

This report, originally released as U.S. Bureau of Reclamation Seismotectonic Report 2008-1, presents new paleoseismic information for two "back-valley" faults on the eastern flank of the Wasatch Range. The Main Canyon (formerly "East of East Canyon" or "East Canyon – East Side") fault and the East Canyon fault are on the east and west sides, respectively, of the East Canyon valley area in Morgan and Summit Counties, Utah. The purpose of the study was to evaluate the Quaternary activity of the two faults as part of a seismic safety assessment of East Canyon Dam. To address this issue, the Bureau of Reclamation made a geomorphic evaluation of both faults, and excavated a trench across the northern part of the Main Canyon fault. The geomorphic evaluation revealed little or no evidence of Quaternary surface faulting on the East Canyon fault, but strong evidence of late Quaternary activity (scarps formed on geologically young deposits, faceted mountain spurs, disrupted drainages) on the Main Canyon fault. Using stratigraphic and structural relations, and radiocarbon and luminescence ages, it was determined that the trench exposed evidence for two surface-faulting earthquakes during the past 30,000 to 38,000 years, with the most recent event possibly as young as shortly before 5000 to 6000 years ago. There was also limited evidence for an unknown number of surface-faulting earthquakes older than 38,000 years. Differences in stratigraphic units on opposite sides of the fault in the trench prevented the determination of either the amount of offset or slip rate of the fault.

Determining well-constrained paleoseismic parameters for Utah's Quaternary faults is important because the new data will help refine fault activity and hazard models and improve earthquake-hazard evaluations for the region, all of which help reduce Utah's earthquake-related risk.

*William R. Lund, Editor*  
*Paleoseismology of Utah Series*

# **Late Quaternary Faulting in East Canyon Valley, Northern Utah**

*by Lucille A. Piety, Larry W. Anderson, and Dean A. Ostenaar*

## **ABSTRACT**

East Canyon valley, a 25-km-long by 5-km-wide “back-valley,” is on the eastern flank of the Wasatch Range about 25 km northeast of Salt Lake City and the Wasatch Front. Previous geologic mapping and the geomorphic expression of this north-northeast-trending valley suggest that East Canyon valley is a middle to late Cenozoic half-graben bounded on the west by the East Canyon fault. The Main Canyon fault, previously referred to as the “East of East Canyon” or “East Canyon – East Side” fault, is a down-to-the-west normal fault that partly coincides with the drainage divides that bound the east side of East Canyon valley. The Main Canyon fault cuts across existing topography, but has nearly continuous expression in the landscape for about 26 km. Previous interpretations have suggested that the Main Canyon fault is a minor structural feature, antithetic to the East Canyon fault.

A trench excavated across a 0.4-m-high, west-facing scarp on unconsolidated sediments near the northern end of the Main Canyon fault exposed a 5-m-wide fault zone that juxtaposes alluvium/colluvium on the footwall against paludal (marsh) deposits on the hanging wall. Recurrent surface ruptures formed upslope-facing scarps that interrupted the east-flowing drainages, which were ponded temporarily along the fault. The trench exposed a record of two faulting events during the past 30,000 to 38,000 years, but the difference in the stratigraphic units on opposite sides of the fault did not allow for an estimate of the amount of displacement. Age estimates based on luminescence and radiocarbon analyses, supported by an assessment of soil development, indicate that the most recent surface-rupturing earthquake likely occurred shortly before 5000 to 6000 years ago, but could be as old as 10,000 to 12,000 years ago.

Recurrent late Pleistocene and Holocene displacement on the Main Canyon fault is consistent with faulting histories determined for other northerly trending, mostly down-to-the-west normal faults east of the Wasatch Range in north-central Utah. Although the overall geomorphology and the trenching results indicate recurrent late Quaternary surface rupturing earthquakes associated with the Main Canyon fault, the East Canyon fault lacks evidence for late Quaternary or Quaternary surface faulting, which suggests that such activity has not occurred or has occurred at a very low rate. Finally, geology and geomorphology suggest that the Main Canyon fault has not had recurrent displacement throughout the late Cenozoic, but instead became active only during the past few million years.

## INTRODUCTION

The East Canyon area (hereafter referred to as East Canyon valley) is on the eastern flank of the Wasatch Range about 25 km east of the range-bounding Wasatch fault (Figure 1). Paleoseismic studies in the northern and central mountains east of the main Wasatch Range indicate that late Quaternary faulting is associated with several northerly trending valleys (e.g., Morgan Valley, Strawberry Valley) east of the range-bounding Wasatch fault (Nelson and VanArsdale, 1986; Sullivan and others, 1988; Figure 1). Although Sullivan and others (1988) discussed the East Canyon area in their assessment of faulting in the central Utah region, they conducted only a brief reconnaissance of the faults in the valley, and this reconnaissance focused on the East Canyon fault. While they failed to identify any late Quaternary fault scarps associated with the East Canyon fault, they concluded that the southern portion of the fault shared some of the characteristics of recognized late Quaternary faults in north-central Utah and hence was a potential seismic source. This assessment of the faults in East Canyon valley was undertaken as part of a reevaluation of fault seismic sources for the probabilistic seismic hazard analyses (PSHA) conducted by the Bureau of Reclamation (BOR) for East Canyon Dam.

A consultant review board that convened in 2006 to review BOR work assessing the safety of East Canyon Dam recommended that “Additional geology and paleoseismic investigations of the East Canyon and East Canyon East Side faults should be undertaken to try to better constrain the slip rates on these faults, the ages of their most recent surface faulting earthquakes, and the surrounding geologic structure.” In previous studies, the East Canyon fault was considered the primary seismic source, despite little detailed work. In response to the Consultant Review Board recommendation in 2006, Dean Ostenaar (formerly in the BOR Seismotectonics and Geophysics Group) began an assessment of the East Canyon area by examining previous reports, published and unpublished literature and geologic maps, and aerial photographs. In August 2006 he conducted a ground reconnaissance of the East Canyon area and noted a possible late Quaternary fault scarp along the northern portion of what we now refer to as the Main Canyon fault. Trench investigations were initiated in the fall of 2006 to try to determine the origin and history of the scarp where it crosses the northern end of East Canyon valley. A trench was excavated, described, sampled, and reviewed in October 2006. The trench exposed evidence for recurrent late Pleistocene and Holocene tectonic surface ruptures on the Main Canyon fault. Interpretations of fault history from the trench exposure are consistent with the geomorphic expression of the fault, which suggests geologically recent displacements on the Main Canyon fault, but no long-term record of movement throughout the late Cenozoic.

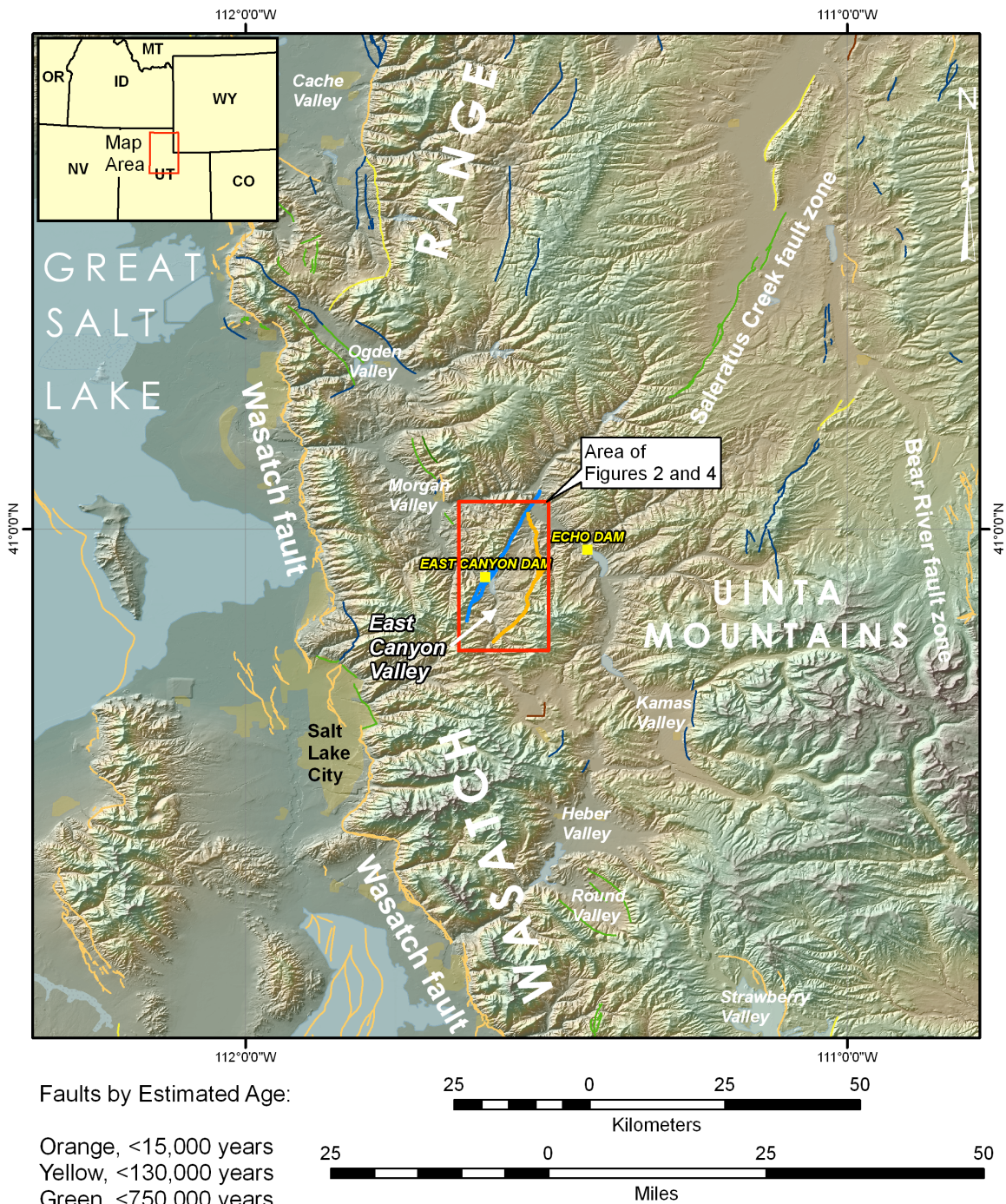


**Figure 1.** East Canyon valley and Quaternary faults in northeastern Utah. Faults and their ages are from the database of Quaternary faults and folds by the U.S. Geological Survey (2010), except for the ages of the Main Canyon and East Canyon faults. The ages for these faults have been modified on the basis of the conclusions of this study.

Additional assessment of the possible tectonic features in East Canyon valley was done in 2007 using existing mapping, black-and-white 1:40,000-scale aerial photographs, additional field reconnaissance, and an aerial overflight. The geologic evidence suggests that displacement on the East Canyon fault, which bounds the west side of East Canyon valley, was primarily responsible for the initial formation of the valley probably late in the middle Cenozoic. However, displacements on the East Canyon fault do not appear to have continued into the late Quaternary.

## **GEOLOGY AND TECTONIC GEOMORPHOLOGY OF EAST CANYON VALLEY**

East Canyon valley formed through a combination of fault displacement, sedimentation, and erosion, similar to other valleys east of the main Wasatch Range (Sullivan and others, 1988). East Canyon valley is defined geologically by the extent of the Norwood Tuff (Tn) and older underlying conglomerate deposited within a Cenozoic basin (Toc or Tc; Bryant, 1990; Figure 2 and Figure 3). Because of the deposition of these units, a valley or basin must have been present in this area during the late Eocene and early Oligocene (about 30 to 40 million years ago). In addition, a linear north-northeast-striking faulted contact between these units and older rocks and increasing backtilting of these units toward the fault with depth indicate that displacement on the East Canyon fault continued during and after deposition of the two units (Figure 2). Surfaces or pediments cut on the erodible Norwood Tuff along the west side of East Canyon valley further suggest that drainages from the west side of the valley dominated, probably because of the topographic escarpment created by displacements on the East Canyon fault and the presence of the resistant Echo Canyon Conglomerate on the footwall. The pediments also suggest that the valley was a closed basin, or nearly so, for a time during the early Pleistocene (about 2 million years ago to several hundred thousand years ago). Subsequently, the present drainages of East Canyon Creek and the Weber River were established (Sullivan and others, 1988). Headward erosion on tributaries to these two main drainages removed sediment from East Canyon valley and left a drainage divide at Hogback Summit (elevation 6250 feet) between East Canyon Creek and the Weber River (Figure 2 and Figure 4). East Canyon Creek enters East Canyon valley from the south, flows across the East Canyon fault at East Canyon Dam, and continues northwest to join the Weber River in Morgan Valley. Thus, the outlet for flow and the lowest point along the drainage in East Canyon valley south of Hogback Summit crosses the East Canyon fault.

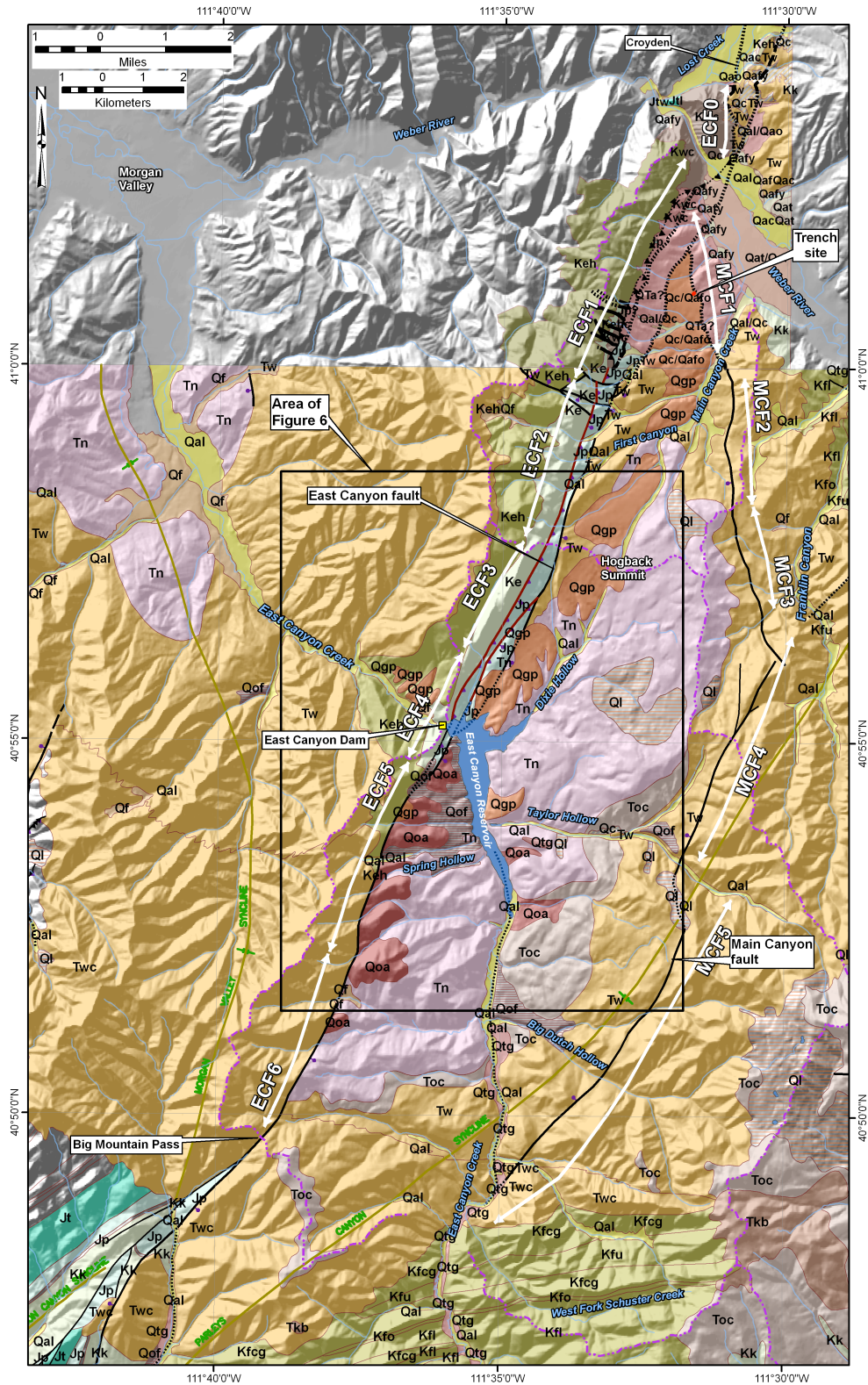


**Figure 2.** Generalized geology of East Canyon valley. Geology south of latitude 41 degrees is from Bryant (1990). Geology north of latitude 41 degrees is from Coogan (2002). See Figure 3 for an explanation of geologic units and symbols.

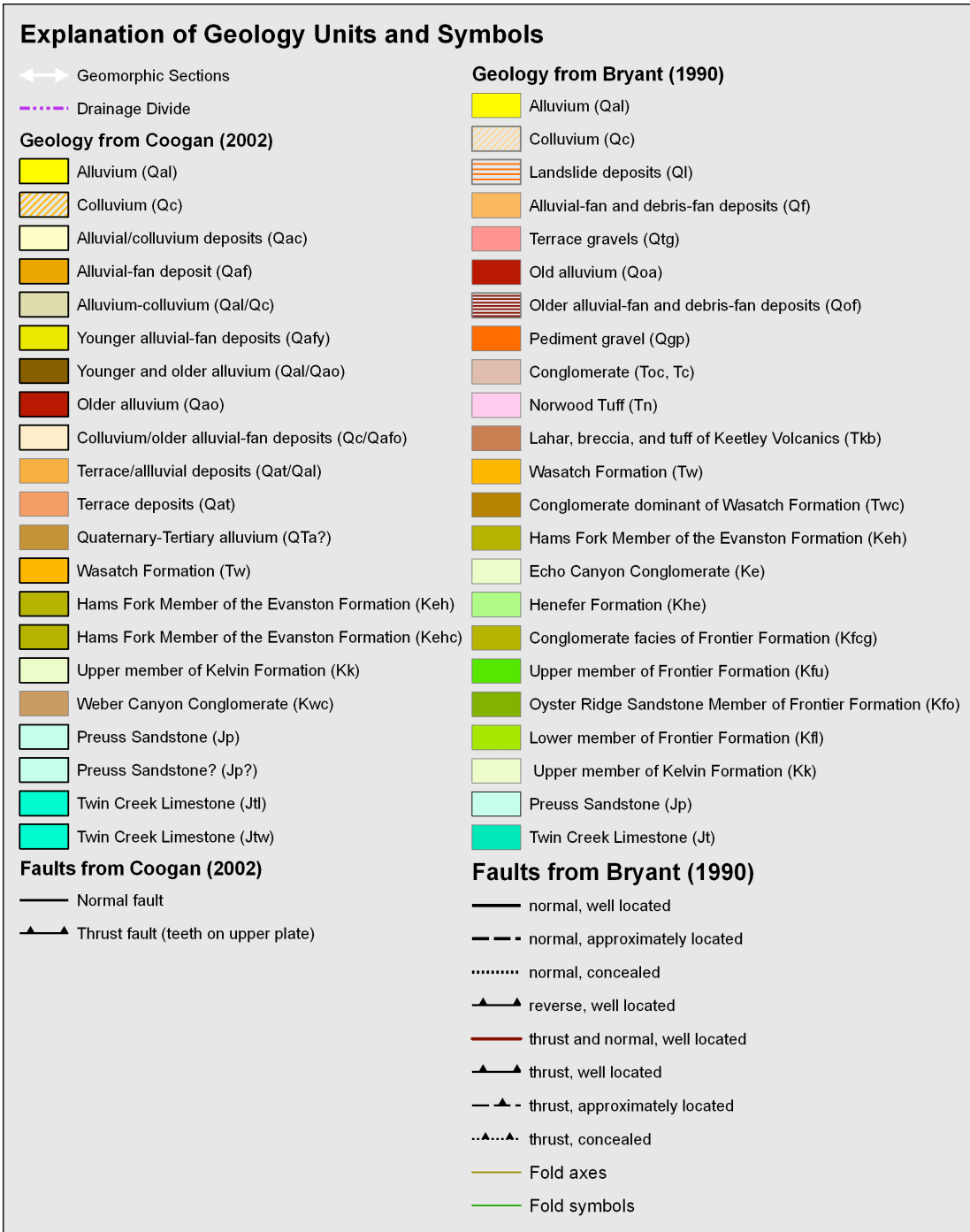
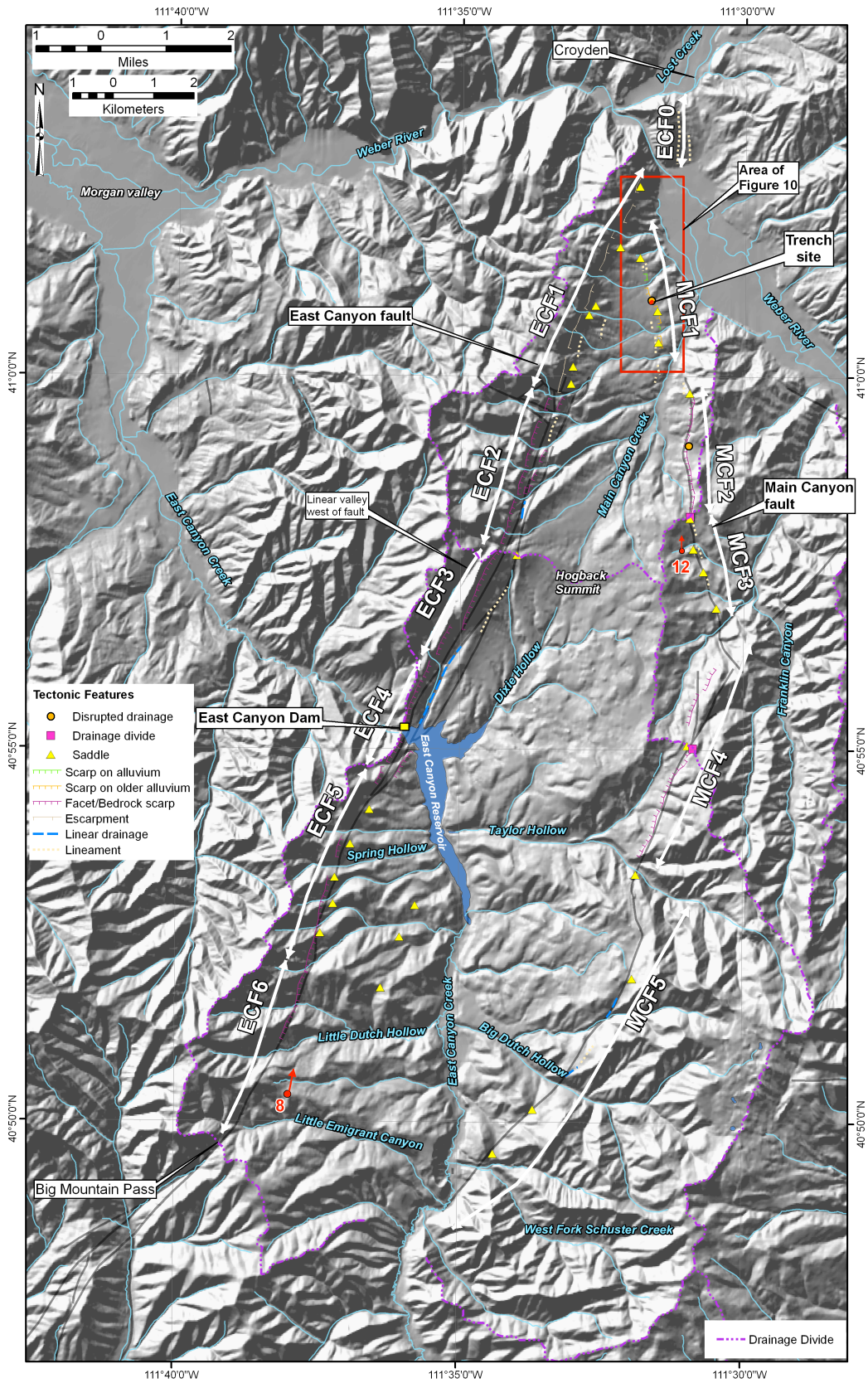


Figure 3. Explanation of geologic units mapped in East Canyon valley (see Figure 2).



**Figure 4.** Geomorphic sections and tectonic geomorphic features along the East Canyon and Main Canyon faults in East Canyon valley. Gray lines show mapped fault traces (Figure 2). Red numbers and arrows indicate the locations of Figure 8 and Figure 12.

Presently, the best topographic expression of East Canyon valley is north of about Spring Hollow (Figure 2). South of this point, older deposits mapped as Norwood Tuff (Tn) by Bryant (1990) are preserved in the west half of the valley, and Wasatch Formation (Tw) and an older conglomerate (Toc) are preserved in the east half (Figure 2). North of Spring Hollow, early Quaternary (younger than about 2 million years) alluvial fans are preserved near East Canyon Reservoir and along Taylor Hollow. North of Taylor Hollow, Pleistocene pediment gravels (Qgp) are present along both Dixie Hollow, which flows southward into East Canyon Reservoir, and Main Canyon Creek, which flows northward into the Weber River. North of First Canyon, younger Pleistocene and Holocene alluvial fans are present in the northern (about 3 km) of the valley.

## **East Canyon Fault**

The Cenozoic East Canyon fault has a length of at least 26 km, extending from near the town of Croyden north of the Weber River to near Big Mountain Pass on the south-southwest (Figure 2). Southwest of Big Mountain Pass, the fault loses its geomorphic expression as it crosses the crest of the Wasatch Range, where the fault then splays into a series of fault strands that apparently die out within the Emigration Canyon syncline (Bryant, 1990). Previous seismotectonic studies subdivided the East Canyon fault into two sections or segments that overlap immediately east of East Canyon Dam. The northern section begins near the Weber River and terminates east of East Canyon Dam. The southern section begins near the dam and ends near Big Mountain Pass.

The primary sources of bedrock mapping for the East Canyon fault are Bryant (1990), Coogan and King (2001), and Coogan (2002). Basically, the East Canyon fault was originally interpreted to be an east-dipping, west-verging thrust fault that was later re-activated as a down-to-the-east normal fault. Typically, this multi-stranded fault juxtaposes resistant west-dipping Cretaceous and early Tertiary rocks against either erodible, steeply east-dipping Jurassic rocks (Preuss Formation; Jp) or early Tertiary sedimentary rocks (Wasatch Formation; Tw) and/or the Norwood Tuff (Tn). In some areas, however, particularly where there are multiple strands of the fault, the Preuss Formation is also faulted (up-on-the-west) against the west-dipping Wasatch Formation or Norwood Tuff. The East Canyon fault is structurally complex due to earlier thrusting and later normal faulting.

The geomorphic expression of the East Canyon fault varies significantly, and for ease of discussion the fault has been subdivided into seven sections (ECF0 through ECF6), which are based on the differences in the geology and geomorphic expression of the fault (Figure 2 and Figure 4). Landscape features that might have a tectonic origin were mapped using aerial photographs and are portrayed on Figure 4.

The northernmost section (**ECF0**), which is about 1.8 km long, is north of the Weber River and juxtaposes Weber Canyon Conglomerate (Kwc) on the west against younger Wasatch Formation (Tw; Figure 2). The Weber Canyon Conglomerate forms a large unnamed hill north of the Weber River. North-trending lineaments along the east side of the hill might be related to the fault, and are the northernmost surficial expression of the East Canyon fault (Figure 4).

In the next section (**ECF1**), about 6 km long, the fault is composed of up to three traces, one of which is the mapped trace of the East Canyon thrust (Figure 2). The western trace of the East Canyon fault south of the Weber River forms an escarpment about 350 m high in resistant Evanston Formation (Keh) and Weber Canyon Conglomerate (Kwc) along the west margin of East Canyon valley. The drainage divide for Main Canyon Creek on the west side of the valley is nearly parallel to and is less than 1 km west of this trace of the fault. East-flowing drainages from the divide have eroded the escarpment, which is embayed (Figure 5). Alluvial fans have been deposited along the base of the escarpment. The eastern trace (or the middle trace of Coogan [2002]) is expressed as lineaments and saddles that are 0.3 to 0.4 km east of the western trace. All three traces are shown as concealed by Coogan (2002). The western and middle traces are concealed by Quaternary-Tertiary alluvium (QTa?). The eastern trace is shown as a concealed contact between Quaternary-Tertiary alluvium and Quaternary colluvium/older alluvial-fan deposits (Qc/Qafo). A few saddles (notches) are present along the middle trace, where hills mapped as Quaternary-Tertiary alluvium are separated from the bedrock escarpment to the west.



**Figure 5.** East-facing escarpment along section ECF1 of the East Canyon fault. Escarpment is formed by resistant Evanston Formation and Weber Canyon Conglomerate. Approximate fault location is shown by arrows. Note the embayed character of the escarpment and the alluvial-fan deposits at the foot of the escarpment.

In the next section to the south (**ECF2**), which is about 5 km long, two fault traces were mapped by Bryant (1990). The western and central traces of Coogan (2002) in section ECF1 merge into the western trace of Bryant (1990). The western trace is expressed as discontinuous, low, east-facing facets or bedrock scarps in very resistant, late Cretaceous

(about 95 to 65 million years ago) Echo Canyon Conglomerate (Ke; Figure 2). The drainage divide for Main Canyon Creek is between 2 and 3 km west of the fault trace, and the facets/bedrock scarps are preserved only on ridges between the incised east-flowing drainages that head at the divide (Figure 4). The eastern trace, mapped by Bryant (1990) between Preuss Formation (Jp) and Wasatch Formation (Tw), is expressed as discontinuous east-facing facets or bedrock scarps, lineaments, and a linear drainage. The area between the two fault traces is topographically low, and is underlain by erodible Preuss Formation. The topographic low is bounded by higher surfaces cut into the Wasatch Formation on the east and into Echo Canyon Conglomerate on the west.

The next section to the south (**ECF3**), which is about 3 km long, has two or three traces (figure 6). The western trace is expressed as nearly continuous linear facets or bedrock scarps in Late Cretaceous Echo Canyon Conglomerate (Ke). The drainage divide for Main Canyon Creek is about 1 km west of the western trace or is coincident with the top of the facet/bedrock scarp along this trace. The facet is only slightly eroded because little drainage reaches it. West-flowing drainage collects in a linear valley immediately west of the facet and east-flowing drainages begin at the top of the facet/bedrock scarp and have little drainage area at the facet (Figure 4). The eastern trace juxtaposes Preuss Formation (Jp) against Wasatch Formation (Tw) or Norwood Tuff (Tn). Bryant (1990) shows this trace as mostly concealed by Quaternary pediment gravels (Qgp). He portrays an additional central fault trace within Preuss Formation (Jp). This trace bounds the west side of a linear ridge; the eastern trace bounds the east side of this ridge. A south-flowing drainage has developed along the central trace.

The next section to the south (**ECF4**) is about 3 km long and just east of East Canyon Dam (Figure 6). Bryant (1990) continues the three traces of ECF3 to East Canyon Creek, but shows only two fault traces south of the creek. This is the area where the north and south sections or segments of Sullivan and others (1988) overlap. North of the reservoir, the west trace juxtaposes Echo Canyon Conglomerate (Ke) and Preuss Formation (Jp), and is expressed as a facet or bedrock scarp. The drainage divide coincides with the top of the facet, so that there is little drainage to erode the facet. The middle trace north of East Canyon Creek is shown within the Preuss Formation. The east trace north of East Canyon Creek is portrayed as concealed by Quaternary pediment gravel (Qgp) and as curving to the west to join the central trace under East Canyon Reservoir.

South of East Canyon Creek, Bryant (1990) shows the East Canyon fault as two traces. The west trace juxtaposes Echo Canyon Conglomerate (Ke) and Preuss Formation (Jp), and is expressed as a facet or bedrock scarp. A portion of this trace is shown as concealed by older (Pleistocene) debris-fan deposits (Qof). Bryant (1990) portrays the east trace as a fault contact between Preuss Formation (Jp) on the footwall and older (Pleistocene) alluvium and debris-fan deposits (Qoa and Qof) on the hanging wall. He

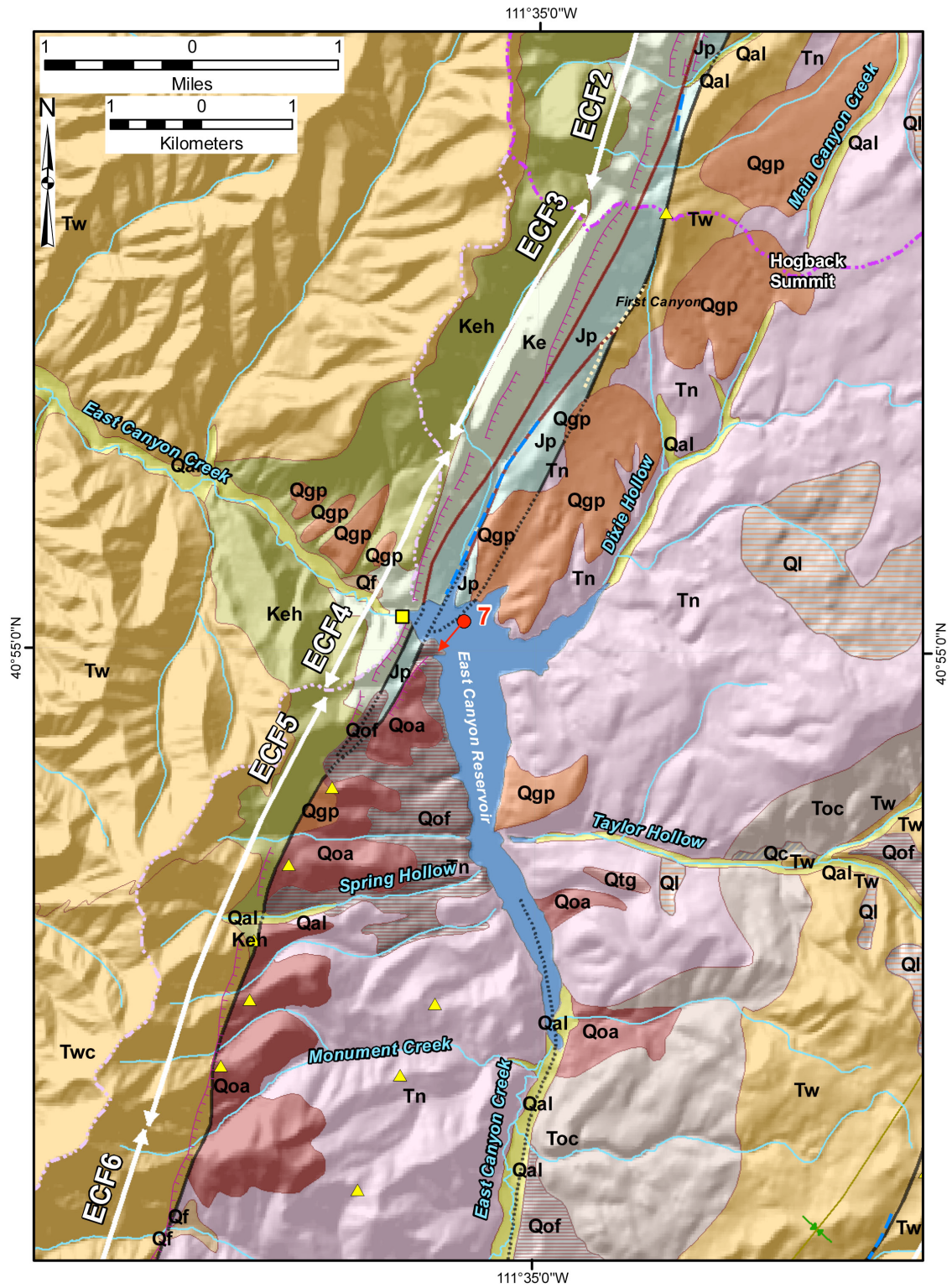


**Figure 6.** Enlargement of geology and geomorphic features along the East Canyon fault near East Canyon Dam (yellow square). Geology is from Bryant (1990). Red arrow shows location of Figure 7. See Figure 3 and Figure 4 for explanation of units and symbols.

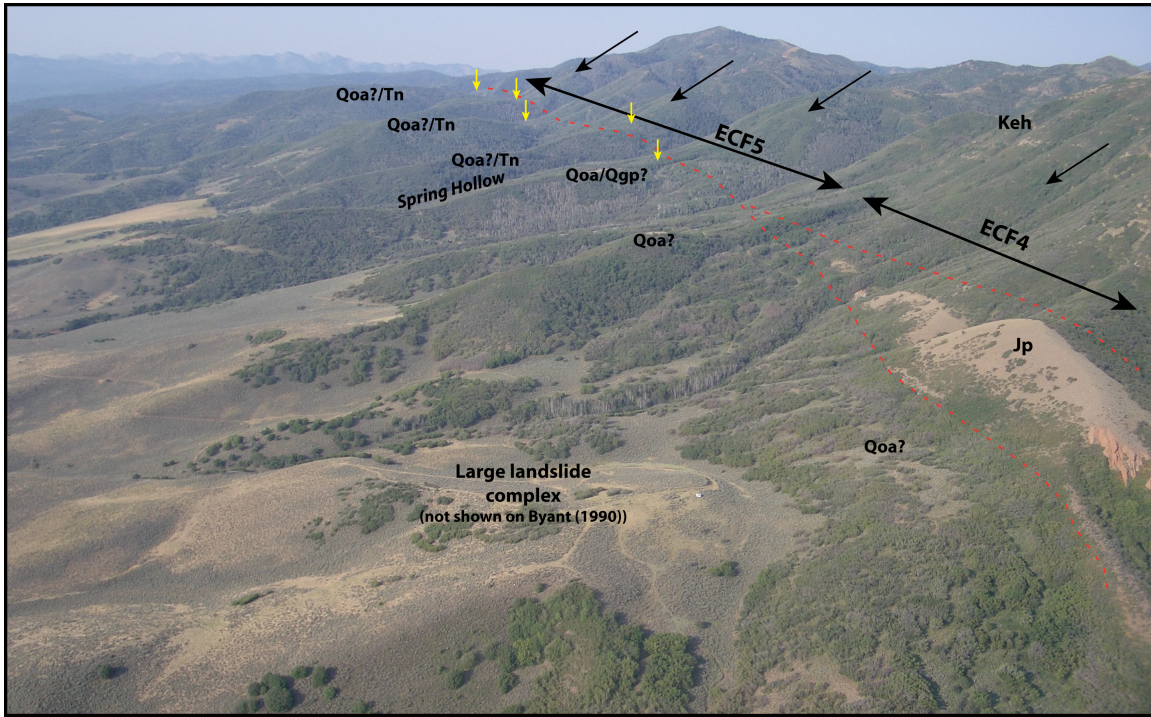


**Figure 7.** Sections ECF4 and ECF5 along the East Canyon fault immediately south of East Canyon Dam (Figure 6). Photograph taken looking southwest. Approximate location of the East Canyon fault is shown by the dotted red lines. Facets in bedrock on the footwall are indicated by black arrows. Saddles or notches at the uphill extent of high surfaces mapped by Bryant (1990) as Pleistocene alluvium or debris-fan deposits are indicated by yellow arrows. Photograph by L.W. Anderson in 2007.

also shows a portion of this trace as concealed by Pleistocene debris-fan deposits. A large unmapped landslide is present just east of the eastern trace (Figure 7).

In the next section to the south (**ECF5**), about 5 km long, Bryant (1990) portrays the East Canyon fault as a single trace (Figure 6) with older (Pleistocene) alluvium (Qoa) and pediment gravel (Qgp) on the hanging wall in fault contact with the Evanston Formation (Keh) or conglomerate within the Wasatch Formation (Twc) on the footwall. Facets or bedrock scarps are present on the footwall (Figure 7). The older alluvium and pediment gravel are preserved on high dissected hills that are disconnected from the bedrock by saddles or notches (Figure 6 and Figure 7)

In sections ECF4 and ECF5, the East Canyon fault is expressed as discontinuous, east-facing facets or bedrock scarps on the footwall and as saddles (Figure 7 and Figure 8). These saddles are topographically low areas between the bedrock and the mapped Quaternary deposits. Although these low areas align with the mapped trace of the East Canyon fault, their origin is unclear. Aerial reconnaissance and limited field studies conducted as part of this investigation did not reveal direct evidence for fault displacement of the Quaternary units as implied by Bryant's mapping. It is possible that the topographic expression is the result of erosion. In addition, the ages of the mapped Quaternary units are unknown.

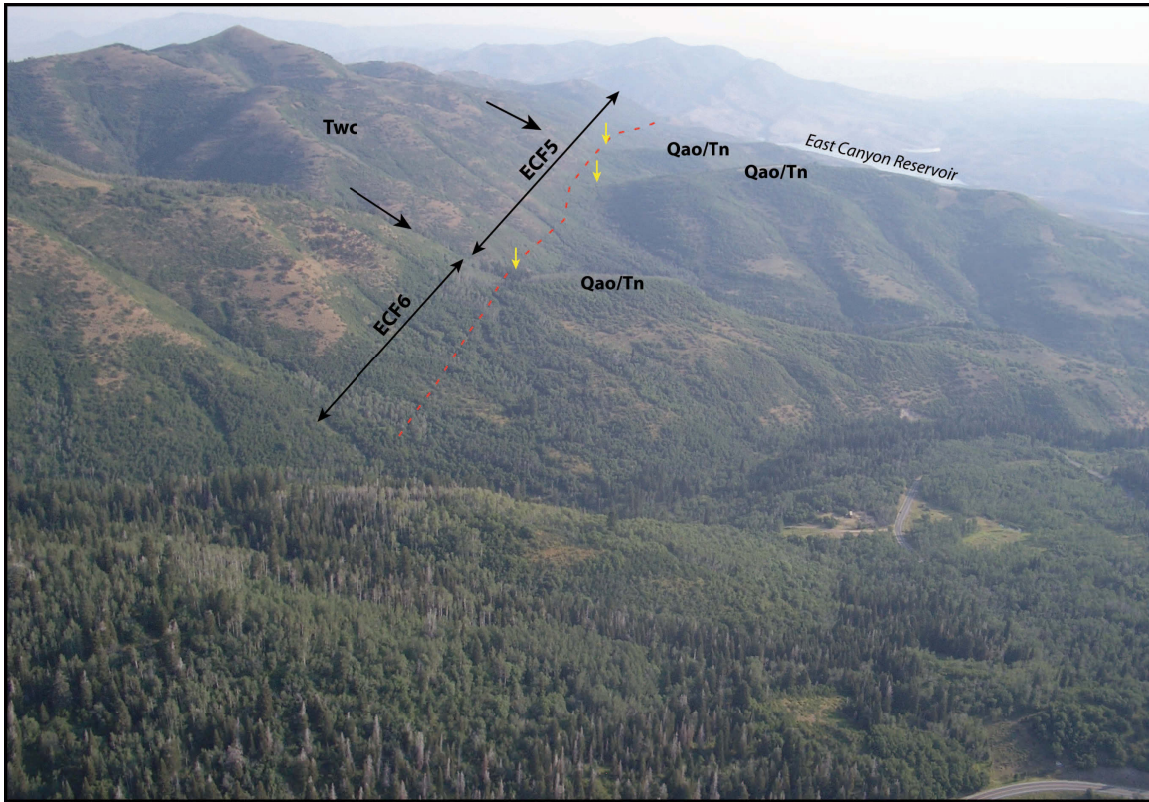


**Figure 8.** Sections ECF5 and ECF6 of the East Canyon fault south of East Canyon Dam (Figure 4). Photograph taken looking north. Approximate location of the East Canyon fault is shown by the red dotted line. Bedrock facets formed in bedrock on the footwall are shown by black arrows. Saddles or notches at the uphill extent of high surfaces mapped by Bryant (1990) as Quaternary alluvium or debris-fan deposits on the hanging wall are indicated by yellow arrows. Photograph by L.W. Anderson in 2007.

The final section at the south end of the fault (**ECF6**), about 4 km long, is shown by Bryant (1990) as a single trace (Figure 2). The fault is expressed as nearly continuous facets or bedrock scarps eroded by east-flowing drainages that head on a divide about 1 km west of the fault trace. High, dissected remnants, shown as Norwood Tuff by Bryant (1990), are preserved on the hanging wall. These remnants decrease in elevation to the south. Geomorphic expression of the East Canyon fault as a normal fault ends near Big Mountain Pass.

The map pattern of the Norwood Tuff and underlying conglomerate suggests that East Canyon valley was present as a topographic depression when these units were deposited during the middle Cenozoic. Rotation of the Norwood Tuff to the west further suggests that displacements continued on the East Canyon fault after deposition of the Norwood Tuff. Quaternary displacement on the East Canyon fault has not been demonstrated. Bryant's mapping implies that Pleistocene alluvium and debris-fan deposits are offset in sections ECF4, ECF5, and ECF6 (the portion of the fault south of East Canyon Dam). However, the nature and ages of any deposits related to these high, dissected surfaces are unknown. The presence of high surfaces of Tertiary Norwood Tuff and possible Quaternary gravels on the hanging wall immediately east of the fault suggests that any Quaternary displacement has been very limited. The notches or saddles along these sections could have an erosional origin. The East Canyon fault in these three sections is still visible in the landscape in large part because of the presence of the resistant Wasatch Formation conglomerate on the footwall. In contrast, the East Canyon fault north of East

Canyon Dam, especially sections ECF1 and ECF2, is expressed as a high escarpment that lacks high surfaces on the hanging wall, although the escarpment is embayed and eroded. North of East Canyon Dam, the fault is shown by Bryant (1990), Coogan and King (2001), and Coogan (2002) as concealed by Quaternary deposits where they are present.

Sullivan and others (1988) concluded that the portion of the East Canyon fault south of East Canyon Reservoir may have been active during the late Quaternary. While our studies have been limited, like Sullivan and others (1988) we have not observed any scarps on what may be late Quaternary or Quaternary deposits or surfaces. Consequently, because direct evidence for or against late Quaternary displacements has not been recognized, we do not know whether or not displacements on the East Canyon fault continued into the Quaternary. Because such displacements cannot be entirely discounted, early Quaternary activity on the East Canyon fault is considered to be possible.

### **Main Canyon Fault**

The Main Canyon fault was mapped by Bryant (1990) as two separate traces: a northern one, about 10 km long that strikes nearly north and extends north into the Ogden quadrangle (Coogan and King, 2001), and a southern one, about 16 km long that strikes northeast (Figure 2). On Bryant's map, both faults are west dipping and located entirely within the Tertiary Wasatch Formation (Tw), except for a 2-km-long section of the fault just south of the Right Fork of Taylor Hollow, where the fault is covered by a landslide (Figure 2). Coogan's (2002) map continues the Main Canyon fault north of latitude 41° N as a concealed trace between Quaternary-Tertiary alluvium on the footwall and Quaternary colluvium over older alluvial-fan deposits on the hanging wall (Figure 2). Coogan's map shows the Main Canyon fault terminating at the eastern trace of the East Canyon fault about 1 km southwest of the Weber River valley.

There is no geologic evidence that the Main Canyon fault existed late in the middle Cenozoic. The extent of the Norwood Tuff can be explained by displacements on the East Canyon fault alone. Displacements on the Main Canyon fault have affected topography, but not in the sense that a middle or late Cenozoic basin had developed. Regardless, the geomorphic expression of the fault is nearly continuous north of Taylor Hollow as bedrock scarps or as lineaments and scarps on alluvium (Figure 4 and Figure 9). The fault cuts across existing topography indicating that displacements on the fault are geologically young, perhaps occurring only during the past few million years. In addition to scarps, the principle geomorphic features produced by the Main Canyon fault are disrupted (abandoned) drainages and differences in the degree of incision along drainages that cross the fault. Because the fault cuts across topography and drainage divides, the geomorphic expression of the fault is highly variable and depends in part on the direction of fault displacements relative to existing drainages.

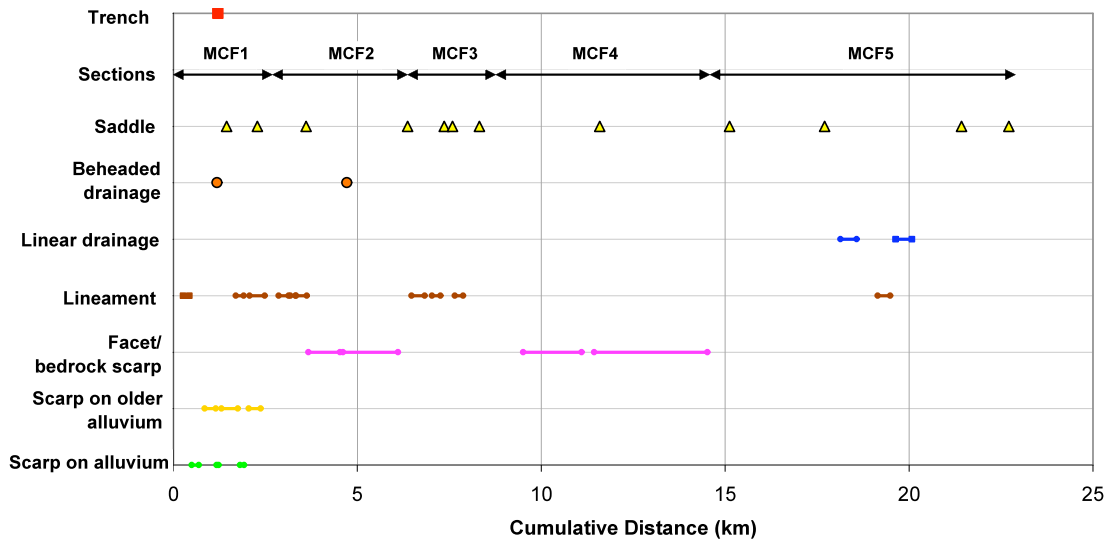


**Figure 9.** Distribution of possible tectonic geomorphic features along the Main Canyon fault. The features are plotted by distance from the north end of the fault. Taylor Hollow is at the boundary between sections MCF4 and MCF5.

For ease of discussion, the Main Canyon fault has been subdivided into five sections (MC1 through MC5) on the basis of differences in geomorphic expression of the fault (Figure 4 and Figure 9). Bryant (1990) shows nearly the entire fault as a single trace. The northernmost section (**MCF1**), which is about 3.5 km long, is that portion of the fault north of Main Canyon Creek. The fault cuts across early Quaternary (less than about 2 million years old) alluvial fans on eastward slopes and has formed upslope-facing (west-facing) scarps (Figure 10). East-flowing drainages from the escarpment along the East Canyon fault are barely incised on the hanging wall, but are markedly incised into older deposits downstream on the footwall (Figure 11; Appendix A). Displacements on the Main Canyon fault flattened gradients of the drainages on the hanging wall, which resulted in ponding adjacent to the fault. Topographic profiles along the smaller drainages flatten at the fault. The fault crosses Main Canyon Creek seemingly without a change in gradient or incision, but this is a much larger drainage that heads at a divide (Hogback Summit) within East Canyon valley. Because of its larger size, Main Canyon Creek may have been able to maintain its gradient after faulting events. The fault also may step to the east at Main Canyon Creek, so that displacements may not have been continuous across the drainage.

In this northern section (MCF1), fault scarps are present on surfaces of two broad age groups: younger alluvial fans and older alluvial fans or gravel deposits. The younger alluvial fans, which form the main part of the valley floor, are now graded to a level below the fault scarps. At least one drainage has been disrupted (cut off from its downstream continuation) because of reversal of gradient caused by fault displacements along this section of the fault (Figure 10). Other small drainages may be disrupted but have not been identified at the scale of the existing mapping.

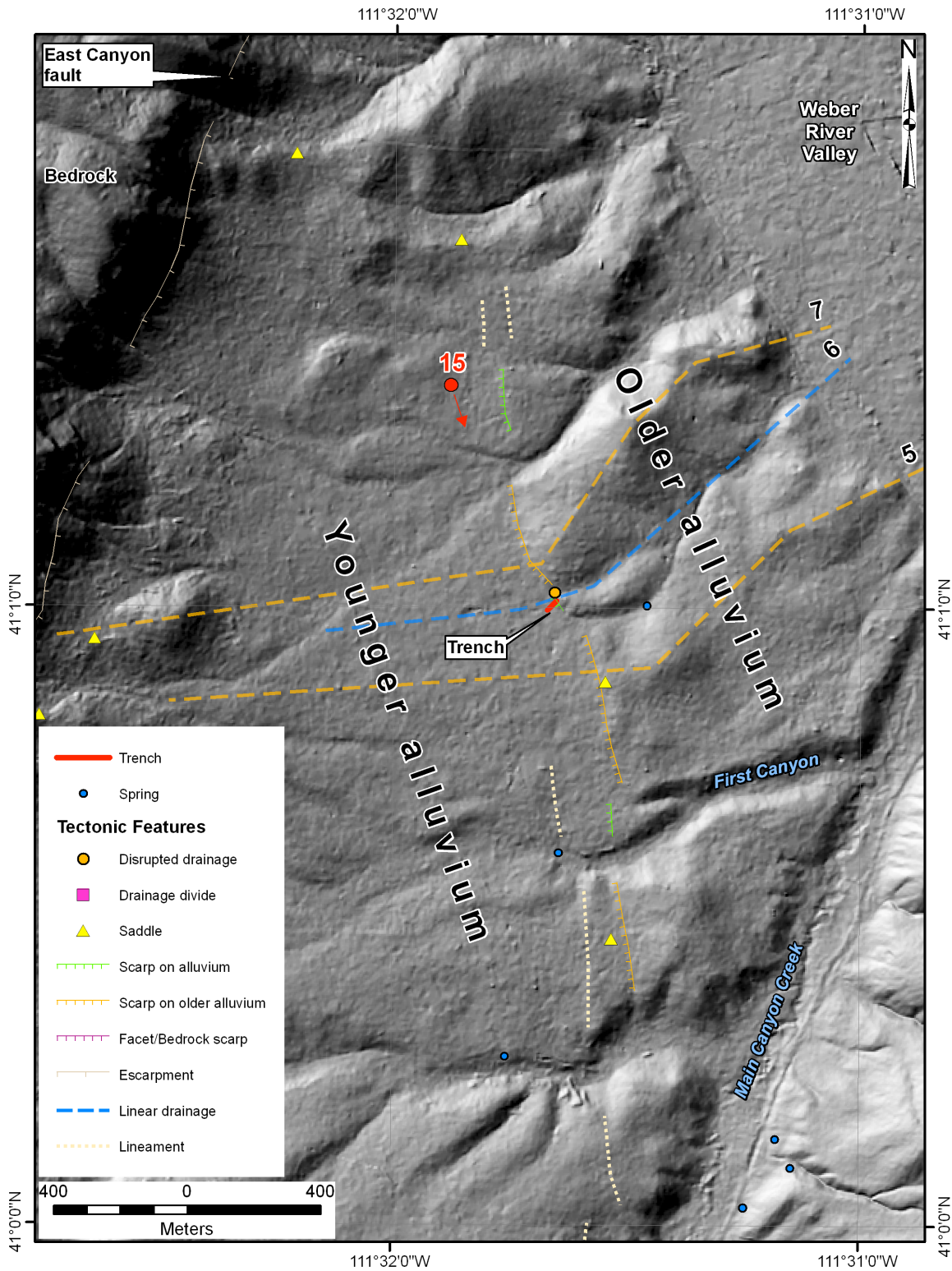


**Figure 10.** Possible tectonic geomorphic features in the vicinity of the trench excavated near the north end of the Main Canyon fault. Older alluvium is preserved east of the fault; younger alluvium is west of the fault. Red arrow shows location of Figure 15. Drainage profile 6 (blue dashed line) and ridge profiles 5 and 7 (orange dashed lines) shown on Figure 11. Background is a hillshade created from 1997 aerial photographs, ground control, and a generated grid.

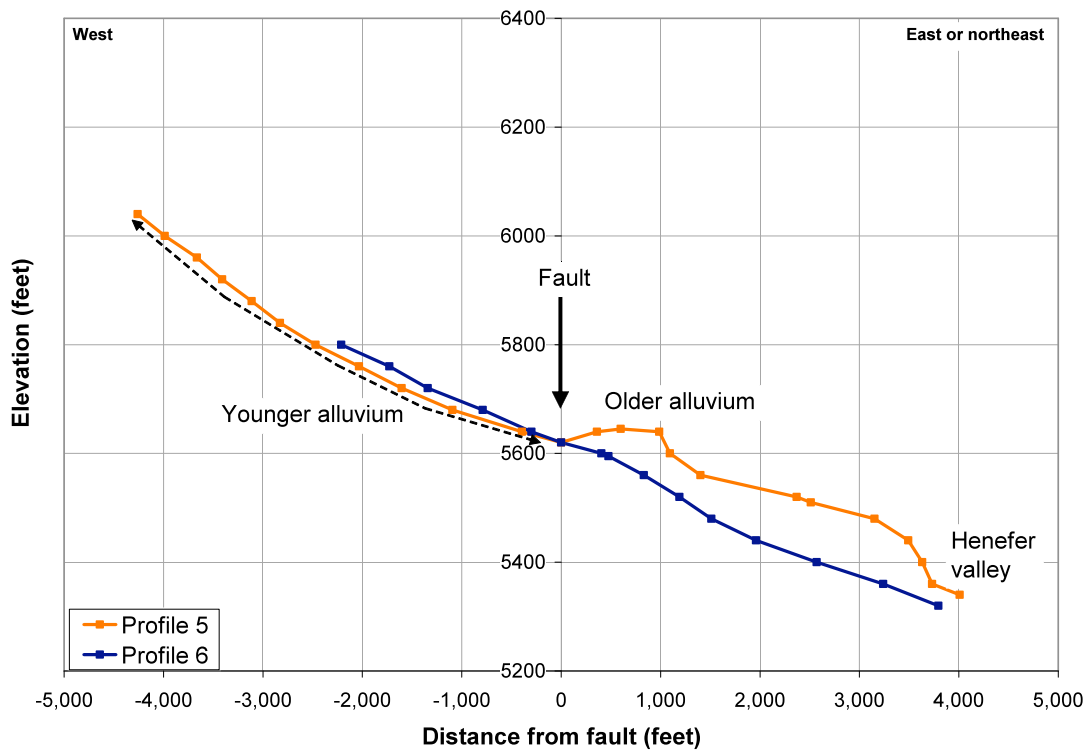
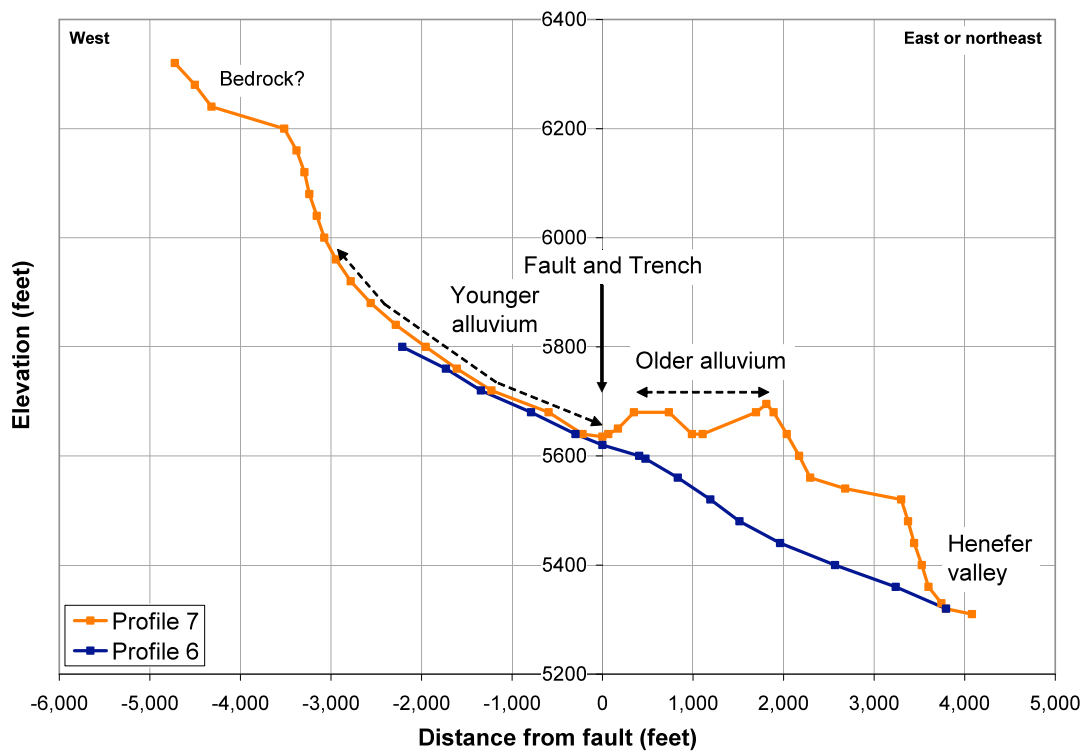


**Figure 11.** Topographic profiles in the vicinity of the trench excavated near the north end of the Main Canyon fault. Differences in incision across the fault are shown by the drainage profile (blue) and the ridge profiles (orange). See Figure 10 for locations of the profiles.

The location of the northern end of the Main Canyon fault is not known with any certainty. Coogan and King (2001) and Coogan (2002) map the north-northwest-striking Main Canyon fault as intersecting the north-northeast-striking East Canyon fault at an oblique angle about 2 km south of the Weber River (Figure 2). However, both fault traces are shown as concealed, and bedrock outcrops in this area are scarce even though the area is fairly well dissected. Possible west-facing scarps and lineaments that were observed by L.W. Anderson on an aerial overflight in July 2007 suggest that the Main Canyon fault could continue with a more northerly trend than that shown by Coogan and King (2001) and Coogan (2002). If the surficial expression of the Main Canyon fault continues north of the Weber River, then the fault could be 1 to 2 km longer than it is presently portrayed, and the structural relation between the Main Canyon fault and the East Canyon fault would be even more uncertain.

In the next section to the south (**MCF2**), about 3 km long between Main Canyon Creek and a drainage divide, displacements on the Main Canyon fault are downslope facing and have produced steep facets or bedrock scarps (Figure 12 and Figure 13). At least one drainage (a tributary to Bachelor Canyon) has been disrupted by fault displacements along this section of the fault (Figure 4 and Figure 14), and a saddle is present where the fault crosses the drainage divide at the south end of this section.

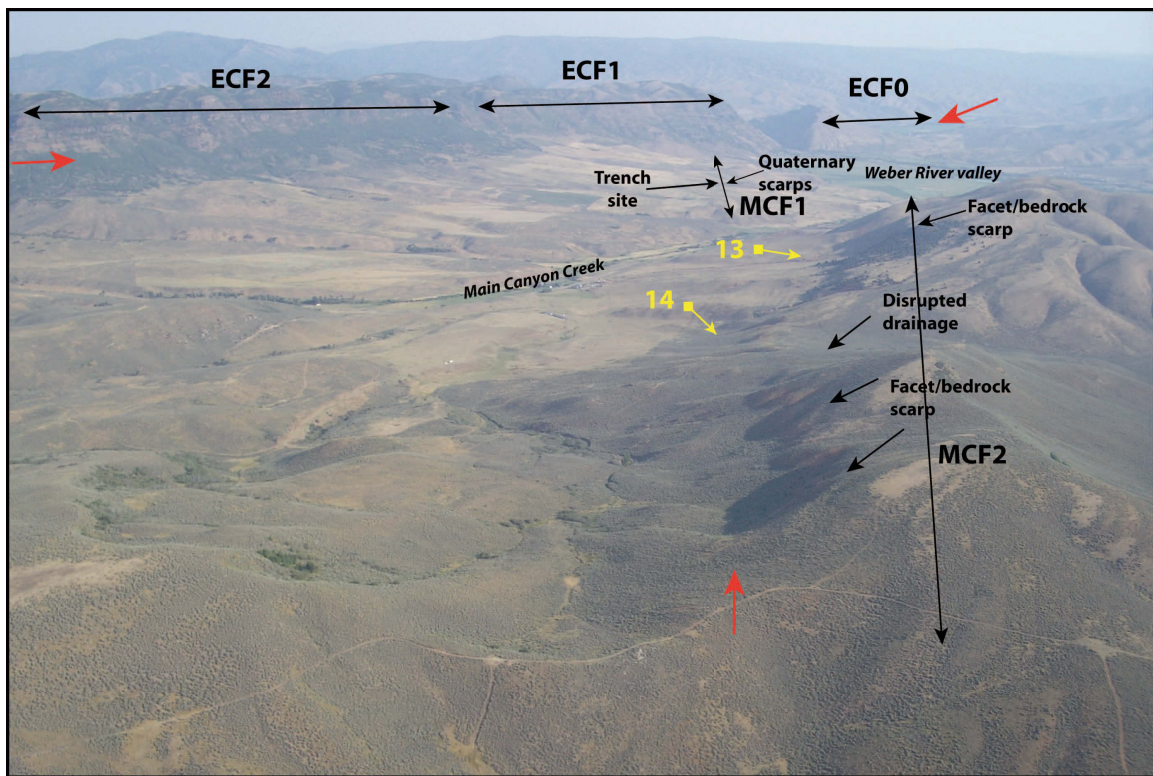


**Figure 12.** Oblique aerial photograph of sections MCF1 and MCF2 of the Main Canyon fault and sections ECFO, ECF1, and ECF2 of the East Canyon fault (Figure 4). Photograph taken looking north. Approximate locations of faults shown by red arrows. Locations of Figure 13 and Figure 14 are shown by the yellow arrows. Photograph taken by L.W. Anderson in 2007.



**Figure 13.** Facets and bedrock scarp (between red arrows) along section MCF2 of the Main Canyon fault (Figure 12). The facets and scarps are on Tertiary Wasatch Formation on the footwall. Quaternary surfaces are preserved on the hanging wall (middle ground). View is to the east. Photograph taken by D.A. Ostenaar in 2006.

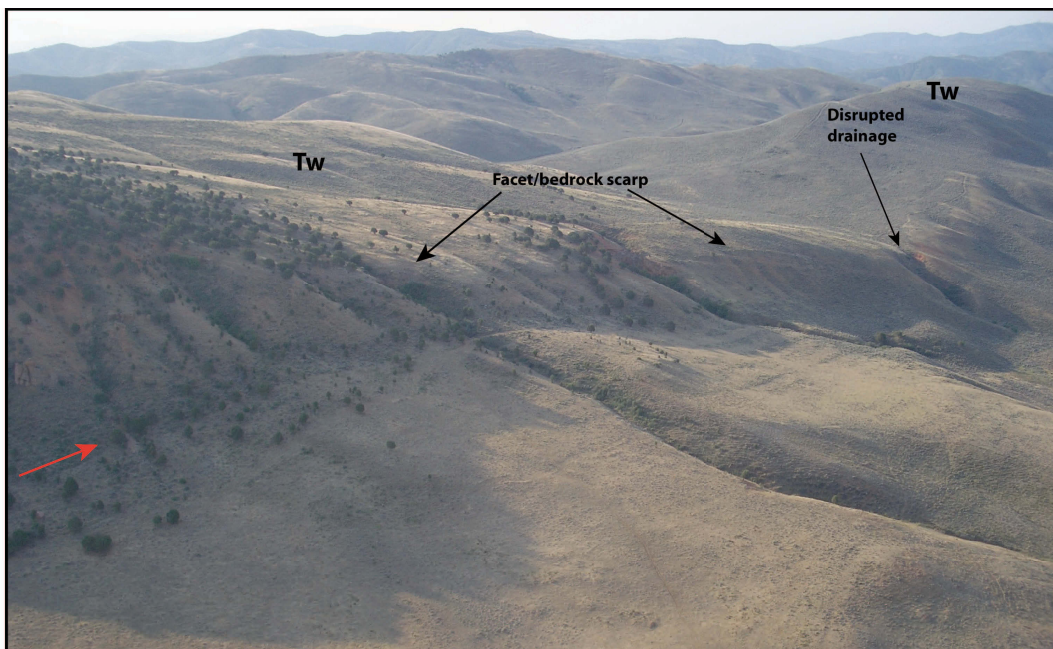


**Figure 14.** Lineaments, facets, bedrock scarps, and disrupted drainage along section MCF2 of the Main Canyon fault (red arrow) (Figure 12). Facets are in Tertiary Wasatch Formation (Tw) on the footwall. Wasatch Formation is also on the hanging wall. View is to the southeast. Photograph by L.W. Anderson in 2007.

In the next section to the south (**MCF3**), about 3 km long between the drainage divide and the Right Fork of Franklin Canyon, displacements on the fault are upslope facing. The fault is expressed as discontinuous lineaments and saddles across ridges (Figure 4 and Figure 9).

In the next section to the south (**MCF4**), 6 km long between the Right Fork of Franklin Canyon and Taylor Hollow, displacements on the fault are downslope facing. The fault in this section is expressed nearly continuously as west-facing facets or bedrock scarps (Figure 4). The facets/bedrock scarps continue to Taylor Hollow, where the fault appears to bound the east side of a higher alluvial surface preserved along the north side of Taylor

Hollow (Figure 2). However, the alluvial surface does not cross the fault, so it cannot be used to evaluate age of displacement.

In the southernmost section (**MCF5**), about 8.5 km long between Taylor Hollow and near West Fork Schuster Creek, the Main Canyon fault is expressed as discontinuous saddles, lineaments, and linear drainages (Figure 4 and Figure 9). Landslides along and near the fault (most not mapped on Figure 2) complicate an assessment of the geomorphic expression of this section of the fault. The trace of the fault curves to the southwest and intersects the canyon of East Canyon Creek, where a short section of that drainage coincides with the fault. Bryant (1990) does not map the fault south of this point, and no geomorphic expression of the fault was noted to the south.

In summary, definite evidence for late Quaternary surface rupture is present only along the northern about 3.5 km of the fault, where it forms west-facing scarps on alluvial fans that are likely late Quaternary. However, geomorphic expression of the Main Canyon fault is nearly continuous from the Weber River valley to Taylor Hollow, and discontinuous south of this point to near West Fork Schuster Creek.

## **LATE QUATERNARY SURFACE RUPTURES**

As noted above, the only potential fault scarps identified on late Quaternary surfaces in East Canyon valley are along the northern 3.5 km of the Main Canyon fault (section MCF1; Figure 4 and Figure 10). A trench was excavated across one of these scarps to determine if the scarp has a tectonic origin and to estimate the age of any fault displacements. A backhoe trench was excavated across a 70-m-long, 0.4-m-high, west-facing scarp on an alluvial fan that is inset into higher surfaces to the north and south (Figure 10 and Figure 15). The scarp is part of a higher, broader, west-facing slope from one of the remnants of uplifted older alluvium.

Alluvial fans from the escarpment along the East Canyon fault to the west are graded to an elevation below the west-facing scarps along the Main Canyon fault (Figure 10 and Figure 16). Drainages on active alluvial fans are only slightly incised on the hanging wall of the Main Canyon fault (Figure 11). The drainages become markedly more incised on the footwall, which has been uplifted relative to the alluvial fans on the hanging wall. The highest (oldest) remnants preserved between the incised drainages on the footwall are capped by subrounded to rounded, quartzite cobbles and boulders and may be remnants of older Pleistocene alluvial-fan deposits or possibly weathered Tertiary Wasatch Formation.

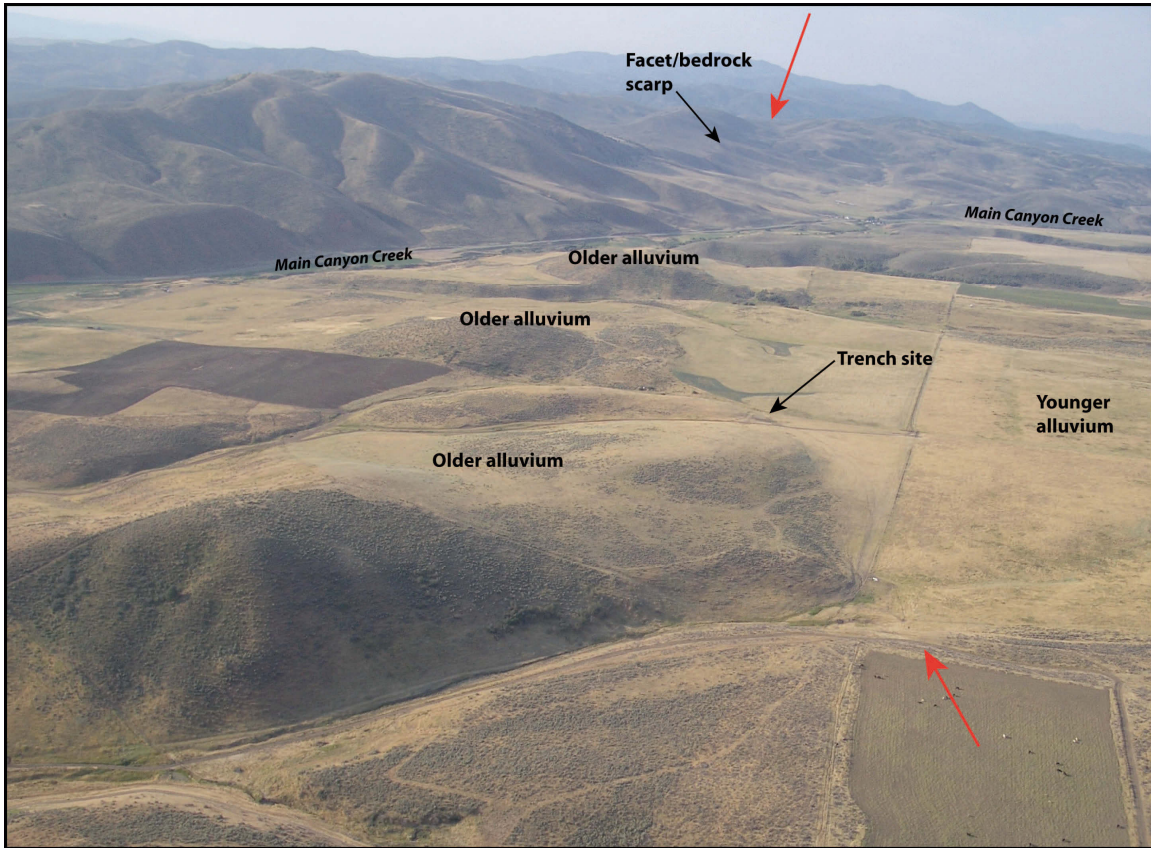


**Figure 15.** Oblique aerial photograph looking south along sections MCF1 (foreground) and MCF2 (background) of the Main Canyon fault (Figure 10). Approximate location of the Main Canyon fault indicated by red arrows. West-facing scarps and trench site are along section MCF1. Photograph taken by L.W. Anderson in 2007.

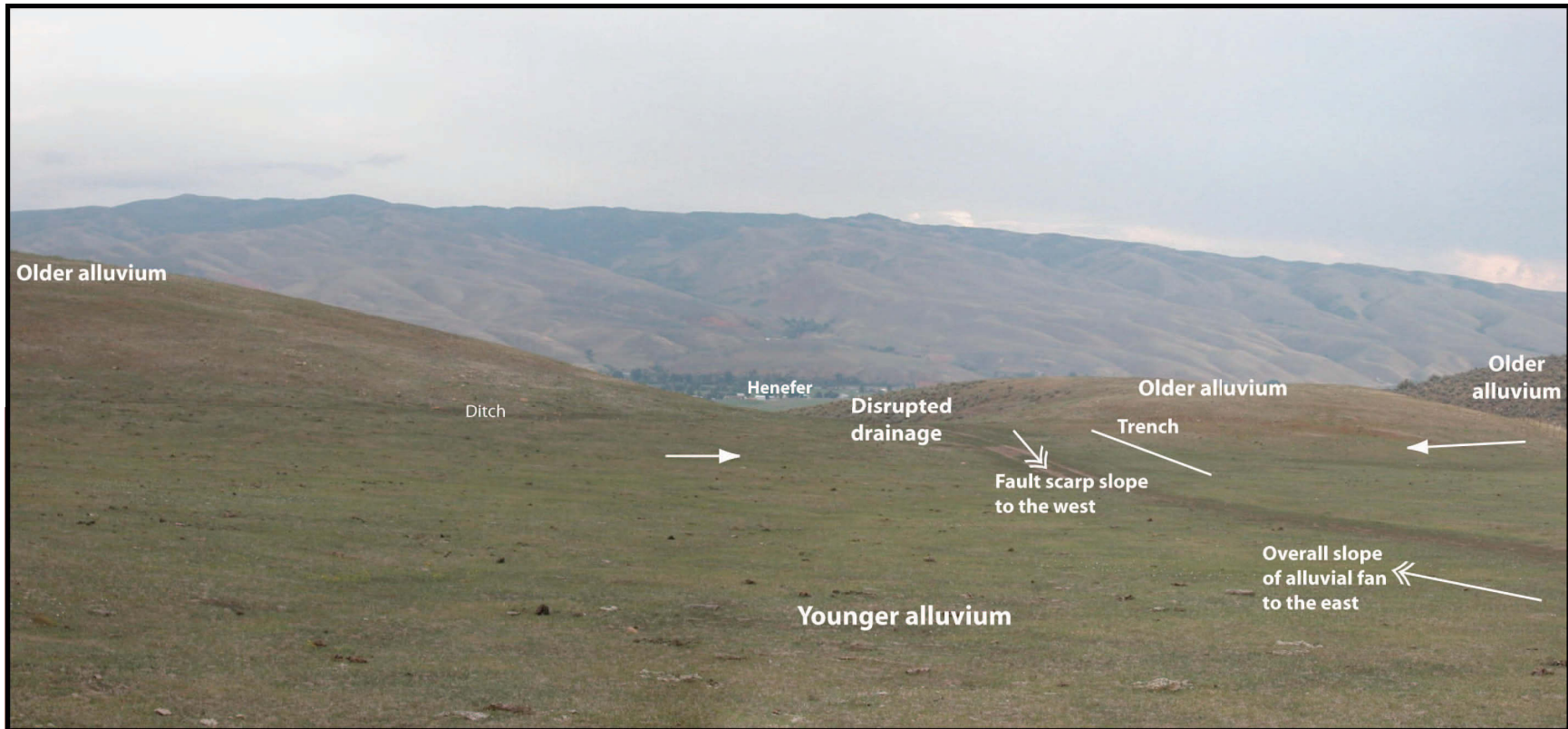


**Figure 16.** Geomorphic features in the vicinity of the trench excavated near the north end of the Main Canyon fault. West-facing fault scarp is indicated by solid-headed arrows. Slope of the scarp is shown by the double-headed arrow. The scarp opposes the overall fan slope to the east as shown by the other double-headed arrow. View is to the east.

The older remnants are shown by Coogan (2002) to be possibly Pleistocene and/or Pliocene alluvium (QTa?; Figure 2). These hills, which are shown as older alluvium on Figure 10, Figure 15, and Figure 16 are about 90 to 120 m above the Weber River valley, and are higher than pre-Bull Lake surfaces reported by Sullivan and others (1988). Their pre-Bull Lake surfaces are between 45 and 70 m above the central Weber River valley and have estimated ages of >200 ka to <500 ka (thousand years), 350 ka to 370 ka, and 440 ka to 470 ka. However, the remnants of older alluvium near the trench site have been uplifted along the Main Canyon fault, and so it is difficult to estimate their original height above the Weber River valley. If late Quaternary displacements on the Main Canyon fault had not occurred, then the alluvial fans should slope more or less evenly to the Weber River to the northeast. The remnants of older alluvium at the trench site are likely at least as old as the pre-Bull Lake surfaces reported by Sullivan and others (1988). It also is possible that the remnants are much older, perhaps on the order of a million years.

West-facing scarps also are present on lower surfaces that appear to be on the order of 30 to 60 m above the valley. The lower elevations of these surfaces relative to the older remnants suggest that the lower surfaces may be remnants of Pleistocene alluvial fans. These remnants are small, and projecting them to the Weber River valley is difficult; however, they may be correlative to the pre-Bull Lake surfaces reported in Sullivan and others (1988). The scarp where the trench was excavated is on one of these surfaces.

Displacements on the Main Canyon fault have flattened the gradients of the east-flowing drainages and small drainages are particularly affected (Appendix A). The drainage immediately north of the trench site has been uplifted to the point that the drainage ponds at the fault and no longer flows to the east through the footwall. Larger drainages appear to be able to adjust to displacements on the fault, and may be affected only temporarily by gradient changes caused by fault displacements.

Although the overall drainage direction is to the east, displacements on the Main Canyon fault form west-facing scarps that create local slopes to the west (Figure 16). At the trench site, colluvium has moved downslope to the west across the scarp. The scarp at the trench site also receives colluvium from the higher scarp preserved to the north of the disrupted drainage. Colluvium has likely filled in the drainage that at one time separated this hill to the north from the trench site after the drainage was disrupted by uplift on the Main Canyon fault. Sediment shed from the slope was no longer removed by the drainage (Figure 16).

### **Trench Across the Main Canyon Fault**

The trench site is on a southwest-facing scarp on a Pleistocene alluvial fan. Younger paludal sediments and alluvium are preserved west of the scarp. The scarp, which is about 0.4 m high and trends about N70°W, aligns with higher scarps to the north and south (Figure 10). The higher scarps are between about 6 and 20 m high. The scarp where the trench was excavated is separated from the higher scarps by drainages.

The maximum slope of the scarp at the trench is about 6° to the southwest. The general slope of the ground surface northeast of the trench is about 2° to the southwest. The ground surface between stations 8 and 13 m is flat or nearly flat. The ground surface southwest of the trench slopes a few degrees to the northeast. Because the scarp faces upslope, overall scarp angle would not vary systematically with scarp age.

A trench about 13 m long and about 2 m wide was excavated across the scarp. The low scarp height and the low scarp angle made it difficult to excavate the trench perpendicular to the trend of the scarp. In addition, the location and strike of the fault associated with the scarp were not well constrained. As a result, the trench as excavated was not perpendicular to the scarp, which trends about N70°W at the trench site (Figure 17). The fault strands that were exposed by the trench strike between N65°W and N85°W.

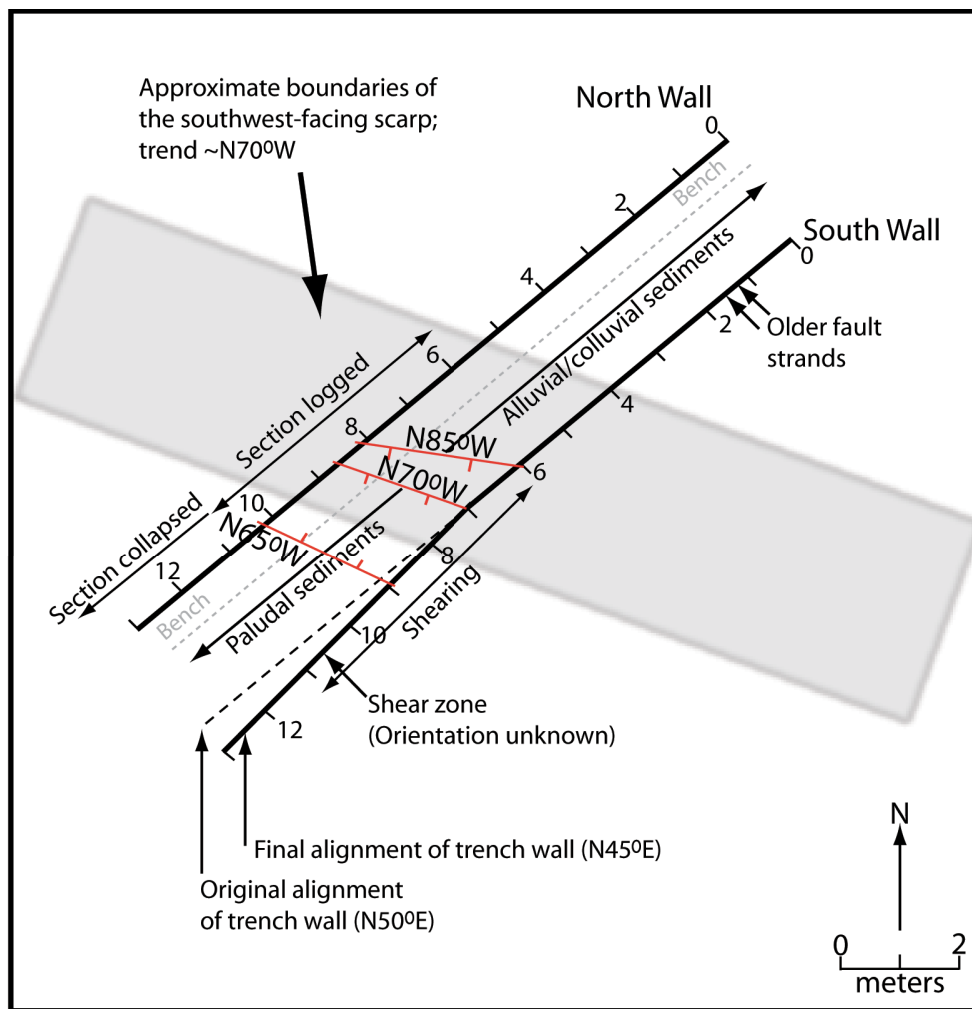


**Figure 17.** Sketch map showing the orientation of the trench relative to the west-facing fault scarp (gray box) and the main shears (shown in orange) exposed in the walls of the trench.

## Methods

The south wall of the trench was excavated vertical for logging, and a bench was dug along the north wall for safety.

Once the trench was excavated, the walls were cleaned with picks, small shovels, and trowels. Horizontal and vertical string lines were set to form a meter grid; secondary lines were established in some areas at 0.5 m and 0.25 m intervals in places to make mapping easier. Color digital photographs were taken of each 1-m square. A photo mosaic of each trench wall was constructed in *Adobe PhotoShop*. These photo mosaics were used to map stratigraphic boundaries and fault-related features (Appendix B).

The trench was initially dug with a trend of N50°E (Figure 17). However, before the trench could be logged, an intense storm filled the trench with water to a depth of about 1.5 m, and portions of both walls at the lower end of the trench collapsed. The water was pumped from the trench, and the south wall between stations 7 and 13 m was re-excavated with a backhoe. The trend of the new section of the south wall was N45°E (Figure 17). The new section was cleaned, and the string grid was resurrected and replaced, where necessary. The lower about 1 m of the south wall that was not re-excavated and the north wall between stations 6 and 11 m were re-cleaned to remove the silty deposits that coated the lower walls. The collapsed section of the north wall, between stations 11 and 13 m, was not re-excavated. A preliminary log of the north wall had been made before the collapse, and this was used (Appendix B).

Because the trench intersects the scarp and fault zone at angles less than perpendicular, the fault zone is exposed in the south wall between stations 6 and 9 m, but is exposed in the north wall between stations 8 and 10 m (Figure 17). The strike of the main shear zone is N70°W near the base of the trench exposure, and has an average dip of 81°W. Other distinct shear zones strike N85°W and N65°W, and have average dips between 70°W and 75°W (Figure 17).

## Characteristics, Ages, and Tectonic Interpretation of the Stratigraphic Units Exposed in the Trench

Twelve stratigraphic units were identified and mapped in the trench (Figure 18; Appendices B and C). Units are generally labeled oldest to youngest in ascending numerical order. The main fault zone is clearly expressed as a steep southwest-dipping shear zone that juxtaposes alluvial/colluvial units on the footwall and paludal (marsh) deposits on the hanging wall (cover photograph). The units on the hanging wall and footwall were subdivided on the basis of depositional unconformities between the units as indicated by erosion surfaces and/or soil development. The only unit that can be traced across the main fault zone is slope colluvium (unit 12) from the higher slope west of the trench. Because the surface ruptures that created the scarp disrupted small drainages on the alluvial fans and caused local ponding along the scarp for some time after surface rupture occurred, correlative stratigraphic units are not present on opposite sides of the

fault. Units on the footwall are primarily slope colluvium and/or alluvium. Units on the hanging wall are primarily paludal deposits, which were deposited in ponded areas that collected loess and fine alluvial sediment from the adjacent low-gradient slopes. At least two mudflow deposits that originated from the adjacent steeper slopes, probably from the hill north of the trench site, are exposed in the trench. One mudflow deposit fills a channel on the footwall (unit 8); the other is on the hanging wall and fills the graben along the scarp (unit 10). The relation between these two deposits cannot be determined directly from the trench exposures. Better soil development on unit 8 suggests that it is older than unit 10.

Ages for the units exposed in the trench were determined from luminescence analyses on nine samples and radiocarbon analysis on one sample (Appendix D). Ages obtained from these methods are supported by the degree of soil development observed in the trench exposure. Soil development was used to estimate the ages of the oldest units, which yielded maximum values from luminescence analyses. Soil development was generally compared to descriptions by Sullivan and others (1988) for dated Quaternary deposits in other valleys in the northern Wasatch Range. The nine samples collected for luminescence analyses were submitted to the Luminescence Dating Laboratory at the U.S. Geological Survey, Denver, Colorado, for analyses (Appendix E). Eight bulk sediment samples were collected and submitted to Paleo Research Institute, Golden, Colorado, for cleaning, examination, and analyses (Appendix F). Only one sample (ECT-C8) yielded enough charcoal for an accelerator mass spectrometry (AMS) age. This sample was sent to the Keck Carbon Cycle AMS Facility at the University of California, Irvine, for analysis (Appendix F).

Dark, rounded pellets with diameters of about 1 mm are common to abundant in most of the paludal deposits exposed on the hanging wall. The pellets were extracted from the bulk sediment samples collected for possible radiocarbon dating and were examined by Paleo Research. They concluded that the pellets are asphaltum and the results from a Fourier Transform infrared spectrometry analysis matched most closely those of man-made asphalt (Appendix G). Additional analyses were recommended. Asphaltum pellets from one sample (ECT-C7) from unit 6 were submitted to Humble Instruments & Services for additional analyses (Appendix G). Results from chromatography and spectrometry indicate that the asphaltum from the trench is not from processed (man-made) hydrocarbons, but is probably from some type of natural oil seep associated with Cretaceous marine or lacustrine rocks and could be from the Wasatch Formation, which is a known oil reservoir. The asphaltum from the trench does not appear to be from gilsonite deposits that are present in northeastern Utah, which would indicate a significant transport distance for the deposits.

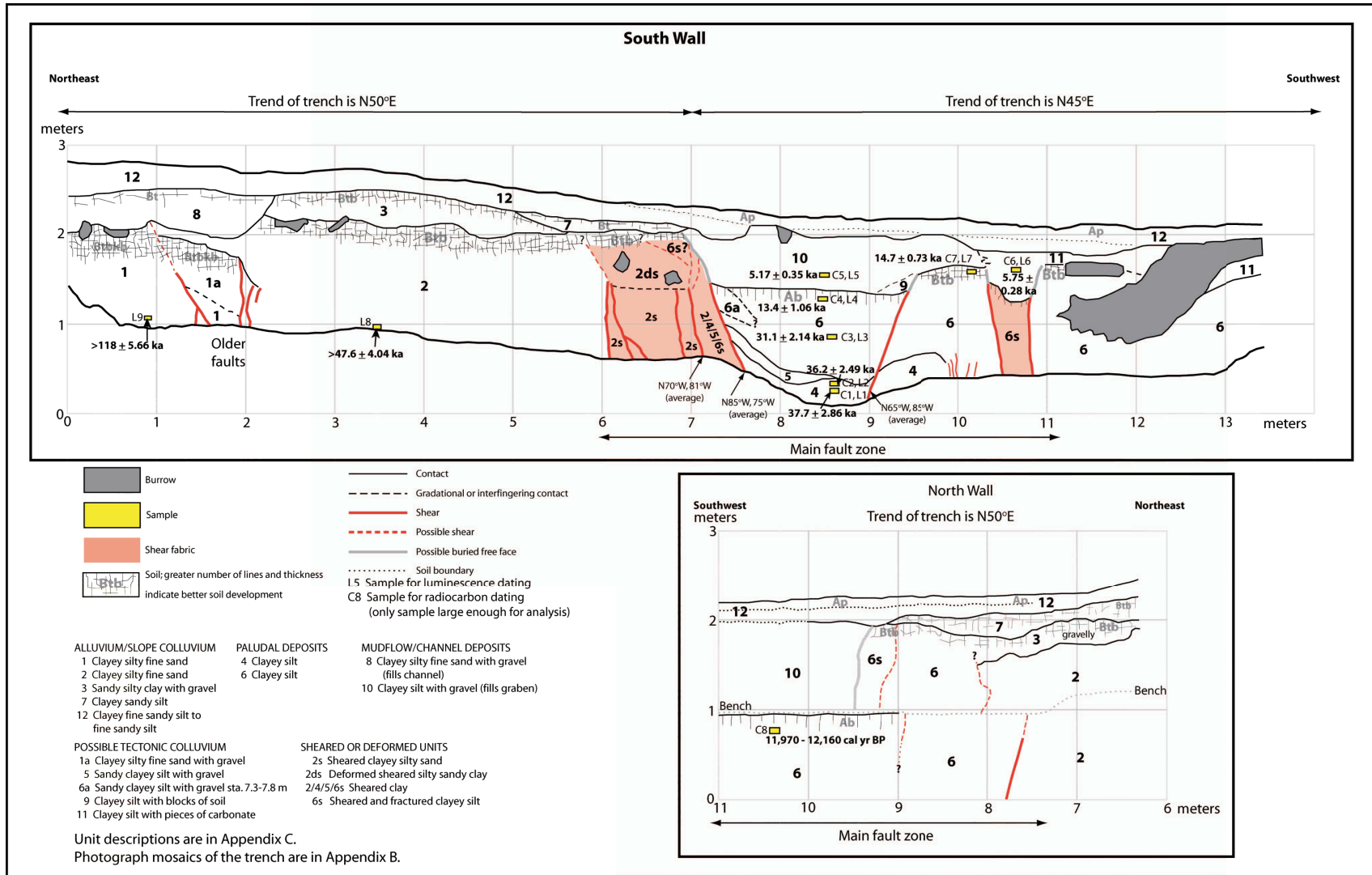


Figure 18. Interpreted log of the trench excavated near the north end of the Main Canyon fault.

## *Units 1, 1a, and 2*

The oldest unit in the trench (unit 1) is alluvium and/or colluvium (Figure 18; Appendices B and C). Distal sediment in this unit may have come from two different directions: either deposited as alluvial fans from the escarpment to the west or as colluvium from the higher fan remnant to the east. The unit is clayey, silty fine sand with a few percent of gravel, either scattered through the deposit or in lenses. The deposit was probably clay-rich initially. Regardless, thick clay films, strong prismatic structure, and stage III carbonate on which the clay films are overprinted suggest that the deposit is quite old, and has undergone several cycles of soil formation and disintegration. A luminescence date for sample L9 of greater than  $118,000 \pm 5660$  years is likely a minimum age (Table 1; Appendix E), because of the problems in applying optically stimulated luminescence (OSL) dating to sediment with strong soil development. The soil development suggests that the deposit is at least several hundred thousand years old (Sullivan and others, 1988), and may be as old as 1 to 2 million years. Carbonate-filled shear zones between stations 1 and 2 m indicate faulting event(s) older than the ones associated with the main fault zone between stations 6 and 11 m.

Unit 1 is displaced near station 2 m against the next oldest unit (unit 2), which has characteristics similar to those of unit 1, and probably has a similar origin. The degree of soil development in unit 2 is much less than that in unit 1 (Appendices B and C). The soil on unit 2 has prominent clay films and is red, but it lacks carbonate and evidence for polycyclic formation that are present in unit 1. A luminescence date from unit 2 near the base of the trench (sample L8) yielded an age of greater than  $47,600 \pm 4040$  years (Table 1; Appendix E), which is likely a minimum because of the problems in applying OSL dating to sediment with strong soil development. Thick red argillic horizons with strongly developed soil structure were interpreted by Sullivan and others (1988) to be correlative with the Bull Lake glaciation, and date from about 60 ka-70 ka to about 130 ka-140 ka. This age range is consistent with the luminescence date.

Unit 1a may be a tectonic colluvial wedge derived from unit 1 due to a faulting event that displaced units 1 and 2. Unit 1a is similar to unit 1, but has slightly more gravel (Appendix C). We interpret unit 1a to be a colluvial wedge on the basis of the gravel content, its limited extent and wedge shape, and its position just downslope of a carbonate-filled shear zone (Figure 18; Appendices B and C).

**Table 1.** Quartz blue-light OSL ages from trench across Main Canyon fault (Mahan, 2007 [Appendix E]).

Sample information expected age: stratum	% Water content <sup>a</sup>	K (%) <sup>b</sup>	Th (ppm) <sup>b</sup>	U (ppm) <sup>b</sup>	Cosmic dose <sup>c</sup> additions (Gy/ka)	Total Dose Rate (Gy/ka)	Equivalent Dose (Gy)	n <sup>d</sup>	Age (ka)
<i>ECT-L5</i>	5 (48)	2.27 ± 0.11	12.5 ± 0.33	3.58 ± 0.13	0.26 ± 0.02	3.59 ± 0.07	18.6 ± 1.22	22 (30)	5.17 ± 0.35 <sup>e</sup>
post MRE sediments (youngest?)									
<i>ECT-L6</i>	13 (57)	3.23 ± 0.06	12.1 ± 0.33	3.30 ± 0.12	0.27 ± 0.02	4.28 ± 0.07	24.6 ± 1.15	29 (35)	5.75 ± 0.28 <sup>e</sup>
<i>ECT-L4</i>	9 (74)	2.15 ± 0.07	12.5 ± 0.32	3.47 ± 0.12	0.26 ± 0.02	3.31 ± 0.06	44.3 ± 1.94	24 (28)	13.4 ± 1.06 <sup>e</sup>
sediment buried by MRE									
<i>ECT-L7</i>	10 (54)	1.62 ± 0.14	11.3 ± 0.27	2.54 ± 0.11	0.26 ± 0.02	2.78 ± 0.06	40.9 ± 3.11	27 (35)	14.7 ± 0.73 <sup>e</sup>
<i>ECT-L3</i>	9 (68)	1.82 ± 0.12	12.0 ± 0.27	3.23 ± 0.12	0.25 ± 0.02	2.98 ± 0.05	92.6 ± 2.18	30 (37)	31.1 ± 2.14 <sup>e</sup>
"Event 1" sediment wedge									
<i>ECT-L2</i>	13 (58)	1.50 ± 0.05	11.3 ± 0.29	3.16 ± 0.11	0.23 ± 0.02	2.65 ± 0.05	96.0 ± 6.21	8 (20)	36.2 ± 2.49 <sup>f</sup>
pre-Event 1 sed/soil									
<i>ECT-L1</i>	15 (51)	1.36 ± 0.06	10.8 ± 0.27	2.55 ± 0.10	0.21 ± 0.02	2.50 ± 0.04	94.2 ± 2.36	15 (15)	37.7 ± 2.86 <sup>f</sup>
pre-Event 1 sed									
<i>ECT-L8</i>	7 (51)	1.56 ± 0.14	11.1 ± 0.23	2.38 ± 0.11	0.24 ± 0.02	2.67 ± 0.05	>127 ± 5.02	16 (29)	>47.6 ± 4.04 <sup>e</sup>
older, weathered, Bt soil development									
<i>ECT-L9</i>	7 (34)	1.68 ± 0.09	11.0 ± 0.24	2.80 ± 0.10	0.24 ± 0.02	2.84 ± 0.05	>334 ± 8.34	21 (24)	>118 ± 5.66 <sup>e</sup>
oldest, stage III carbonate soil, reddened									

<sup>a</sup>Moisture value used in calculation of age (usually 45% of total saturation, except ECT-9 which was 60%). Figures in parentheses indicate the complete sample saturation %.

<sup>b</sup>Analyses obtained using laboratory Gamma Spectrometry (low resolution NaI).

<sup>c</sup>Cosmic doses and attenuation with depth were calculated using the methods of Prescott and Stephans (1982) and Prescott and Hutton (1994). See Appendix E for details and references.

<sup>d</sup>Number of replicated equivalent dose (De) estimates used to calculate the mean. Figures in parentheses indicate total number of measurements made including failed runs with unusable data.

<sup>e</sup>Dose rate and age for fine-grained 90-125 µm quartz sand. Linear and exponential fit used on age, errors to one sigma.

<sup>f</sup>Dose rate and age for fine-grained 90-250 µm quartz sand. Exponential fit used on age, errors to one sigma.

### ***Unit 3***

Unit 3 was deposited on unit 2 after a period of erosion. Unit 3 is gravelly slope colluvium and contains more gravel than the older, underlying units. The gravel is likely from the gravel deposit upslope because of its high percentage of quartzite stones that are also present in the gravel deposit upslope. Soil development, while still relatively strong, is much less than the soils developed in units 1 and 2. The soil in unit 3 has thick, dark clay films, and strong blocky structure. Pedogenic carbonate is absent. This soil is similar to those described by Sullivan and others (1988) for deposits from about 60 ka-70 ka to about 130 ka-140 ka. Unit 3 does not intersect any tectonic features.

### ***Unit 4***

Unit 4, which is preserved within the main fault zone, is the oldest paludal (or marsh) deposit exposed in the trench. The unit is massive, brown clayey silt with about 1 percent gravel. The unit has stage II+ carbonate, which includes irregularly shaped, elongated nodules that are oriented horizontally or subhorizontally. Two luminescence dates (samples L1 and L2) from this unit yielded ages of  $37,700 \pm 2860$  years and  $36,200 \pm 2490$  years (Table 1; Figure 18; Appendix E). Because the marsh was likely present due to ponding against a fault scarp, displacement on the fault zone would have occurred before this time. The base of unit 4 was not exposed in the trench, so its total thickness is not known. The presence of a marsh along the scarp suggests that the drainages from the escarpment to the west were not through going at this location at the time. This implies that displacement on the Main Canyon fault had uplifted the drainages enough so that flow to the northeast was disrupted on the smaller drainages.

### ***Unit 5***

Unit 5 is a reddish, 0.1-m-thick bed with about 5 percent gravel just below unit 6 between stations 7.5 and 8.5 m on the south wall. On the basis of its position adjacent to the fault zone, gravel content, and wedge shape, unit 5 is interpreted to be scarp-derived colluvium. Unit 5 would have been deposited just after the earthquake that created the topographic low that became the marsh into which unit 6 was deposited.

### ***Units 6 and 6a***

Unit 6 includes paludal deposits, which are up to 0.7 meters thick in the trench, but their base is not exposed so their total thickness is not known. The unit is massive, brown clayey silt with about 1 percent gravel. The unit is present both within the fault zone between stations 7 and 11 m, and west of the fault zone (stations 11 to 13 m). A higher gravel content (5 to 10 percent), gravel clasts oriented with a slope to the southwest, and wedge shape suggest that some of unit 6 near the fault zone may be scarp-derived colluvium. This sediment is designated unit 6a. A luminescence date (sample L3) from a depth of about 1 m in unit 6 yielded an age of  $31,100 \pm 2140$  years, slightly younger than the dates from underlying unit 4 (Table 1; Appendix E). The scarp-derived colluvium (unit 5) just below unit 6 suggests that an unconformity is present between units 4 and 6,

although the time represented may be only a few thousand years. The faulting event that resulted in deposition of scarp colluvium (unit 5) and created the marsh into which unit 6 was deposited occurred between  $36,200 \pm 2490$  years and  $31,100 \pm 2140$  years, the bracketing ages from units 4 and 6.

Two luminescence samples (L4 and L7) near the top of unit 6, one near station 8.5 m and one near station 10.2 m, yielded ages of  $13,400 \pm 1060$  years (L4) and  $14,700 \pm 730$  years (L7). A radiocarbon age of 11,970 to 12,160 cal years BP (L8; Appendix F) from the north wall is consistent with the luminescence ages. The difference in the ages from samples separated by about 0.3 m vertically on the south wall suggests that it took several tens of thousands of years for the fine sediment (alluvial and eolian) to accumulate in the marsh created by displacement on the fault about 30 ka to 38 ka. Unit 6 within the graben has an A horizon developed in it. Unit 6 outside of the graben has a Bt horizon. The difference in soil development may be the result of different landscape positions once a portion of unit 6 was downdropped into the graben. This area would have been wetter and received a greater influx of finer sediment than the portion of unit 6 outside of the graben. Unit 6 is displaced along several shears within the broad shear zone between stations 7 and 11 m.

### ***Unit 7***

Unit 7 is slope colluvium that has a stone line with about 30 percent gravel at its base. The rest of the unit has about 15 percent gravel. The unit has characteristics similar to those of unit 3, and likely has a similar source. The stratigraphic relation, the stronger soil developed in unit 3, and the stone line at the base of unit 7 suggest an unconformity between units 3 and 7. Unit 7 overlies sheared blocks of unit 2 between stations 6 and 7 m, and does not appear to be displaced. On the north wall, slope colluvium with similar characteristics (e.g., 25 percent gravel, Bt soil horizon) is present between stations 6 and 9 m. The slope colluvium on the north wall also overlies the east end of the main fault zone, as does unit 7 exposed on the south wall. For these reasons, the slope colluvium on the north wall is tentatively correlated with unit 7.

### ***Unit 8***

Unit 8 is on the footwall only, between stations 0 and 2 m on the south wall. (The area where this unit would be present on the north wall was destroyed during the initial excavation.) This unit is a mudflow deposit of clayey, silty fine sand with up to 5 percent gravel. It appears to fill a channel. An argillic (Bt) horizon has formed in the unit and has moderately thick clay films and strong, medium blocky structure. The soil is less developed than the soils in the older units on the footwall.

### ***Unit 9***

Unit 9 is a 0.3-m-thick, wedge-shaped unit between stations 9 and 9.5 m on the south wall. This unit contains blocks of soil that appear to be rotated. On the basis of its position adjacent to a fault zone, blocks of soil, and wedge shape, unit 9 is interpreted to

be scarp-derived colluvium. Unit 9 would have been deposited just after the faulting event that downdropped unit 6 and created the graben into which unit 10 was deposited.

### ***Unit 10***

Unit 10 is a mudflow deposit that is visible in both trench walls. It is massive clayey silt with up to 5 percent gravel that is dispersed throughout the unit without stratification or bedding. The unit is thickest within the graben, where it is about 0.6 m thick. Soil on unit 10 has an A horizon only. Pedogenic carbonate is not present. A luminescence (L5) from near the base of the unit at a depth of 0.7 m yielded an age of  $5170 \pm 350$  years (Table 1; Figure 18). Unit 10 buries unit 6 in the graben. The burial is likely the result of a tectonic event on the fault that created a new scarp or enhanced a preexisting one and downdropped unit 6. The soil developed on this part of unit 6 is a dark A horizon that contains more silt in its upper 30 cm than in the rest of the soil. Because unit 6 within the graben was buried by unit 10, the soil on this part of unit 6 is less developed than the soil developed on unit 6 between stations 9.5 and 10 m, an area outside of the graben (Figure 18). The luminescence age from unit 10 indicates that the earthquake that displaced unit 6 and created the graben in which unit 10 was deposited occurred before  $5170 \pm 350$  years. The luminescence ages from the upper part of unit 6 suggest that this displacement occurred after  $13,400 \pm 1060$  years and  $14,700 \pm 730$  years, the ages from the upper part of unit 6.

### ***Unit 11***

Unit 11 is gray clayey silt with about 1 percent gravel that is visible on the south wall between stations 10.5 and 13 m. Between stations 10.5 and 11.75 m, the unit contains small pieces (<1 mm) of carbonate that appear to have been eroded from unit 6. Unit 11 was deposited above a 0.5-m-wide shear zone in which unit 6 had been downdropped. The pieces of carbonate indicate that erosion of free faces above the bounding faults in this small shear zone provided some of the material for unit 11. We interpret unit 11 to be fine-grained, scarp-derived colluvium on the basis of its geometry, relation to the adjacent free faces, and sedimentological properties. The unit has an A horizon only; no pedogenic carbonate was visible in the unit. A luminescence sample at a depth of about 0.6 m within the unit near station 10.5 m yielded an age of  $5750 \pm 280$  years (L6; Table 1; Figure 18). The relation between unit 11 and unit 10, the similar characteristics of the two units, their relations to the shear zones, the lack of a marked contact between the two units, and the luminescence ages suggest that the units are correlative in age.

### ***Unit 12***

Unit 12 is slope colluvium that is present along the length of the trench. Its texture varies from clayey, fine sandy silt between stations 0 and 7 m to fine sandy silt between stations 7 and 13 m. Gravel content is highest, up to 10 percent, between stations 0 and 7 m. Unit 12 is sediment that has eroded from the higher slope of the hill to the east of the trench since the last faulting event. The gravel content decreases near station 7 m at a point that coincides with a decrease in large boulders on the ground surface. The unit

does not have any visible soil development other than an Ap (plow) horizon along most of the trench. The unit is present in both the south and north walls, and it overlies all of the other units in the trench. The unit is not visibly offset along the shear zone, and the unit does not markedly thicken across the shear zone.

### **Sequence of Faulting, Deposition, and Erosion**

Figure 19 is a schematic drawing of the how the trench site may have looked at times during the sequence of events that deposited and displaced the exposed units. Brief descriptions of these events are given below.

***Older than 38,000 years ago (could be as long ago as 1 million to 2 million years)  
(Figure 19A)  
(Before the two most-recent surface-faulting earthquakes on the main fault zone)***

Unit 1 is deposited, probably as alluvial-fan deposits from the escarpment along the East Canyon fault to the west of the trench site.

Recurrent fault ruptures likely occur, and eventually the toes of the alluvial fans are uplifted and older alluvial-fan deposits or Wasatch Formation is exposed on the footwall of the Main Canyon fault. The only direct evidence of fault displacement during this time is a zone of shears between stations 1 and 1.5 m and a possible tectonic colluvial wedge downslope of one shear (unit 1a).

Soil develops on unit 1 (and 1a) during several climatic cycles.

Fault displacement on a shear near station 2 m offsets the tectonic colluvial wedge (unit 1a) against unit 2, alluvial-fan deposits from the west or colluvium from the scarp or slope to the east.

Soil develops on unit 2.

If the tectonic ruptures formed marshy (or ponded) areas west of the fault scarp as they did in later events, there is no evidence for them in this part of the trench. The lack of ponded sediment may indicate that the uplift along the Main Canyon fault had not yet been enough to strand (reverse or disrupt) the drainages flowing to the northeast toward the Weber River from the escarpment along the East Canyon fault. This could imply that displacement on the Main Canyon fault was initiated during the late Quaternary, or possibly the middle Quaternary.

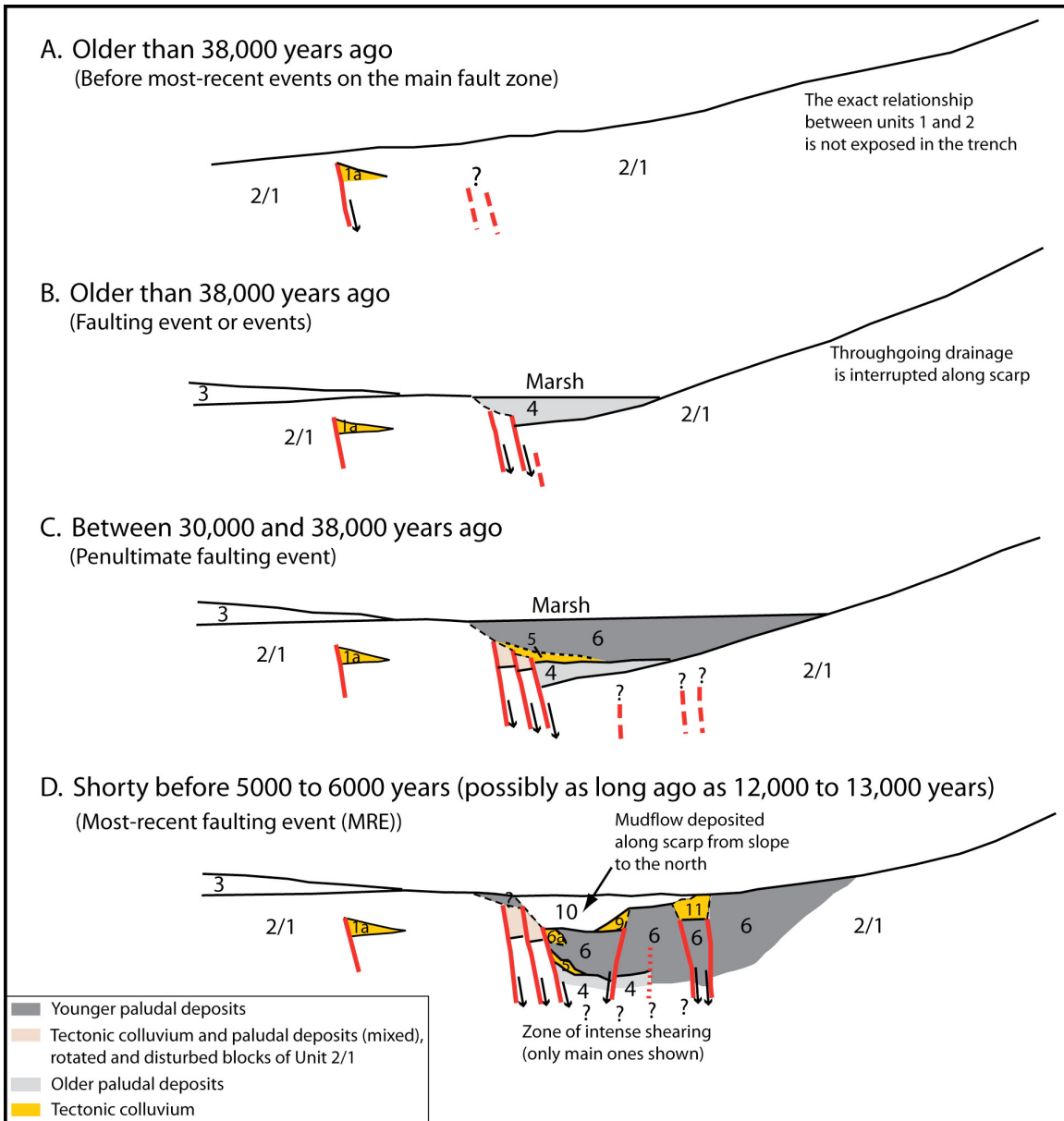


**Figure 19.** Schematic drawing (looking south) of possible sequence of events interpreted from the trench exposure. Dashed red lines indicate the locations of fault strands with future displacements.

**Older than 38,000 years ago (Figure 19B)**  
**(Faulting event or events)**

At least one, and more likely several, fault displacements occur on shears between stations 6 and 7.5 m.

Displacements shear and disrupt unit 2.

The youngest of these ruptures blocks drainage from the west, and a marsh forms along the scarp. (Marshes may have formed during older faulting events, but we do not have direct evidence for this exposed in the trench.)

Unit 4 is deposited as fine sediment from the adjacent slopes washes into the marsh and as loess (eolian silt and fine sand) settles into the marsh.

As the marsh fills with sediment, it is repeatedly wetted and dried. The soil development suggests that this area on the hanging wall was not subaerial for any length of time. The soil consists primarily of carbonate that is concentrated into irregularly shaped nodules.

Unit 4 may have buried or nearly buried the scarp.

The upper part of unit 2 is eroded between stations 2 and 7 m. Unit 3 is deposited as slope colluvium from the higher remnant to the east on the footwall.

***Between about 30,000 and 38,000 years ago (Figure 19C)  
(Penultimate surface-faulting earthquake)***

Fault displacement on at least one of the shears between stations 7 and 7.5 m.

Displacement also may have occurred on other shears.

Unit 4 is displaced.

Deposition and erosion after faulting event.

Unit 5 is deposited as tectonic colluvium through erosion of the west-facing scarp (primarily from unit 2) that formed during the faulting event.

The west-facing scarp that formed during the event blocks east-flowing drainage, and a marsh forms along the scarp.

Unit 6 is deposited in the marsh through a combination of alluvial and eolian processes.

Based on the relative extent of the units exposed in the trench, the marsh when unit 6 was deposited may have been larger than the marsh when unit 4 was deposited.

However, it may be that the shapes of the two marshes differed, but this cannot be resolved by the two-dimensional trench exposure.

As the marsh fills with sediment, a cumulic soil develops in unit 6.

The soil development suggests that the area was probably subaerial, but still wet at least at times.

***Shortly before about 5000 to 6000 years ago, possibly 12,000 to 15,000 years ago  
(Figure 19D)  
(Most-recent surface-faulting earthquake, MRE)***

Fault displacement on the shears between stations 7 and 11 m.

Unit 6 is displaced in a graben between stations 7.5 and 9 m.

Graben is bounded by scarps that formed during the faulting event.

Shortly after the scarps formed, unit 9 is deposited at the base of a scarp near station 9 m as the scarp degrades. Soon afterwards, a mudflow (unit 10), possibly from the relatively steep slope to the north of the trench site, fills the graben and buries unit 9 and the downdropped portion of unit 6. Unstable slopes created by the surface faulting may have contributed to the occurrence and size of the mudflow. The mudflow may have occurred before scarp-derived colluvium was deposited along the scarp at station 7.5 m, or any scarp-derived colluvium at this location may have been incorporated into the mudflow deposit.

Soil development changes and slows on the portion of unit 6 within the graben once the unit is buried and in a different landscape position.

Soil development continues on the portion of unit 6 west of the graben (stations 9.5 to 13 m). This portion of unit 6 remains near the ground surface.

A fault zone between stations 10.5 and 11 m also has displacement, and unit 6 is also sheared and downdropped here.

Unit 11 is deposited between stations 10.5 and 12 m as scarp-derived colluvium. Pieces of carbonate that appear to be from the soil developed in unit 6 are incorporated into unit 11.

This faulting event, the MRE, likely occurred shortly before 5 ka to 6 ka, the ages from near the base of units 10 and 11 that fill the graben formed during this event. Unit 10 is interpreted to be a mudflow deposit that was deposited relatively quickly. The buried A horizon in the upper part of unit 6 in the graben and the sharp contact between units 6 and 10 support this interpretation. If unit 10 accumulated slowly, then a cumelic soil would have formed and incorporated any soil developed in unit 6. However, it is possible that the MRE could be closer to the maximum bracketing age (12,000 to 15,000 years).

At some point, a channel is cut into units 2 and 3 between stations 0 and 2 m. The channel fills with a mudflow deposit (unit 8). This mudflow likely originated on the higher slope north of the trench. The soil developed on unit 8 suggests that some time interval elapsed between the deposition of unit 8 and the deposition of unit 12.

***Since about 5000 and 6000 years ago  
(Not shown on Figure 19)***

Once units 10 and 11 are deposited, soils begin to develop on them.

As part of the scarp degradation processes and continued slope processes, slope colluvium (unit 12) is deposited across the scarp. Unit 12 is likely the material that continuously moves down this slope.

Soil develops on unit 12.

Plowing has disturbed the upper few centimeters of unit 12.

## CONCLUSIONS

Exposures in the trench confirm that the scarps along the northern Main Canyon fault have a tectonic origin, and were likely formed by recurrent surface-faulting earthquakes. Stratigraphic units, ages, and tectonic events interpreted from the trench are summarized in Figure 20. Dating of faulted and unfaulted deposits exposed in the trench suggests that two surface-rupturing earthquakes have occurred since about 30,000 to 38,000 years ago. The MRE likely occurred shortly before 5000 to 6000 years ago, but could be as old as 12,000 to 15,000 years. Characteristics of the sediment filling the graben and a distinct, buried A horizon preserved on unit 6 beneath the graben fill (unit 10) suggest that this earthquake occurred closer to the minimum bracketing age than to the maximum bracketing age. The orientation of the fault and its sense of displacement relative to the landscape resulted in fault scarps that face upslope. When scarps formed, the generally

east-flowing drainages were blocked at least temporarily, and fine alluvial and eolian sediments were trapped in the resulting ponds and marshes. Consequently, the alluvial-fan and colluvial deposits that are preserved on the footwall were not exposed in the trench on the hanging wall, and neither the amount of offset nor a slip rate could be estimated. The penultimate faulting earthquake occurred between about 30,000 and 38,000 years ago, when a marsh also formed in response to scarp formation. Evidence for older surface-faulting earthquakes (older than 38,000 years ago) on the Main Canyon fault is present in the trench, but the timing of these events could not be estimated with any accuracy from the available exposures.

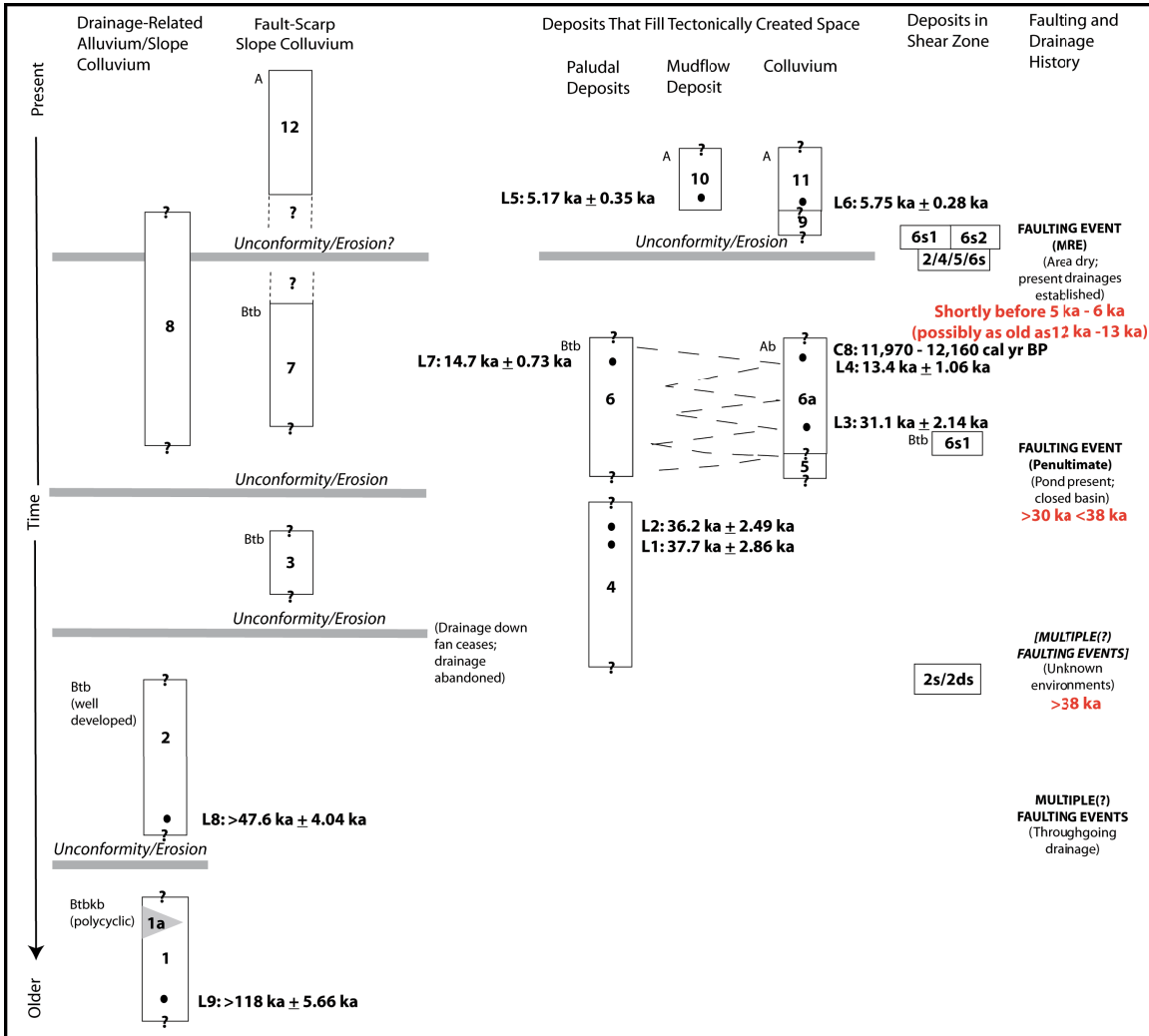


**Figure 20.** Stratigraphic units, ages, and tectonic events interpreted from the trench excavated near the north end of the Main Canyon fault.

The geomorphic expression of the Main Canyon fault is consistent with the faulting history interpreted from the trench exposure. Although late Quaternary tectonic scarps have been recognized only at the north end of the fault, between Main Canyon and the Weber River valley, facets or bedrock scarps, saddles, and lineaments are present nearly continuously to Taylor Hollow, a distance of at least 20 km. The fault cuts across topography, and its geomorphic expression varies depending upon whether the offsets

face upslope or downslope. The geomorphic expression of the southern about 6 km of the Main Canyon fault (south of Taylor Hollow) is more discontinuous than it is to the north, but is still present. Thus, the total length of late Quaternary rupture could be as long as 26 km. The lack of an escarpment or a late Cenozoic basin along the fault suggests that the fault did not experience surface ruptures during the entire Cenozoic, but has only been recently active.

The geomorphic expression of the East Canyon fault is quite different than that of the Main Canyon fault. The East Canyon fault has produced an eroded escarpment in resistant rocks at its north end, and facets/bedrock scarps along about 26 km of the fault. No obvious scarps on late Quaternary or Quaternary deposits have been observed associated with the East Canyon fault, in contrast to the Main Canyon fault. This expression, along with the pattern of Tertiary rocks preserved in East Canyon valley, suggests that displacements occurred earlier on the East Canyon fault than on the Main Canyon fault, beginning some time before the Norwood Tuff was deposited during the Oligocene and continuing for some time thereafter. The lack of evidence for late Quaternary or Quaternary activity associated with the East Canyon fault suggests that such activity has not occurred or has occurred at only a very low rate.

## **ACKNOWLEDGMENTS**

We appreciate the cooperation of Ron Taylor of Henefer, Utah, who graciously allowed us to excavate a trench on his property. Without his consent, this study could not have been done.

Mike Talbot and Cory Baker from BOR's Provo Area Office, Provo, Utah, contributed in many ways to this study. Mike provided much-needed logistical support, and was always ready to help even when our requests were made at odd hours. Cory excavated and re-excavated the trench. He designed and built a covering for the trench that was indispensable in bad weather and allowed us to complete the trench log.

Matt Jones (BOR Seismotectonic and Geophysics Group) generated hillshades for the East Canyon valley study area by obtaining images from the U.S. Geological Survey (USGS) National Aerial Photography Program (NAPP) along with camera calibration files. He then obtained ground control by finding features visible on the aerial photographs, going to the area, and recording GPS coordinates of the control locations. With this information, he was then able to run an aerotriangulation solution in a photogrammetry system and generate a grid across the study region. The NAPP photographs provided a standardized set of cloud-free aerial photographs. The photographs for the East Canyon area were acquired from a flight at an altitude of 20,000 feet in September and October 1997.

Because of the importance of accurate chronological dating to the results of our study, we are indebted to Shannon Mahan (Luminescence Dating Laboratory, USGS, Denver, Colorado) for providing luminescence ages for nine samples from the trench. Kathryn

Puseman (Paleo Research Institute, Golden, Colorado) processed bulk sediment samples from the trench, identified potentially datable charcoal from the samples, and provided an AMS date for one charcoal sample. In addition, Paleo Research Institute performed the initial identification of the asphaltum spheres collected from the trench using Fourier Transform infrared spectrometry.

B.M. Jarvie and D.M. Jarvie (Humble Geochemical Services Division, Humble Instruments and Services, Inc., Humble, Texas) conducted geochemical analyses on an asphaltum sample from the trench.

We appreciate the helpful comments made by Jim McCalpin (GEO-HAZ, Consulting, Inc., Crestone, Colorado) during a field review of the trench. Mike Machette (USGS, Denver) and Gary Christenson, Mike Hylland, Greg McDonald, and Chris DuRoss (all from the Utah Geological Survey, Salt Lake City) also examined the trench and participated in discussions that helped us refine our interpretations of the trench exposure and faulting history.

This report greatly benefited from a thorough and thoughtful review by Susan Olig (URS Corporation, Oakland, California), and William Lund, Mike Hylland, and Steve Bowman (UGS).

## REFERENCES

- Bryant, B., 1990, Geologic map of the Salt Lake City 30' by 60' quadrangle, north-central Utah, and Uinta County, Wyoming: U.S. Geological Survey Miscellaneous Investigations Series Map I-1944, 2 sheets, scale 1:100,000.
- Coogan, J.C., 2002, Progress report geologic map of the Devils Slide quadrangle, Morgan and Summit Counties, Utah [unpublished draft]: Utah Geological Survey, scale 1:24,000.
- Coogan, J.C., and King, J.K., 2001, Progress report—Geologic map of the Ogden 30' x 60' quadrangle, Utah and Wyoming (Year 3 of 3): Utah Geological Survey Open-file Report 380, scale 1:100,000.
- Nelson, A.R., and VanArsdale, R.B., 1986, Recurrent late Quaternary movement on the Strawberry normal fault, Basin and Range – Colorado Plateau Transition Zone, Utah: *Neotectonics*, v. 1, p. 7-37.
- Sullivan, J.T., Nelson, A.R., LaForge, R.C., Wood, C.K., and Hansen, R.A., 1988, Central Utah seismotectonic study for USBR dams in the Wasatch Mountains: Denver, Colorado, Bureau of Reclamation Seismotectonic Report 88-5, 269 p.
- U.S. Geological Survey, 2010, Quaternary fault and fold database of the United States: Online, <<http://earthquake.usgs.gov/regional/qfaults/>>, accessed October 25, 2010.

**Appendix A.**  
**Topographic Profiles Across the Main Canyon Fault**  
**in the Vicinity of the Trench**

## Methods and Discussion

Twelve topographic profiles were measured in the vicinity of the trench across the Main Canyon fault (*Figure 1*). Seven of the profiles are along ridges; five are along intervening drainages. The profiles were measured on 1:24,000-scale topographic maps with 40-foot contour intervals. Points were measured along the topographic lines at each contour, at each bend in the profile, and at the fault.

The ridge profiles show the relationship between the fault and the low hills on the footwall (east side) of the fault (*Figure 2*). The hills are armored with quartzite cobbles and boulders and could be remnants of older alluvial fans as mapped by Coogan (2002) or a conglomerate within the Wasatch Formation. The hills have been uplifted along the Main Canyon fault. Incision has occurred in the uplifted area between the fault and the Henefer valley to the northeast. The ridge profiles also show the relationship between these hills on the footwall and younger alluvial-fan deposits on the hanging wall. The trench exposure shows that paludal deposits are preserved on the hanging wall adjacent to the fault. Marshes formed when surface rupture on the fault created a west-facing (upslope-facing) scarp that ponded drainage. The marshes slowly filled with fine-grained eolian and alluvial sediment between faulting events, and at least at times became dry enough that soils formed on the fine sediment. Lineaments that are visible on 1:40,000-scale aerial photographs south of the trench site may indicate the extent of the infilled marshes.

The drainage profiles were done to see if any change in gradient could be detected across the fault (*Figure 3*). Profile 6 and perhaps profiles 2 and 8 may show a change in stream gradient at the fault. Profile 8 has a slight inflection as it crosses the fault. Profile 4 does not have a gradient change at the fault. This profile is along a relatively large drainage that may regrade faster than the smaller drainages. Also, the 40-foot contour interval is likely too large to detect small changes in the gradients of the drainages.

In summary, possible changes in gradients of the smaller drainages, geomorphic features that may have a tectonic origin (e.g., scarps, saddles), and differences in incision on opposite sides of the fault are evident on the topographic profiles. Although drawn from the topographic quadrangles with a 40-foot contour interval, these profiles suggest that displacements on the Main Canyon fault have influenced topography in this area.

## Reference

Coogan, J.C., 2002, Progress report geologic map of the Devils Slide quadrangle, Morgan and Summit counties, Utah [unpublished draft]: Utah Geological Survey, map scale 1:24,000.

Appendix A. Topographic Profiles Near the Trench

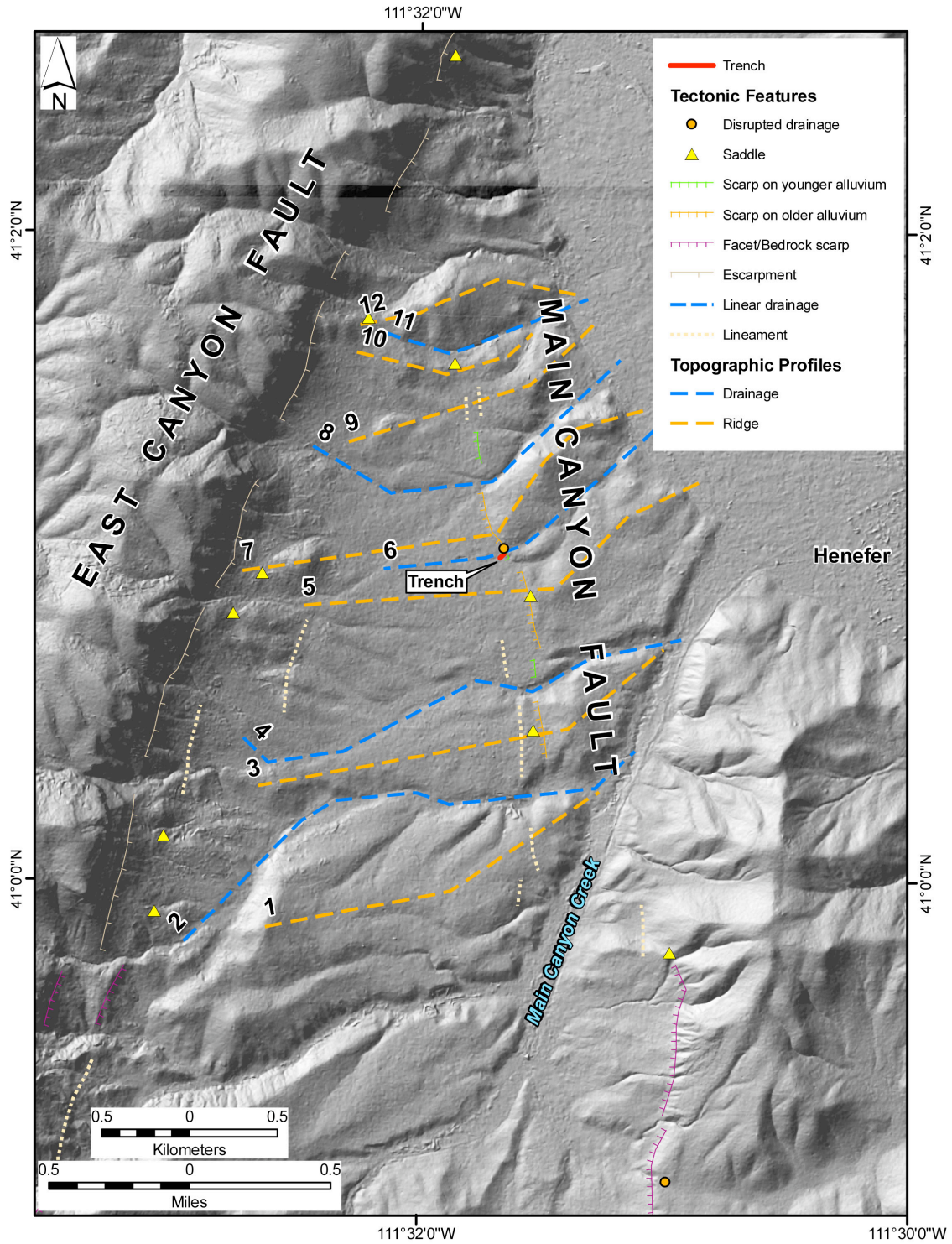
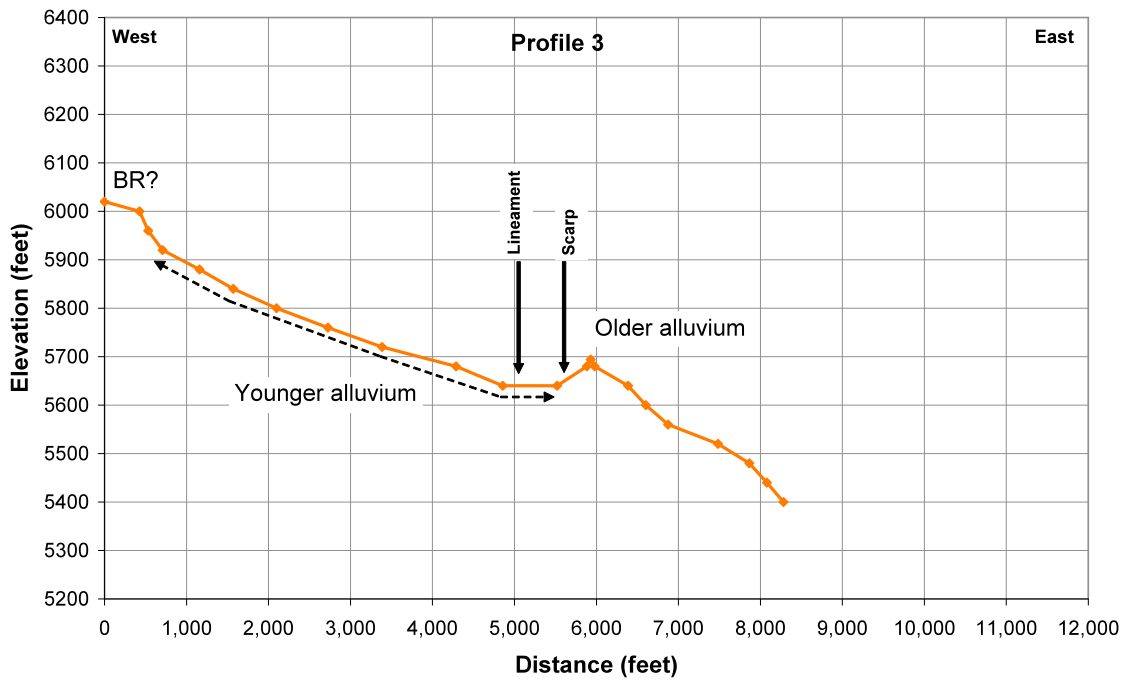
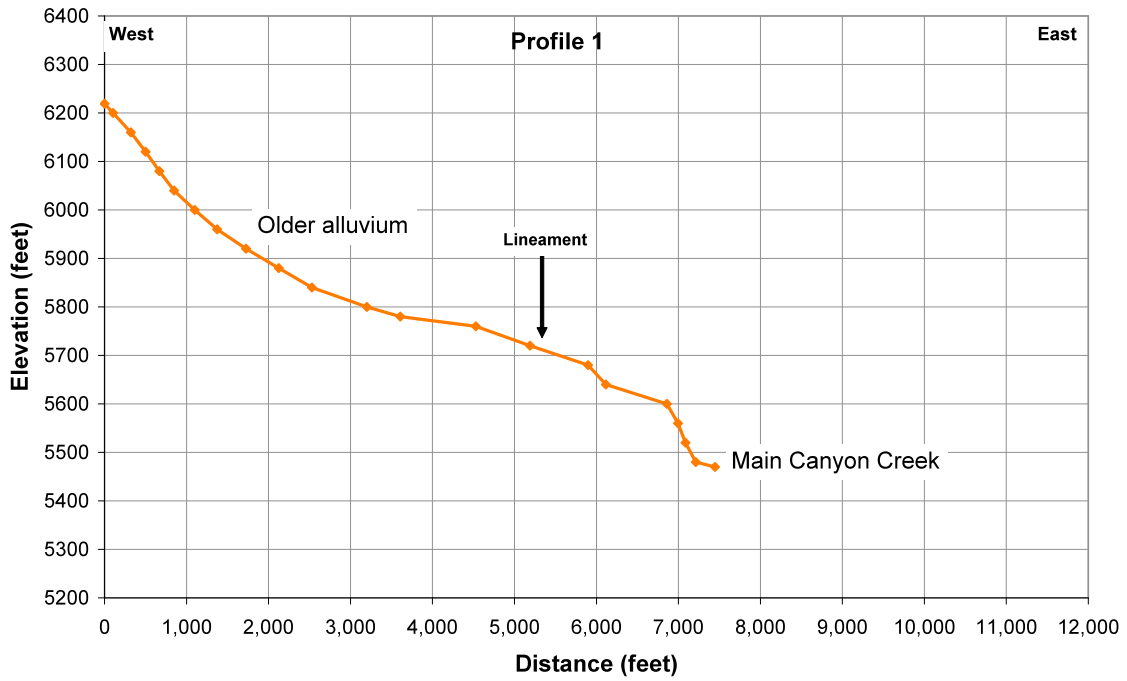
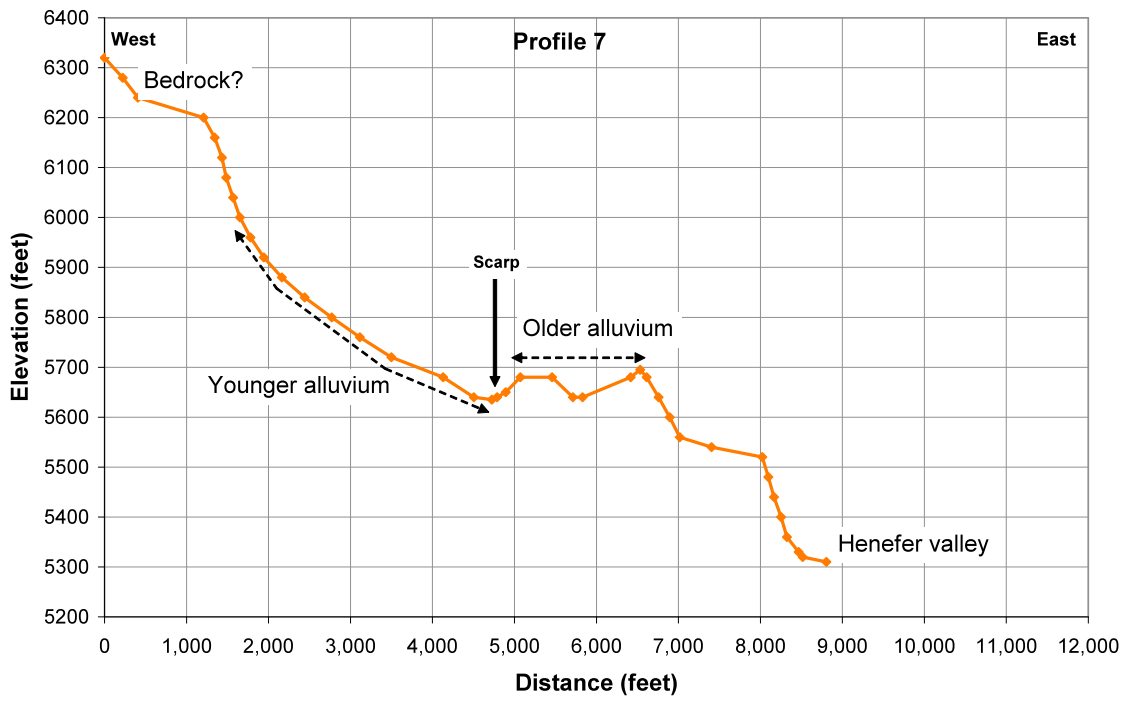
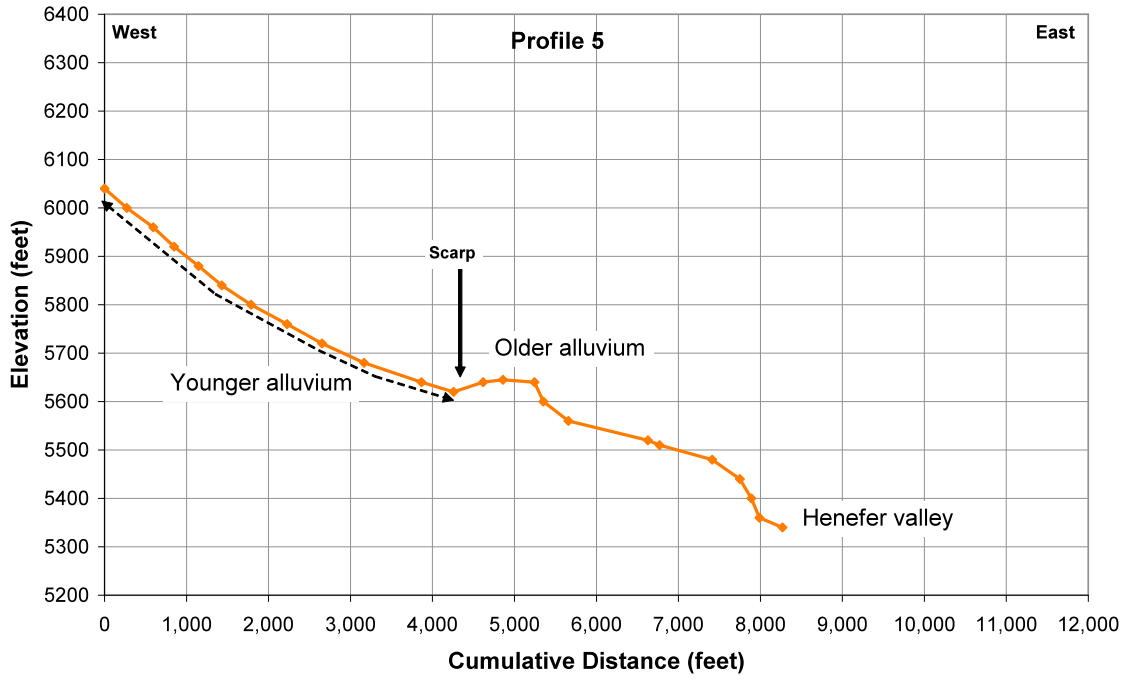


**Figure 1.** Location of topographic profiles across the northern portion of the Main Canyon fault. Background is a hillshade created from 1997 aerial photographs, ground control, and a generated grid.

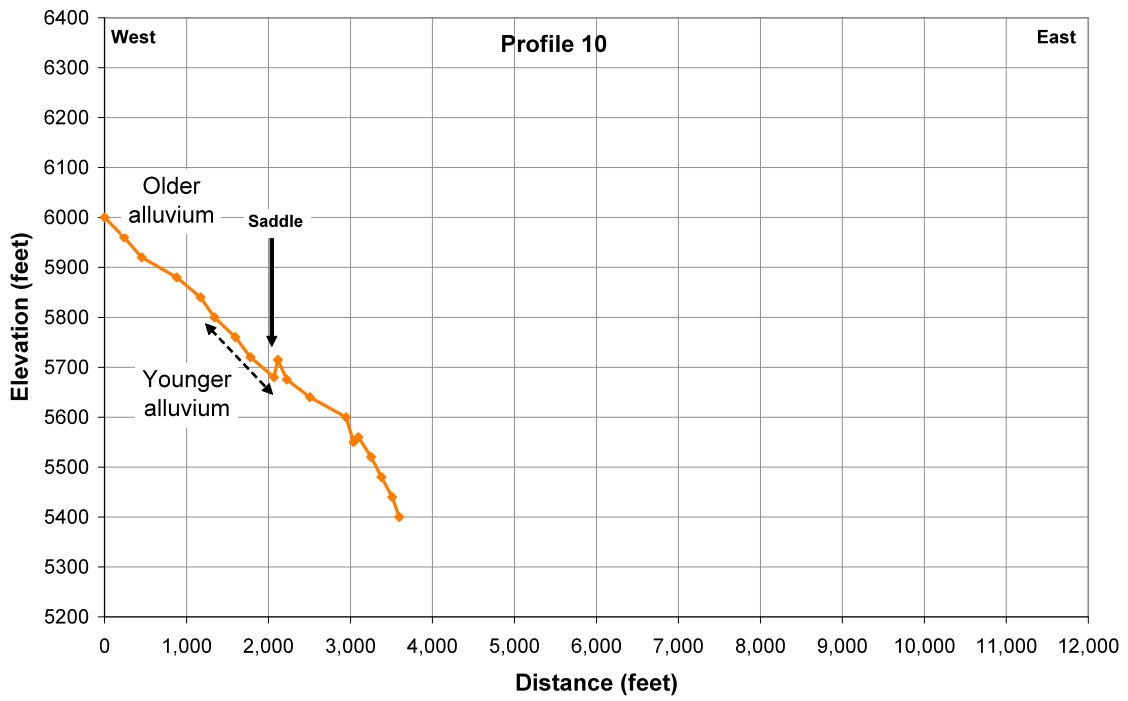
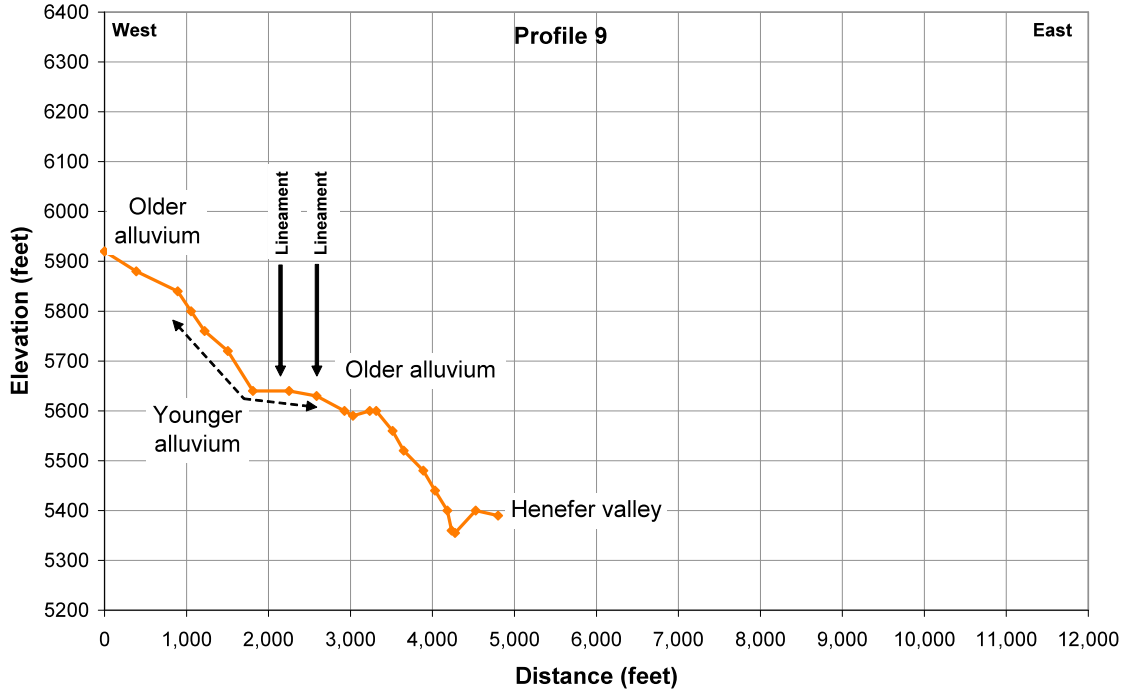
## Profiles Along Ridges



## Appendix A. Topographic Profiles Near the Trench



## Appendix A. Topographic Profiles Near the Trench



## Appendix A. Topographic Profiles Near the Trench

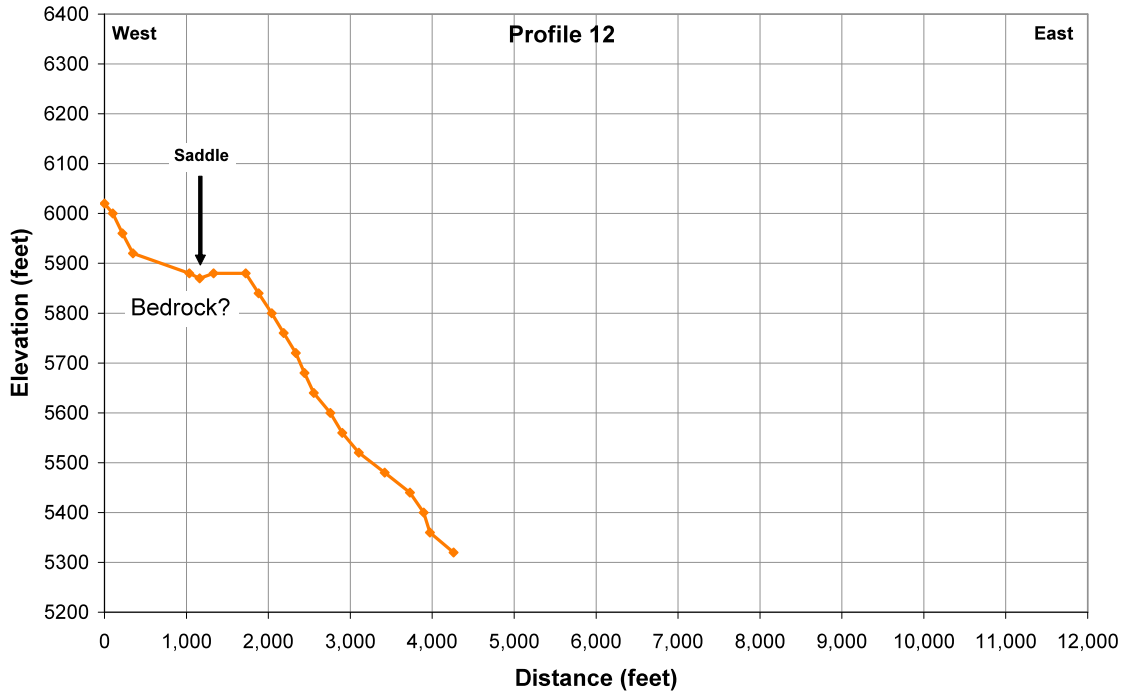
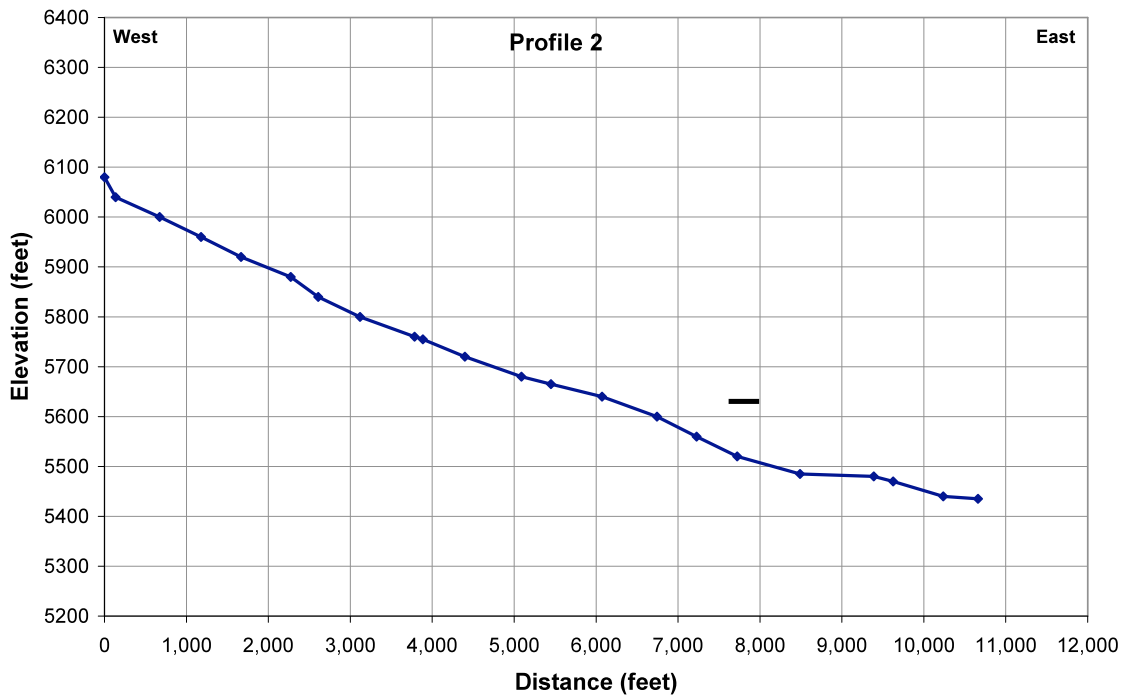
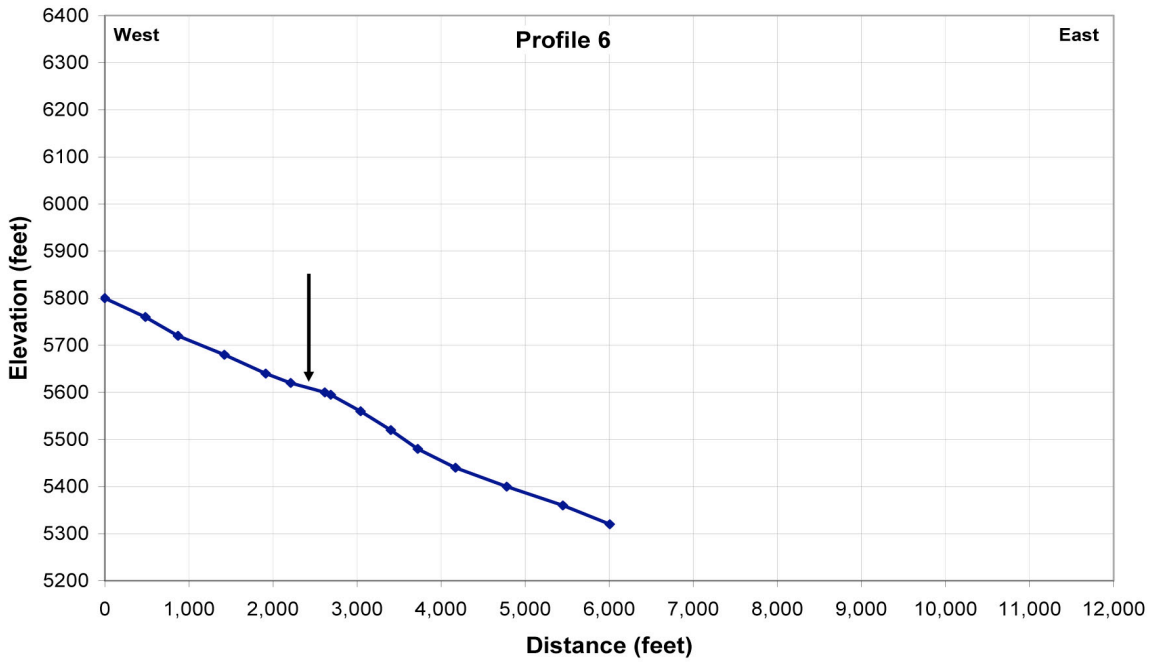
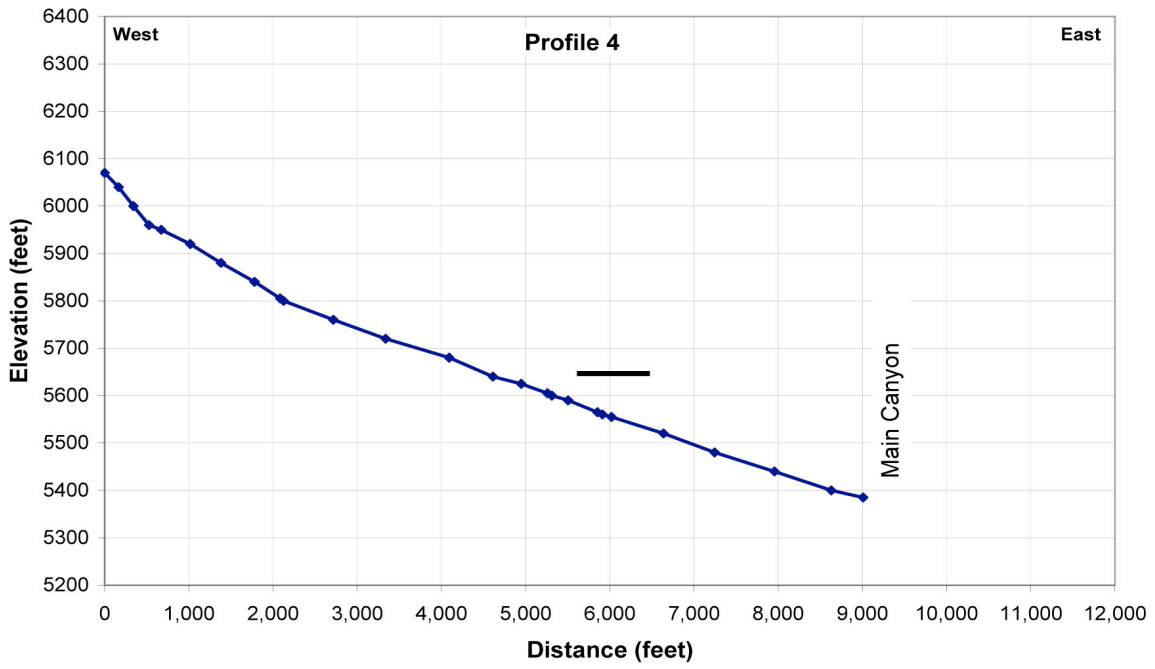


Figure 2. Topographic profiles along ridges across the northern portion of the Main Canyon fault. Arrows indicate the location of possible tectonic geomorphic features as indicated.

## Profiles Along Drainages



# Appendix A. Topographic Profiles Near the Trench



## Appendix A. Topographic Profiles Near the Trench

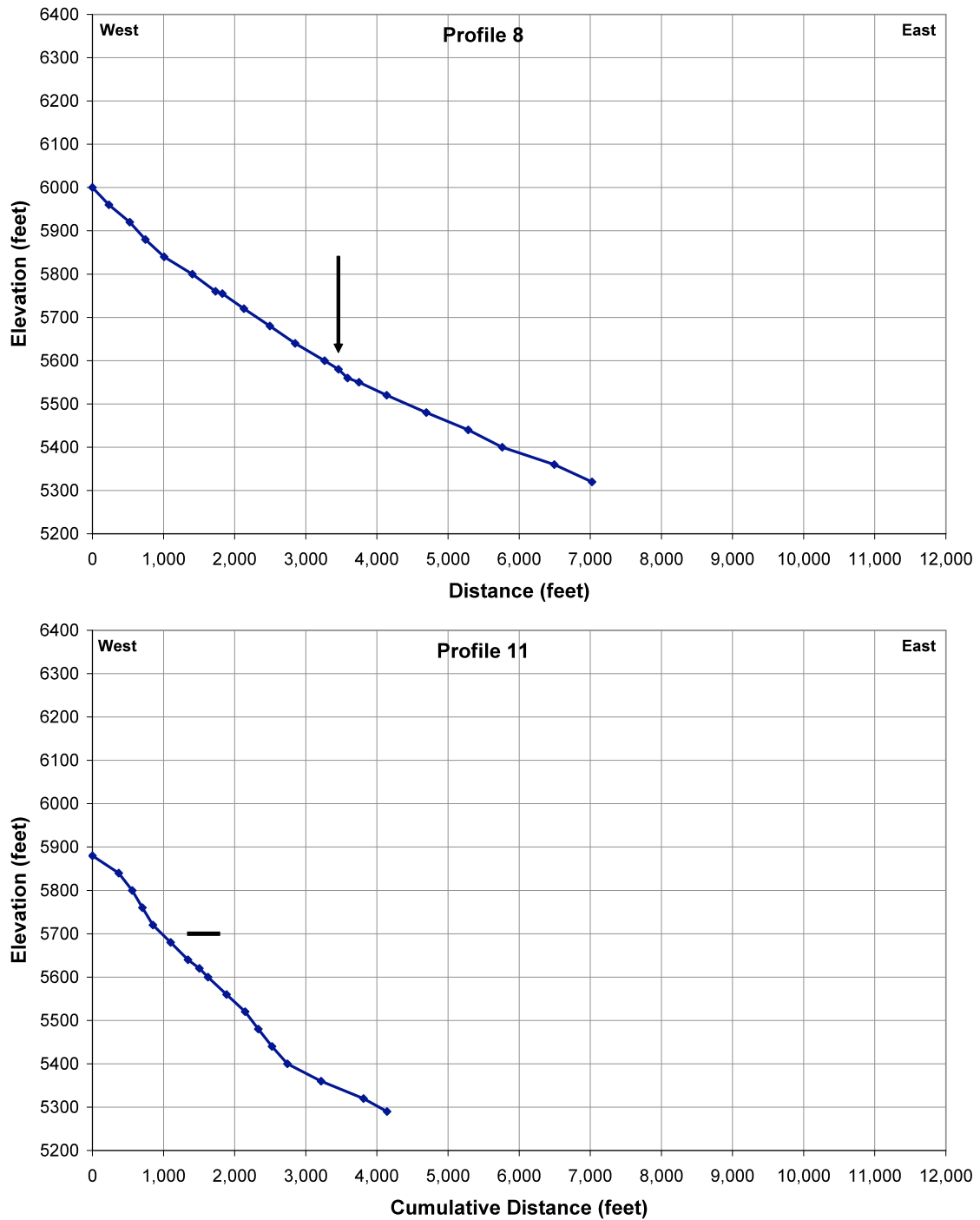


**Figure 3.** Topographic profiles along drainages across the northern portion of the Main Canyon fault. Arrows or black horizontal lines show the location of possible tectonic features on ridges adjacent to the drainages.

**Appendix B.**  
**Photograph Mosaics and Interpretative Logs of Trench**  
**Across the Main Canyon Fault, Utah**

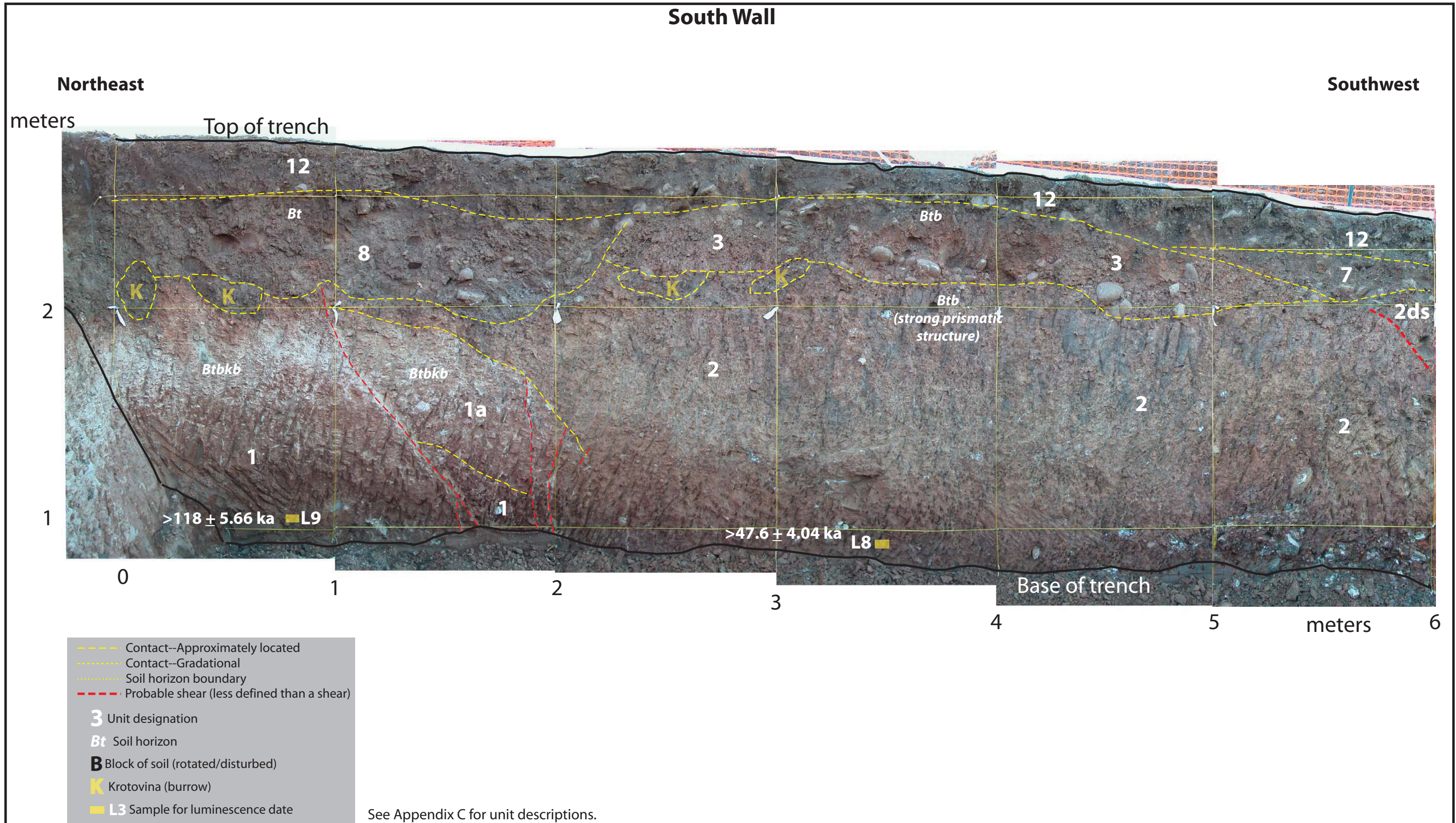


Figure 1. Log shown on photograph mosaic for the south wall between stations 0 and 6 meters of trench across the Main Canyon fault, Utah

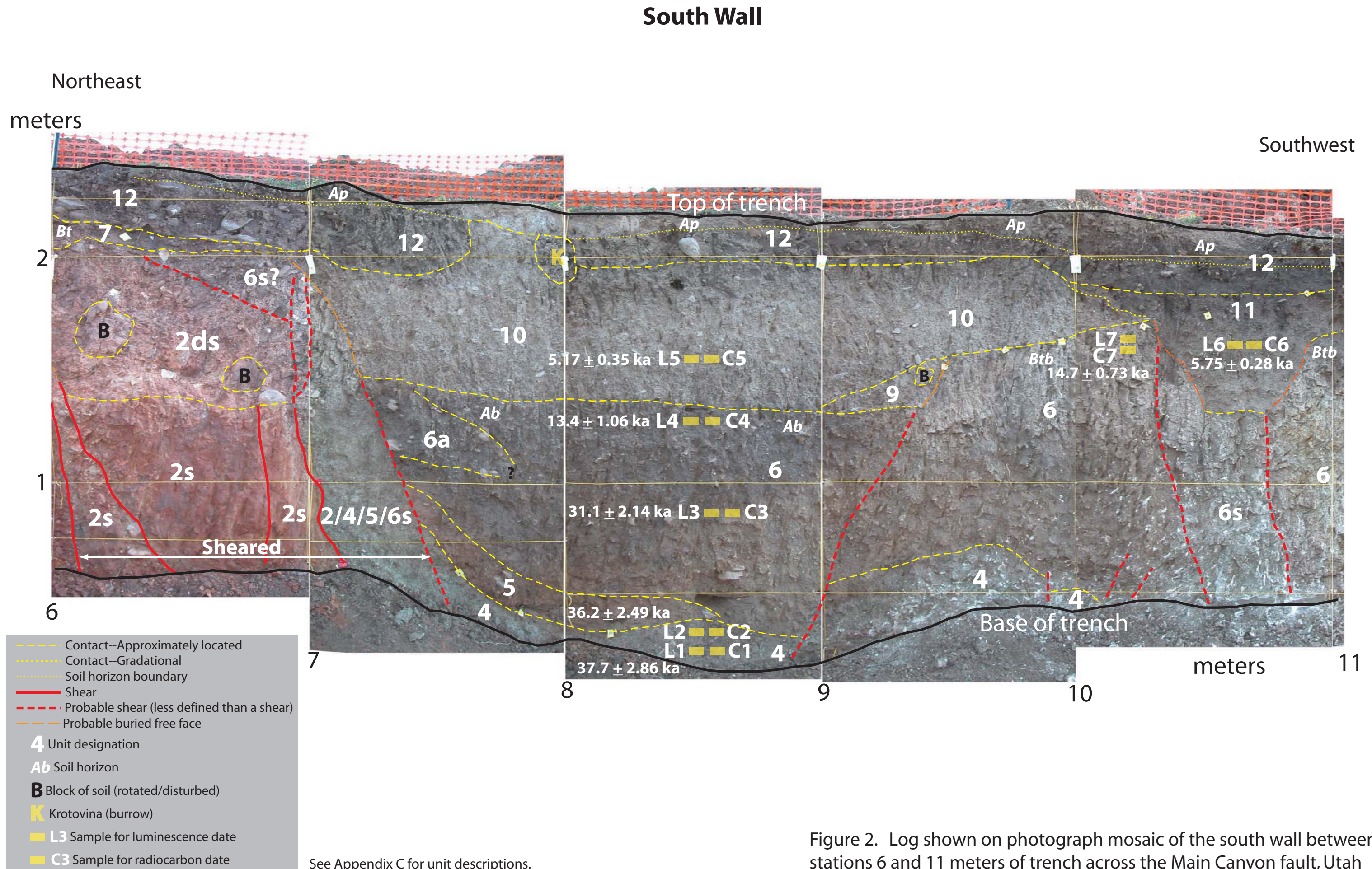
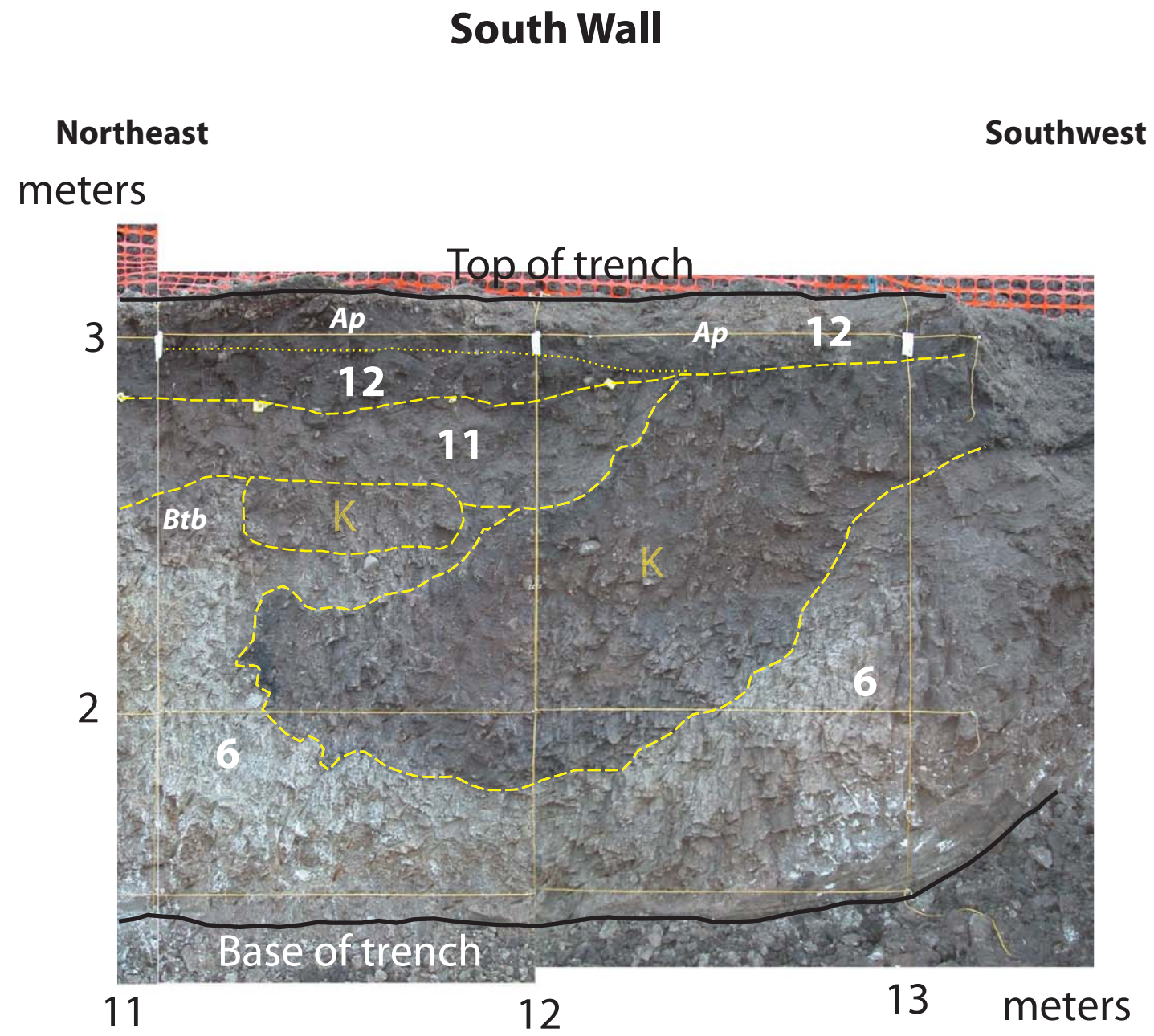


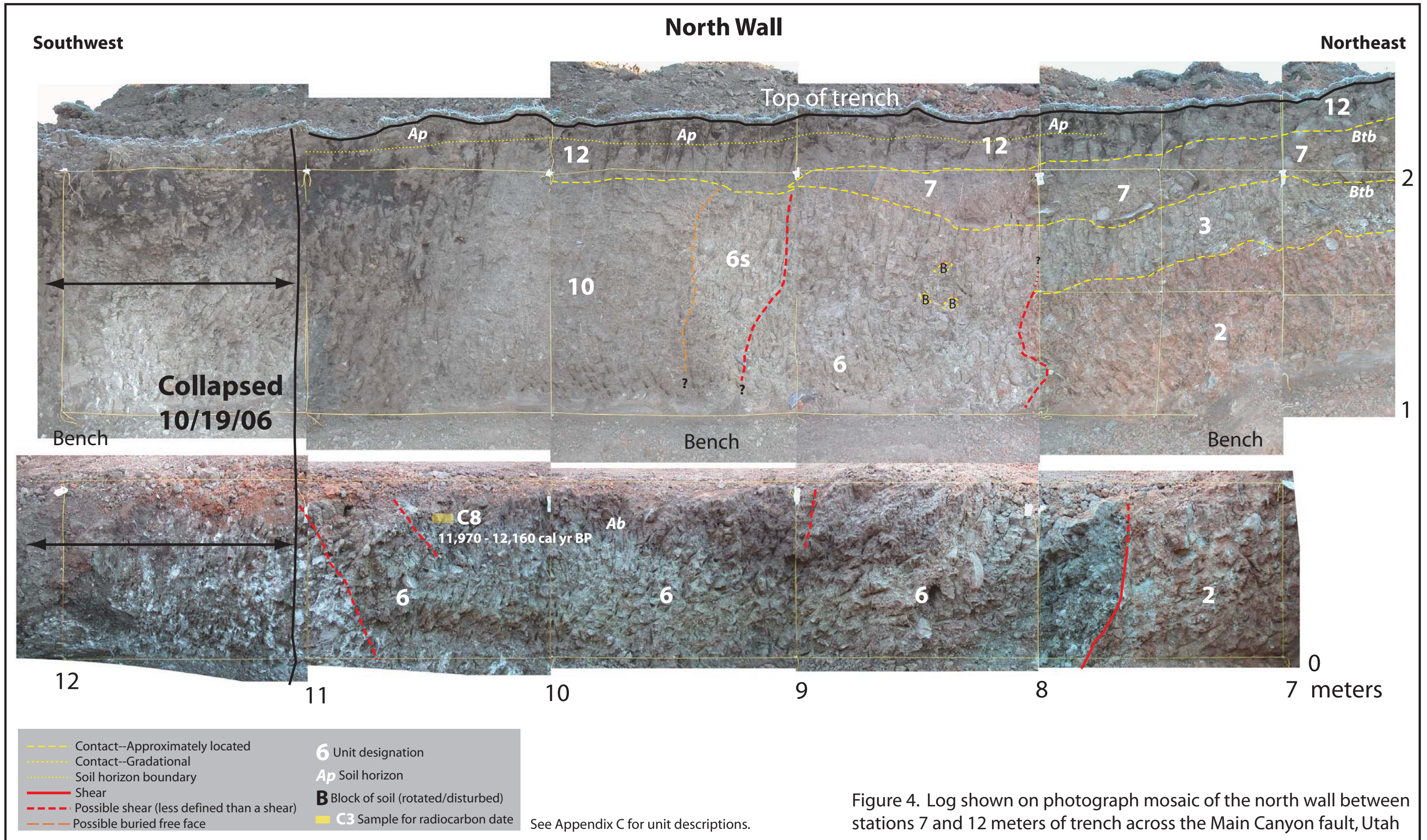
Figure 2. Log shown on photograph mosaic of the south wall between stations 6 and 11 meters of trench across the Main Canyon fault, Utah



- Contact--Approximately located
- Contact--Gradational
- Soil horizon boundary
- 6** Unit designation
- Ap* Soil horizon
- K** Krotovina (burrow)

See Appendix C for unit descriptions.

Figure 3. Log shown on photograph mosaic of south wall between stations 11 and 13 meters, trench across Main Canyon fault, Utah



**Appendix C.**  
**Complete Descriptions of Stratigraphic Units and Soils Exposed in**  
**Trench Across the Main Canyon Fault, Utah**

Unit	Subunit	Description	Soil Development
1		<p><b>ALLUVIUM/SLOPE COLLUVIUM:</b> Clayey, silty fine sand; &lt;1% gravel; angular to well-rounded; angular stones are often split rocks; largest stones have intermediate diameters of about 5 cm; most stones have intermediate diameters of 1 to 2 cm; stones primarily quartzite; some reddish sandstone; massive; no stratification; some stones have a subhorizontal orientation (possibly a weak indication of bedding); soil is markedly better developed than it is in unit 2; red (2.5YR 4/6); unit includes steep, near-vertical, carbonate-filled fractures between stations 1.5 and 2 m that extend downward from unit 1a into unit 1; probably not Wasatch formation, but alluvium/colluvium that is derived from Wasatch formation and older units; present and described between stations 0 and 1 m on south wall; slope of unit appears to be to the northwest; unit also present on north wall near station 0 m</p>	<p><b>Buried and faulted soil:</b>  <i>Btbk1b horizon:</i> Very red clayey sediment (probably a Bt horizon) with carbonate overprinted on it (polycyclic); maximum carbonate development is stage III (carbonate continuous, but matrix is not completely whitened); thickness of maximum carbonate development is about 35-50 cm; carbonate is light red (2.5YR 7/6); matrix is light red (2.5YR 6/6)  <i>Btbk2b horizon:</i> Carbonate in stringers; horizon about 15 cm thick  <i>Btb horizon:</i> Very red clayey horizon (Bt horizon?); horizon about 20 cm thick</p>
	1a	<p><b>POSSIBLE TECTONIC COLLUVIAL WEDGE DERIVED FROM UNIT 1:</b> Same as unit 1, except that it contains slightly more gravel (~5% of unit) in a wedge-shaped deposit that extends downslope from a carbonate-filled shear zone between stations 1 and 1.5 m within unit 1; at least two steep, carbonate-filled fractures extend upward through unit 1 at station 2 m; unit truncated near station 2 m at a depth of about 1.25 m; abrupt, irregular basal contact with unit 1; maximum thickness of unit is about 0.5 m near station 1.5 m; present and described between stations 1.5 and 2 m on south wall</p>	<p><b>Buried and faulted soil (weaker than soil in unit 1):</b>  <i>Btbkb horizon:</i> Clayey sediment (possibly a Bt horizon) with carbonate overprinted on it (polycyclic); maximum carbonate development is stage II (carbonate in 25-30% of unit as nodules and filaments; filaments are on ped faces and in fractures); carbonate is reddish yellow (5YR 7/6); matrix is yellowish red (5YR 5/6)  <i>Bkb horizon:</i> Carbonate in stringers along fractures in the hanging wall of the main shear between stations 1 and 1.5 m; matrix noneffervescent</p>

Unit	Subunit	Description	Soil Development
2		<p><b>SLOPE COLLUVIUM/ALLUVIUM:</b> Clayey, silty fine sand; &lt;1% gravel; angular to well-rounded; angular stones are often split rocks; largest stones have intermediate diameters of about 5 cm; most stones have intermediate diameters of 1 to 2 cm; stones primarily quartzite; some reddish sandstone; massive; no stratification; some stones have a subhorizontal orientation (possibly a weak indication of bedding); red (2.5YR 4/8); thickness of unit is &gt;1.3 m; basal contact not exposed; ~5% of unit has black nodules (manganese?) that are angular and about 1 mm in diameter; black nodules are concentrated in some areas, but are distributed throughout unit; present and described between stations 2 and 6 m on south wall; also present on north wall between stations 0 and 8 m</p>	<p><b>Buried soil:</b>  <i>Bt1b horizon:</i> Coarse, strong prismatic structure with dark clay films on ped faces and stones; mixed color is red (2.5YR 5/6); clay films are commonly reddish brown (2.5YR 4/3); darkest clay films are weak red (2.5YR 4/2); interior of peds are red (2.5YR 4/6); horizon is best developed in upper 40 to 50 cm of horizon  <i>Bt2b horizon:</i> Coarse, moderate to weak prismatic structure with some dark clay films; horizon 15 to 30 cm thick</p>
	<b>Gravel lenses</b>	<p><b>SLOPE COLLUVIUM WITHIN UNIT 2:</b> Unit 2 includes gravel lenses that make up about 2% of entire unit; lenses contain about 50% gravel; angular to well-rounded, mostly subrounded; smaller stones tend to be more angular; angular stones are often split rocks; largest stones have intermediate diameters of about 20 cm; most stones have intermediate diameters between 2 and 5 cm; stones primarily quartzite; a couple of medium-grained crystalline rocks are grussified; lenses up to 25 to 30 cm thick; present and described between stations 2 and 6 m on south wall; prominent lens is present near base of trench near station 6 m</p>	
	<b>2s</b>	<p><b>FRACTURED AND SHEARED UNIT 2:</b> Same as unit 2, except for vertical mottling related to fractures and shears, which are most common near station 7 m; weak to moderate vertical fabric; mottled red (2.5YR 4/8) and reddish yellow (7.5YR 7/8); reddish yellow is &lt;10% of unit; ~5% of unit has black nodules (manganese?) that are angular and about 1 mm in diameter; present and described between stations 6 and 7 m on south wall below a depth of about 0.75 m</p>	<p><b>Buried and faulted soil:</b>  <i>Btb horizon:</i> Clay films on ped faces and stones in upper about 50 cm of unit</p>

Unit	Subunit	Description	Soil Development
	2ds	<p><b>DISTURBED/SHEARED BLOCK OF UNIT 2:</b> Silty, sandy clay; gravel content similar to that described for unit 2, except for a gravelly lens, which has about 5% gravel, along the base of the unit; present between stations 6 and 7 m, between a shear zone/free face near station 6 m and a shear zone near station 7 m; red (2.5YR 4/6-4/8 (slightly moist)); basal contact gradational with unit 1; unit appears to be an area of mostly in-place unit 2 that has been broken, primarily along soil peds; peds are not continuous; reddish brown (5YR 4/3) clay films; contains areas of peds that may be disturbed blocks; some blocks have large prismatic peds (from unit 2?); some blocks have smaller blocky peds (from unit 3?); gravel and other sediment has filled in the spaces between the fractured peds; prismatic peds have been rotated between 10 to 20 degrees to the west from the general slope of the ground surface; sediment has probably not been totally re-deposited; present between stations 6 and 7 m on south wall</p>	
3		<p><b>SLOPE COLLUVIUM:</b> Sandy, silty clay; variable gravel composition; 1 to 2% gravel between stations 2 and 3 m; 30% gravel along base of unit and about 10% gravel in rest of unit between stations 3 and 5.5 m; gravel angular to well-rounded, mostly subrounded to well-rounded; angular (split) stones common; largest stones have intermediate diameters of about 15 cm; most stones have intermediate diameters of 2 to 10 cm; stones primarily quartzite; stones parallel to basal contact between stations 2 and 5.5 m (slight slope to the west); abrupt basal contact erosional on unit 2; unit truncated along an east-sloping contact by unit 8 (debris flow deposit in channel) near station 2 m, and along a west-sloping contact by unit 7 (slope colluvium) between stations 5 and 5.5 m; present and described between stations 2 and 5.5 m on south wall</p>	<p><b>Buried and present? soil:</b>  <i>Btb horizon:</i> Strong, coarse blocky structure to weak, fine prismatic structure in upper part of unit where gravel content is lower; strong, coarse to medium blocky structure in areas where gravel content is higher; thick, prominent dark clay films on peds and stones; reddish brown (2.5YR 4/4) for horizon; clay films weak red to reddish brown (2.5YR 4/2-4/3); horizon is present through entire thickness of unit; upper boundary of horizon parallels ground surface</p>

Unit	Subunit	Description	Soil Development
<p><b>3</b> <b>North wall</b></p>		<p><b>SLOPE COLLUVIUM:</b> Clayey silt between stations 7 and 8 m grading into sandy, clayey silt near station 6.25 m; laterally variable gravel content that is highest near station 6.25 m and decreases to station 8 m; 15% gravel between station 6.25 and 7 m; angular to well-rounded, mostly subrounded and rounded; angular stones are often split rocks; largest stones have intermediate diameters of about 15 cm; most stones have intermediate diameters of 3 to 5 cm; stones primarily quartzite; 1% gravel between stations 7 and 8 m; mostly angular to subangular; most stones have intermediate diameters of 1 to 3 cm; ~5% of unit between stations 7 and 8 m is hard, dark, rounded clasts <math>\leq 5</math> mm diameters; clasts could be shale, coal, or carbon; well sorted; no stratification or bedding; abrupt, irregular basal contact eroded into unit 2; present and described between stations 7.5 and 8 m on north wall; probably correlative with unit 3 on the south wall</p>	<p><b>Buried soil:</b> <i>Btb horizon:</i> Weak, fine to medium blocky structure where gravel content is higher; strong, medium prismatic structure and distinct, moderately thick brown (7.5YR 5/4) clay films on peds in areas where gravel content is lower; pale brown (10YR 6/3) for interior portions of peds; also in 1% of horizon has prominent, thick yellowish red (5YR 5/8) clay films on prismatic peds between stations 8 and 8.5 m</p>
<p><b>4</b></p>		<p><b>PALUDAL DEPOSITS (MOTTLED WITH CARBONATE):</b> Clayey silt, 1% gravel; subangular to subrounded stones; largest stones have intermediate diameters of about 5 cm; ~3% of unit is hard, dark, rounded clasts <math>\leq 5</math> mm diameters; clasts could be shale, coal, or carbon; well sorted; no stratification or bedding; mottled: brown (7.5YR 5/4 and 10YR 5/3); includes carbonate between depths of 95 and 120 cm to the base unit and trench exposure with maximum development of stage II+ (nodules up to 1 to 2 cm diameters compose about 50% of unit; matrix whitened); nodules are irregular shaped; in places, nodules are elongate with lengths of up to 5 cm; elongated nodules oriented horizontal or subhorizontal; brown (10YR 5/3); carbonate may be related to pond/marsh conditions, but could be a buried soil; basal contact is not exposed; unit extends to the base of the trench exposure; unit truncated by possible shear zone near station 10.5</p>	

Unit	Subunit	Description	Soil Development
		m; present and described between stations 7.5 and 10 m on south wall	
5		<b>TECTONIC COLLUVIAL WEDGE:</b> Silty, sandy clay; with about 5% gravel between stations 7.3 and 8.5 m; angular to well-rounded; stones have intermediate diameters ranging between about 3 and 10 cm; larger stones tend to be in the lower part of the unit; stones have a slight downslope orientation; unit is red (7.5YR 5/6)	
6		<b>PALUDAL DEPOSITS:</b> Clayey silt or sandy clayey silt; 1% gravel; angular to rounded; angular to well-rounded; most stones have intermediate diameters of 1 to 2 cm; well sorted; massive; not stratified; stones randomly oriented; brown (7.5YR 5/4 (dry) and 7.5YR 4/4 (moist)); between stations 9 and 10 m, unit is mottled brown and pale brown; contains common, hard, dark, rounded clasts ≤5 mm diameters; clasts are asphaltum (Appendix G); clear and smooth to slightly wavy basal contact with units 4 and 5; unit is truncated along a steep, well-defined shear with unit 2/4/5/6s between stations 7.25 and 7.5 m; unit also is truncated by a steep, east-sloping poorly defined shear between stations 9 and 9.5 m; description is based on the unit primarily between stations 7.25 and 9.25 m and between stations 9.5 to 10.25 m on south wall	<b>Buried soil between stations 9.5 and 10.5 m:</b> <b>Btb horizon:</b> Strong, very coarse prismatic structure; thin clay films on peds and stones; matrix brown (7.5YR 5/3); clay film brown (7.5YR 4/3) near top of horizon; pale brown (10YR 6/3) for middle of horizon; brown (10YR 5/3) for lower part of horizon; horizon about 55 cm thick <b>Bkb horizon:</b> Maximum carbonate has stage II development (nodules up to 1 cm diameters compose about 5% of unit); brown (10YR 4/3-5/3 (slightly moist)); horizon about 40 cm thick <b>Buried soil between stations 7.5 and 9.5 m:</b> <b>Ab horizon:</b> Clayey silt; silt content seems to be highest in the upper 30 cm of horizon between stations 7 and 8 m; highest silt content is in the darkest part of the horizon; silt also decreases in a downslope direction from a maximum content between stations 7 and 8 m; brown (7.5YR 4/3); dark brown (7.5YR 3/2) for the darkest areas

Unit	Subunit	Description	Soil Development
<b>6 North wall</b>		<b>PALUDAL DEPOSITS:</b> Clayey silt; 1 to 3% gravel; angular to rounded; <1% unit near station 8.5 m includes angular red (7.5YR 5/6) pieces between 5 and 10 cm diameter that appear to be pieces of unit 1; ~5% of unit is hard, dark, rounded clasts $\leq 5$ mm diameters; clasts are asphaltum (Appendix G); brown to yellowish brown (7.5YR 5/3-5/4 to 10YR 5/3-5/4); well sorted; no stratification or bedding; basal contact is not exposed; unit extends to the base of the trench exposure; unit contains steep, poorly defined shears between stations 7.5 and 9 m; present and described between stations 8 and 9 m on north wall	<b>Buried soil:</b> <b>Btb horizon:</b> Strong, coarse prismatic structure; distinct, moderately thick clay films on peds; horizon 50 to 55 cm thick; strongest horizon development in upper 30 cm of unit
	<b>6a</b>	<b>TECTONIC COLLUVIAL WEDGE:</b> Similar to unit 6, except it contains about 10% gravel; stones have intermediate diameters ranging between 4 and 8 cm; stones oriented approximately parallel to unit contacts; unit interfingers with unit 6 near station 7.8 m; gradual decrease in gravel content	
	<b>6s</b>	<b>FRACTURED AND SHEARED PALUDAL DEPOSITS DERIVED FROM UNIT 6:</b> Similar to unit 6, except that elongated carbonate nodules are oriented vertically and extend throughout unit; basal contact not exposed; unit extends to base of trench; unit truncated laterally by steep, poorly defined shears between stations 10 and 11 m within unit 6; present and described between stations 10 and 11 m on south wall	
	<b>6s North wall</b>	<b>FRACTURED AND SHEARED PALUDAL DEPOSITS DERIVED FROM UNIT 6:</b> Fine sandy, clayey silt; 3% gravel that is present mostly along a steep, poorly defined shear at station 9.5 m; gravel angular or rounded; stones have intermediate diameters of up to about 10 cm; most angular stones are split rocks; between stations 7 and 8, ~5% of unit includes hard, dark, rounded clasts $\leq 5$ mm diameters; clasts are asphaltum (Appendix G); well sorted; massive; no stratification or bedding; brown (7.5YR 5/4); unit tapers with depth; appears to join a shear zone	<b>Buried soil:</b> <b>Btb horizon:</b> Moderate to strong, medium prismatic structure

Unit	Subunit	Description	Soil Development
		that is visible below the bench at station 9.5 m; unit truncated laterally by a steep, poorly defined shear at stations 9 m with unit 6, and by a steep probably free face at station 9.5 m with unit 10; present and described between stations 9 and 10 m on north wall	
	2/4/5/6s	<b>SHEARED CLAY DERIVED FROM UNITS 2, 4, 5, AND 6:</b> Clay; no gravel, except in shear zone near station 7 m; rounded, black, soft?, clasts $\leq 5$ mm diameters present below soil horizon; percent of clasts increases lower in exposure; $\leq 5\%$ just below soil horizon to 10 to 15% with depth; contact with sediment from unit 2s near station 7 m is a shear zone in which the unit is mixed with unit 2s from about 10 cm below the base of the Bt horizon to the base of the trench exposure; mixed zone is about 10 cm wide, includes clasts from unit 2, and overlies a well-defined shear; shear texture is not visible within the Bt horizon; shearing and disturbance of the clay indicated by the way in which the clay breaks out from trench wall; pale brown (10YR 6/3); carbonate nodules present at a depth of about 1.3 m and extend to the base of the trench; nodules compose 10 to 15% of unit in this area; basal contact not exposed; unit extends to the base of the trench; unit truncated by steep shear along units 2s and 2ds at station 7 m; unit truncated by a steep shear (below a depth of 0.75 m) with unit 6 and a steep erosional contact (above 0.75 m) with unit 10; present and described between stations 7 and 7.5 m on south wall	<b>Buried soil:</b> <b>Bt1b horizon:</b> Strong, coarse prismatic structure; prominent, moderately thick reddish brown (5YR 4/3) clay films on peds; matrix light reddish brown to reddish brown (5YR 6/3 ranging to 5YR 5/4); horizon 55 cm thick <b>Bt2b horizon:</b> Moderate, medium blocky structure; light brown (7.5YR 6/3); horizon about 10 cm thick; soil extends to a depth of about 0.75 m below the present ground surface
7		<b>SLOPE COLLUVIUM:</b> Clayey, sandy silt; 30% gravel along base of unit; 15% gravel above; angular, subrounded, and rounded; most stones are angular (split); basal stone line 2 to 5 cm thick; unit about 20 cm thick; reddish brown (5YR 4/4); abrupt, slightly wavy basal contact; contact erosional on units 2 and 3; unit truncated by a west-sloping contact eroded into unit 2 and unit 2ds between stations 5 and 6.5 m; present and described between stations 5 and 6.5 m on south wall	<b>Buried and present(?) soil:</b> <b>Bt horizon:</b> Strong to moderate, fine blocky structure; prominent, moderately thick clay films on stones; prominent, thin clay films on blocky peds; horizon is present through entire thickness of unit

Unit	Subunit	Description	Soil Development
7 North wall		<b>SLOPE COLLUVIUM:</b> Sandy, silty clay; unit fines downslope; 5 to 25% gravel; angular to subrounded; angular stones, which are split rocks, dominate; a stone line at the base of the unit between stations 7 and 8 m is composed of angular (broken) stones; largest stones have intermediate diameters of about 15 to 20 cm; larger stones predominate upslope near stations 6.25 to 7 m; stones primarily quartzite; poorly sorted; color variable; brown (7.5YR 5/4-4/4) near station 6.25; brown (7.5YR 5/4) between stations 8 and 9 m; maximum thickness of unit is about 25 cm; thickness varies between 18 and 28 cm; unit truncated near station 9 m by erosional contact with unit 12; abrupt, slightly wavy basal contact, in part defined by the stone line; unit conformable with underlying units; present and described between stations 6.25 and 9 m on north wall	<b>Buried soil:</b> <b>Btb horizon:</b> Strong, fine to medium blocky structure; prominent, moderate thick clay films on stones; faint, thin clay films on peds
8		<b>MUDFLOW DEPOSIT FILLING CHANNEL:</b> Clayey, silty fine sand; 3 to 5% gravel; angular to well-rounded; angular stones are often split rocks; largest stones have intermediate diameters of about 20 cm; stones have a weak subhorizontal orientation; stones are approximately parallel to the channel margin near station 2 m; poorly sorted; massive; no stratification or bedding; reddish brown (5YR 4/3); abrupt, irregular basal contact eroded into unit 1; unit truncates unit 2 near station 2 m as an erosional contact at the channel margin; present and described between stations 0 and 2.5 m on south wall	<b>Bt horizon:</b> Strong, medium blocky structure; prominent, moderately thick, dark reddish brown (5YR 3/3) clay films on peds and stones; organic coatings on peds; occasional very weak effervescence around fine roots
9		<b>POSSIBLE TECTONIC COLLUVIUM:</b> Clayey silt between stations 9.0 and 9.5 m; includes rotated pieces of soil	
10		<b>MUDFLOW DEPOSIT FILLING GRABEN:</b> Clayey silt; 3-5% gravel; angular to well-rounded; angular and subangular stones common; angular stones are often split rocks; largest stones have intermediate diameters of about 3 cm; most stones	<b>A horizon</b> No visible pedogenic carbonate; no effervescence to base of unit

Unit	Subunit	Description	Soil Development
		<p>have intermediate diameters of 1 to 2 cm; matrix supported; unsorted; massive; no stratification or bedding; brown (7.5YR 4/3-5/3); upper about 50 cm has common worm burrows; some burrows open; others filled with dark, organic-rich sediment; clear, smooth basal contact with unit 6; unit truncated by a steep erosional contact with unit 2/4/5/6s between stations 7 and 7.25 m; unit interfingers with unit 11 or pinches out near station 10.25 m; present and described between stations 7 and 10 on south wall; also present on north wall between stations 9.5 m and at least 11 m; source of debris flow was likely the slope north of the trench</p>	
11		<p><b>TECTONIC COLLUVIUM:</b> Clay; 1% gravel; subangular to subrounded; stones have intermediate diameters between 1 and 3 cm; lower 15 cm of unit between station 10.5 and 10.75 m contains very small (<math>\leq 1</math> mm) pieces of carbonate that appear to have been eroded from unit 6 (locally derived); upper 25 to 35 cm has 1 to 5% worm burrows; some burrows open; others filled with dark, organic-rich sediment; burrows more common in upper part of unit; unit has a maximum thickness of 20 to 50 cm; unit interfingers with unit 10 or pinches out near station 10 m, and is cut out by a large burrow(?) near station 12 m; similar unit is present near station 13 m; abrupt, irregular basal contact eroded into unit 6s; pinkish gray (7.5YR 6/2, slightly moist); present and described between stations 10 and 13 m on south wall</p>	<p><i>A horizon</i> No visible pedogenic carbonate; only effervescence is on the detrital carbonate; no other effervescence to base of unit</p>
12		<p><b>SLOPE COLLUVIUM:</b> Variable texture; clayey, fine sandy silt between stations 0 and 7 m; fine sandy silt (less clay) between stations 7 and 13 m; variable gravel content (highest between stations 0 and 7 m); 1 to 10% gravel between stations 0 and 7 m; subangular to rounded; angular stones are often split rocks; largest stones have intermediate diameters of about 10 to 15 cm; most stones have intermediate diameters of 2 to 5 cm; stone line intermittent along base of unit; 1 to 3% gravel between stations 7</p>	<p><i>A horizon</i> No visible pedogenic carbonate; no effervescence to base of unit</p>

Unit	Subunit	Description	Soil Development
		<p>and 13 m; gravel content decreases in downslope direction; rounding similar to that between stations 0 and 7 m; largest stones have intermediate diameters of about 5 to 10 cm (one stone this size is present about every 1 m); most stones have intermediate diameters of &lt;2 cm; large stones are not present downslope of station 10 m; unsorted, massive, and not stratified between stations 0 and 13 m; sharp wavy basal contact between station 0 and 13 m; between stations 0 and 7 m, stones oriented mostly parallel or subparallel to the ground surface and the basal contact of unit; unit eroded into underlying units (units 3 and 7) between stations 3 and 7 m; unit conformable with underlying units (units 10 and 11) between stations 7 and 13 m; upper 10 to 15 cm of unit has been plowed between stations 8 and 13 m; brown (7.5YR 5/3) between stations 0 and 2 m and brown (7.5YR 4/3) between stations 2 and 4 m; dark brown (7.5YR 3/3, slightly moist) between stations 9 and 10 m; brown (7.5YR 4/3) between stations 10 and 11 m</p>	

Descriptions are for south wall unless otherwise indicated. Colors are for dry samples, unless otherwise indicated. Soil nomenclature follows Birkeland, P.W., Machette, M.N., and Haller, K.M., 1991, Soils as a tool for applied Quaternary geology: Utah Geological and Mineral Survey Miscellaneous Publication 91-3, 63 p.

**Appendix D.**  
**Descriptions of Samples Collected From the Trench**  
**Across the Main Canyon Fault, Utah**

## Appendix D. Locations and Descriptions of Samples Collected From Trench

*Table 1. Locations of samples collected for luminescence analysis.*

Sample Number	Type of Sample	Trench Stratigraphic Unit	Station (m)	Approximate Depth (cm) below Ground Surface	Depth (cm)	Trench Wall	Notes
ECT-L1	Tube	4 (lower)	8.45-8.50	215	35-45 below lowest string	South	
ECT-L2	Tube	4 (upper)	8.45-8.50	200	22-28 below lowest string	South	
ECT-L3	Tube	6 (lower)	8.50-8.55	133	5-10 below middle string	South	
ECT-L4	Tube	6 (upper)	8.48-8.53	100	23-28 above middle string	South	
ECT-L5	Clods (2)	10	8.65-8.75	70	40-50 below upper string	South	Could not collect a tube sample
ECT-L6	Tube	11	10.56-10.61	60	35-40 below upper string	South	
ECT-L7	Clods (2)	6	9.80-9.91	67	38-50 below upper string	South	Could not collect a tube sample
ECT-L8	Tube	2	3.50-3.55	155	2-8 below lower string	South	
ECT-L9	Tube	1	0.62-0.69	139	8-13 above lower string	South	
ECT-L1 (bulk)	Bulk sediment	4 (lower)	8.55-8.70	215	35-45 below lowest string	South	
ECT-L2 (bulk)	Bulk sediment	4 (upper)	8.50-8.55	200	22-28 below lowest string	South	
ECT-L3 (bulk)	Bulk sediment	6 (lower)	8.47-8.58	133	2-12 below middle string	South	Sample taken around ECT-L3
ECT-L4 (bulk)	Bulk sediment	6 (upper)	8.46-8.55	100	21-30 above middle string	South	Sample taken around ECT-L4
ECT-L5 (bulk)	Bulk sediment	10	8.65-8.75	70	40-50 below upper string	South	
ECT-L6 (bulk)	Bulk sediment	11	10.61-10.70	60	33-43 below upper string	South	Sample taken around ECT-L6
ECT-L7 (bulk)	Bulk sediment	6	9.80-9.91	67	38-50 below upper string	South	
ECT-L8 (bulk)	Bulk sediment	2	3.48-3.58	155	1-9 below lower string	South	Sample taken around ECT-L8
ECT-L9 (bulk)	Bulk sediment	1	0.60-0.70	139	7-15 above lower string	South	Sample taken around ECT-L9

## Appendix D. Locations and Descriptions of Samples Collected From Trench

*Table 2. Locations of samples collected for radiocarbon analysis.*

<b>Sample Number</b>	<b>Trench Stratigraphic Unit</b>	<b>Station (m)</b>	<b>Approximate Depth (cm) below Ground Surface</b>	<b>Depth (cm)</b>	<b>Trench Wall</b>	<b>Notes</b>
ECT-C1	4 (lower)	8.55-8.70	203-213	35-45 below lowest string	South	
ECT-C2	4 (upper)	8.50-8.70	188-196	20-28 below lowest string	South	Sample collected from 5 cm below contact with unit 6
ECT-C3	6 (lower)	8.50-8.70	120-130	2-12 below middle string	South	
ECT-C4	6 (upper)	8.40-8.60	88-98	20-30 above middle string	South	
ECT-C5	10	8.38-8.58	53-73	35-55 below upper string	South	
ECT-C6	11	10.60-10.75	45-55	33-43 below upper string	South	
ECT-C7	6	9.80-9.91	70-90	50-70 below upper string	South	
ECT-C8	6 (upper)	10.35-10.65	142	About 20 below old string line for center of sample	North	Sample from below bench on north wall; location approximate; old string line correlates with the middle string line on the south wall

**Appendix E. Report from USGS Luminescence Dating Laboratory**

**Appendix E.  
Informal Memo From USGS Luminescence Dating Laboratory  
By  
Shannon Mahan  
U.S. Geological Survey  
Luminescence Dating Laboratory  
Federal Center  
Denver, Colorado**

Appendix E. Report from USGS Luminescence Dating Laboratory



**INFORMAL MEMO FROM USGS LUMINESCENCE DATING LAB**  
**FEBRUARY 28, 2007**  
**REPORT TO DEAN OSTENAA AND LUCY PIETY ON EAST CANYON FAULT**  
**TRENCH, HENEFER, UTAH**

## Appendix E. Report from USGS Luminescence Dating Laboratory

### U.S. Geological Survey

This report contains the data and final luminescence ages generated from this data on samples ECT-L1 through samples ECT-L9. These samples were collected from a trench across the East Canyon fault near Henefer, Utah by Dean Ostenaar and Lucy Piety. The samples were primarily composed of either clayey silt (ECT-L1 through ECT-L7) or silty sand (ECT-L8 and ECT-L9) with the occasional pebble (see attachment B for detailed particle size analyses). The preferred size for optically stimulated luminescence (OSL) dating is between 250 and 90  $\mu\text{m}$ . I obtained sufficient quantities of sand size grains of quartz for most of the samples after the first pass through wet sieving (except for ECT-L1 and ECT-L2, which had the least amount of sand). The samples had field moistures of 5.2% to 14.5% and total saturation moistures of 48% to ~100% (due to the very high abundance of clays). Saturated water content was obtained by weighing dry bulk soil material in a centrifuge tube, saturating and mixing, centrifuging, suctioning off the supernatant and weighing the resulting saturated soil.

Since mountainous Utah is classified as a mollisol xerolls regime (continuously dry in summer for long periods, moist in winter), I constructed a simple model to estimate average moisture content for the samples. This model assumed moisture contents between 20% and 25%, even though it was obvious some samples would be more saturated (or hold water better) than others.

OSL analyses were carried out in subdued orange-light conditions. One and a half centimeters of sediment was removed from the outer part of the OSL samples to prevent the possibility of contaminated sediments being dated. This left very little sample for OSL analyses as the PVC tubes were only 6 cm long. Luminescence

## Appendix E. Report from USGS Luminescence Dating Laboratory

measurements were made on the central sections of sediment that were least likely to have been exposed to sunlight during sampling.

Samples were treated with 10% HCl and 30% H<sub>2</sub>O<sub>2</sub> to remove carbonates and organic matter, and then sieved to extract the 90-125 µm-size fractions (170 to 120 mesh size apertures). Quartz and feldspar grains were separated by density using Li-Na tungstate ( $\rho=2.58 \text{ gcm}^{-3}$ ). The quartz fraction was etched using 40% HF for 40 min followed by 4N HCl for 45 min to remove the outermost layer affected by alpha radiation. The quartz grains were mounted on stainless steel discs using Silkospray, generally about 150-200 grains centered in the middle of the disc in a single aliquot. Light stimulation of the quartz was achieved using a RISØ array of blue LEDs centered at 470 nm. Detection optics comprised Hoya 2-U340 and Schott BG-39 filters coupled to an EMI 9635 QA Photomultiplier tube. Measurements were taken with a RISØ TL-DA-15 reader.  $\alpha$  radiation was applied using a 25 mCi <sup>90</sup>Sr/<sup>90</sup>Y in-built source.

The single-aliquot regenerative dose (SAR) protocol (Murray and Wintle, 2000) was used to determine the equivalent dose (see attachment A for more detail). A five-point measurement strategy was adopted with three dose points to bracket the equivalent dose, a fourth zero dose and a fifth repeat-equivalent dose point. The repeat equivalent dose was measured to correct for sensitivity changes and check that the protocol was working correctly (see figure 1 for details). All measurements were made at 125°C for 40 seconds after a pre-heat to 240°C for 10 seconds. For all aliquots the recycling ratio between the first and the fifth point ranged within 0.83-1.21. Data were analyzed using the ANALYST program of Duller (1999). Equivalent dose measurements were made on

## Appendix E. Report from USGS Luminescence Dating Laboratory

aliquots of 9.6 mm diameter. In each case 15-30 aliquots from each sample were analyzed (except for ECT-2 for which only 8 usable aliquots were obtained) (table 1).

The dose rate (see attachment A for complete detail) was obtained by gamma spectrometry analyses. Most ionizing radiation in the sediment is from the decay of isotopes in the uranium and thorium decay chains and the radioactive potassium 40. In the laboratory the bulk samples were counted in a gamma spectrometry lab for elemental concentrations (table 1). The cosmic-ray dose rate was estimated for each sample as a function of depth, altitude and geomagnetic latitude (Prescott and Hutton, 1994). Alpha and beta contributions to the dose rate were corrected for grain-size attenuation, if needed (Aitken, 1985).

### **2. Discussion of OSL results:**

These samples showed normal dispersion of equivalent dose scatter, except for ECT-5, ECT-9 and ECT-2 (figure 2). ECT-5 and ECT-9 show one or two outliers (positive skew) that are probably related to incomplete bleaching of grains in those aliquots that make up the outliers. ECT-2 showed a large variation in the grain population, but I could not resolve whether the problem can be attributed to the small number of aliquots (or equivalent doses) which was due to the fact that the sample had very little sand size grains (statistical problem) or whether the sample had many more partially bleached grains (geological problem). However, some of the samples exhibited a tighter than normal distribution (ECT-4, 5, 6, and 7) and look like they were very well bleached at deposition (perhaps having been exposed at the surface for some time before burial??).

## Appendix E. Report from USGS Luminescence Dating Laboratory

In general, the older the sample, the more dispersion it displays. Samples that have a fluvial depositional history (i.e. terrace or colluvium) or short transport path, also display more dispersion than will a sample composed of mainly eolian grains or grains that were sub aerially exposed before burial (point bar deposits). A set of “individual value plots” from all accepted equivalent doses generated for each sample are shown in figure 2. Histograms for the luminescence samples from the upper, middle and lower units within the trench were also generated (figures. 3, 4, 5). Please note that the thick curve over the histograms bins is the normal distribution curve generated for that data set and that the simple mean is shown for the equivalent dose, not the weighted mean as was used in table 1.

The bin width of the histograms can be determined for the samples by defining it as the value of the standard deviation (see figures 3, 4, 5; Lepper and McKeever, 2002). I have attempted to come close to these standard deviation values while retaining a clear data presentation of multiple graphs in one group for comparison purposes. Histograms are unable to display the precision with which each  $D_e$  value is obtained, but the standard deviation generated for each sample is shown.

The comparison of equivalent doses (figure 2) shows tight clusters for ECT-4, ECT-5, ECT-6 and ECT-7, which attest to their well-bleached characteristics (except for the above mentioned outlier in ECT-5). ECT-3, ECT-1 and (of course) ECT-2 show a much broader distribution (and larger standard deviations), more like that of sediment from a fluvial environment or sediment that contains a strong component of partial bleaching. For this reason the mean on ECT-2 was weighted such that those grains that exhibited lower equivalent doses and more precise errors (i.e. well-bleached grains)

## Appendix E. Report from USGS Luminescence Dating Laboratory

would control the total equivalent dose (96 Grays weighted vs. 111 Grays). ECT-2 also had outliers that probably should have been removed, but the outliers to the right of the fit were nulled by weighting the data. The other samples (except ECT-1 and ECT-3 in a minor way) did not really require a weighted mean, but nonetheless were reported in this way. This weighted mean affected the ages generated in only a minimal way (see subtitles in histogram figures for variations).

Material used to calculate the dose rates did not vary significantly in any way for the U and Th, although there was an increase in K at the top of the trench (table 1). It is unclear what this increase means, but it did not point to any disequilibrium problems in the bulk samples.

There were difficulties with the older samples returning reliable ages. The difficulty was not a problem with the laboratory applied SAR protocol on samples ECT-8 and ECT-9, as the samples did not show monotonic (saturating) behavior, did not show a lack of proportionality between the regenerative and test-dose signals and there was no difference in sensitivity corrections between the natural and the regenerative cycles. The excessive scatter and high standard deviations for the samples are instead attributed to problems in the geology of the sediment. The very weathered, red-colored alluvium (Bt soil and carbonate soil of Stage III development) simply presented too many mixing and overprinting problems to sort out using OSL. It was impossible to tell whether young equivalent doses were a result of bioturbation, short transport paths (one side of the fault to the other), clay migration or true burial ages. Older equivalent doses could not be separated out into those that were a result of non-bleaching (residual luminescence held), partial bleaching or true burial ages.

### 3. Conclusion:

Samples at the top of the trench, in sediment deposited after the MRE (unconformity/erosion boundary), are dated at 5.2 ka to 5.8 ka. Samples below the MRE faulting event are dated at 13.4 ka to 14.7 ka. A sample of charcoal collected near the OSL age of 13.4 ka returned an age of 12.1 ka (12,160-11,970 cal yr BP). The OSL age overlaps with the radiocarbon age when the error is applied (table 1). All of the upper OSL samples showed well bleached conditions before final burial.

OSL samples from the middle of the trench (event 1 or pre-event 1) are dated between 31.1 ka to 37.7 ka. These samples also show a fluvial origin and a broader distribution in bleaching conditions, with some aliquots containing many unbleached or partially bleached grains (these grains would carry a small residual luminescence that was not reset at burial, see ECT-2).

OSL samples from the bottom of the trench in older, weathered sediment (strong Bt soil development) could only be minimally dated at >50 ka and >120 ka. That is, these samples obviously contained many grains that were either partially bleached or not bleached at all (figures 1 and 5). Although the histograms may look acceptable, the quartz protocol used in obtaining the resultant ages was returning systematic underestimations. This is not attributed to differences in sensitivity corrections using the SAR protocol, but is attributed to problems with trying to date Bt soils or older overprinting carbonate (stage II or higher) soils using the OSL technique.

### 4. References

- Aitken, M.J. (1985). *Thermoluminescence Dating*. Academic Press, London, 359 pp.
- Aitken, M.J. (1998). *An Introduction to Optical Dating: The dating of Quaternary sediments by the use of photon-stimulated luminescence*. Oxford University Press, New York, 267 pp.

## Appendix E. Report from USGS Luminescence Dating Laboratory

- Friedman, J.M., Vincent, K.R., and Shafroth, P.B. (2005) Dating floodplain sediments using tree-ring response to burial, *Earth Surface Processes and Landforms*, v. 30, no. 9, p. 1077-1091.
- Galbraith, R.F., Roberts, R.G., Laslett, G.M., Yoshida, H. and Olley, J.M. (1999). Optical dating of single and multiple grains of quartz from Jinmium rock shelter, Northern Australia: Part I, Experimental Design and Statistical Models. *Archaeometry*, **41(2)**, 339-364.
- Lepper, K. (2001). Development of an objective dose distribution analysis method for luminescence dating and pilot studies for planetary applications. Ph.D. Thesis, Oklahoma State University, Stillwater, OK, 288 pp.
- Lepper, K. and McKeever, S.W.S. (2002). An objective methodology for dose distribution analysis. *Radiation Protection Dosimetry*, **101**, 349-352.
- Murray, A. and Wintle, A.G. (2000). Luminescence dating of quartz using an improved single-aliquot regenerative-dose protocol. *Radiation Measurements*, **32**, 57-73.
- Murray, A.S., Olley, J.M. and Caitcheon, G.G. (1995). Measurement of equivalent doses in quartz from contemporary water-lain sediments using optically stimulated luminescence. *Quaternary Science Reviews*, **14**, 365-371.
- Olley, J., Caitcheon, G. and Murray, A. (1998) The distribution of apparent dose as determined by optically stimulated luminescence in small aliquots of fluvial quartz; implications for dating young sediments. *Quaternary Science Review*, **17(11)**, 1033-1040.
- Prescott, J.R. and Hutton, J.T. (1994). Cosmic ray contributions to dose rates for luminescence and ESR dating: large depths and long-term time variations. *Radiation Measurements*, **23**, 497-500.
- Wallinga, J. (2002). Optically stimulated luminescence dating of fluvial deposits: a review. *Boreas* **31(4)**, 303-322.

# Appendix E. Report from USGS Luminescence Dating Laboratory

rw-12.bin Disc: 47

Date: 1/31/07

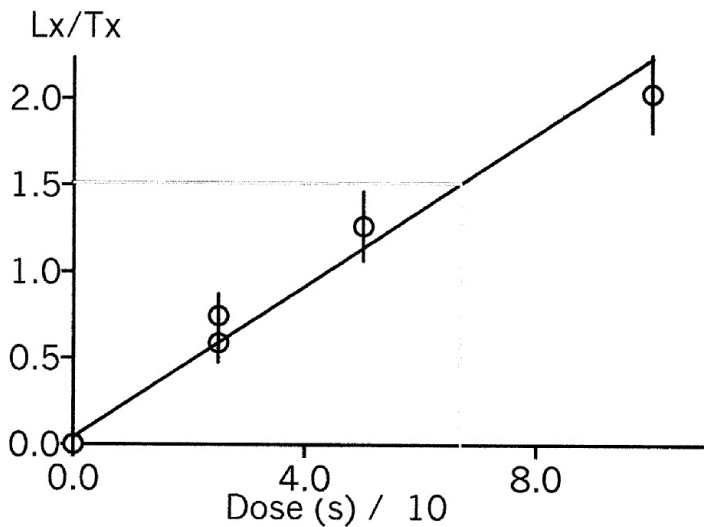
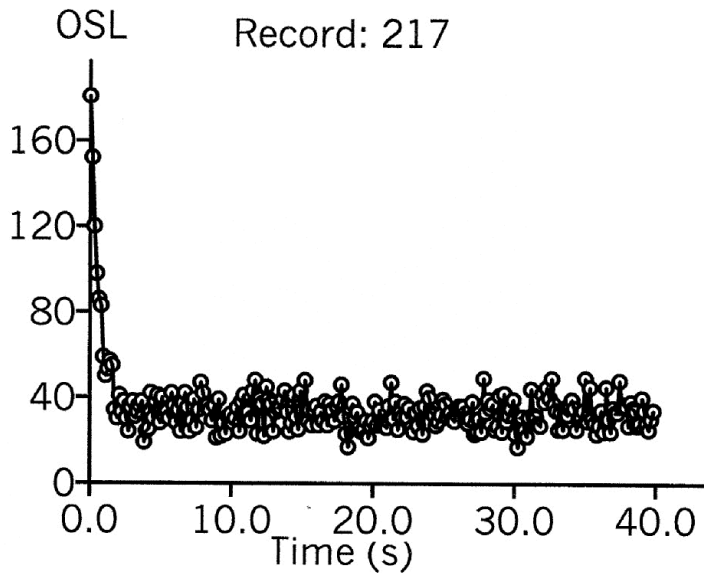


**Figure 1a.** OSL decay curve for ECT-5, showing quartz signal as measured with blue-light wavelength emitting diodes. Time is measured in seconds (s) and OSL is measured in photons counts/second.

**Figure 1b.** ECT-5 growth curve, with the natural plotted on the Lx/Tx axis near 1.5 as a gray line. Regeneration proceeded “normally”, with a recycle within 22% of the first measurement and increases in responses to increasing beta radiation. Dose is measured in seconds x 10 (not / by 10) and OSL is measured in normalized OSL sensitivity measurements (Lx/Tx).

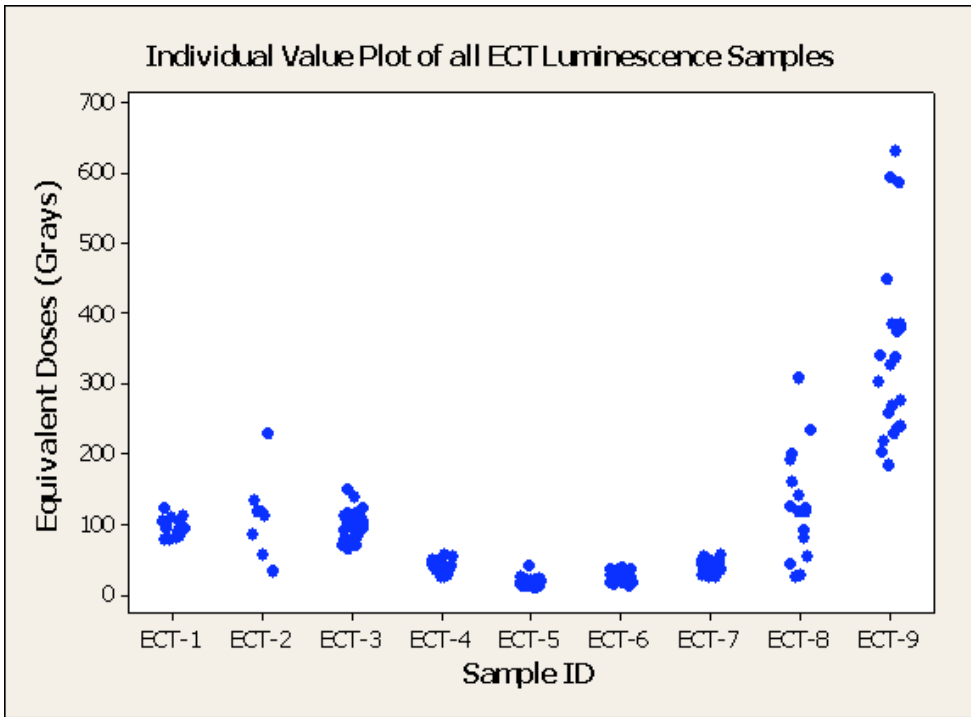


**Figure 2.** Comparison of dispersion (scatter) in the equivalent doses for the East Canyon Trench samples. Note the small number of aliquots in ECT-2.

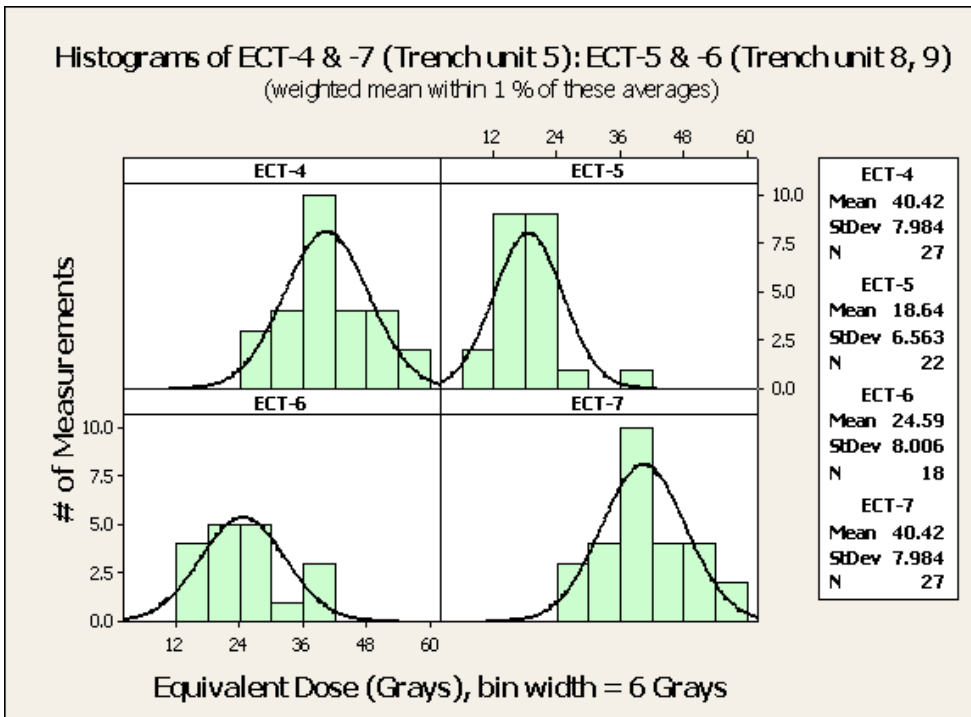


**Figure 3.** Multiple histograms for the upper trench units (no outliers have been removed).

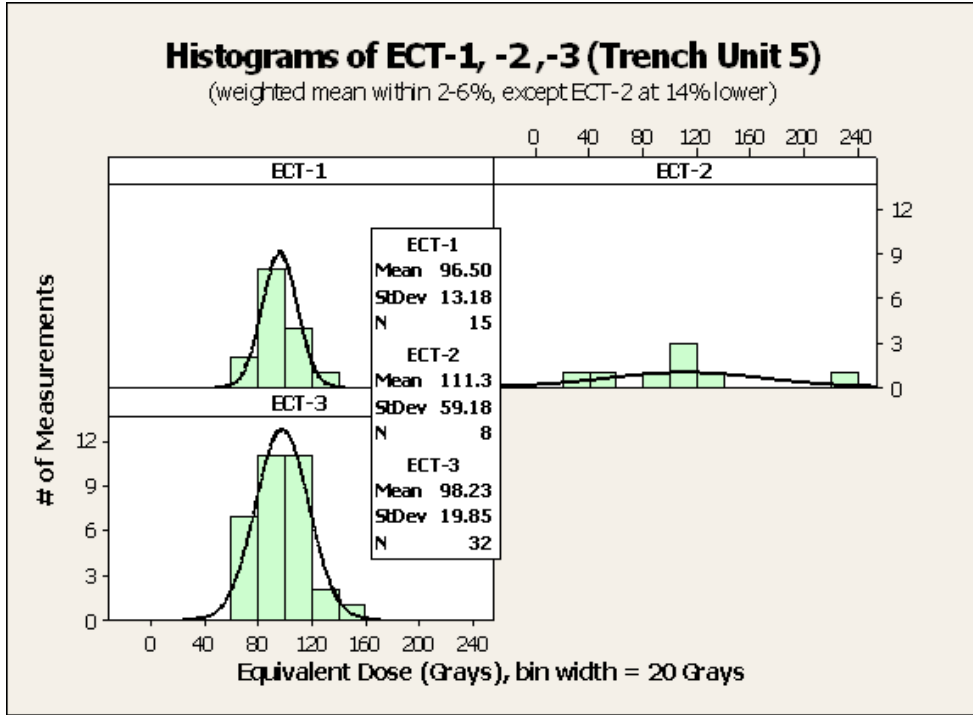


Figure 4. Multiple histograms for the middle trench units (no outliers have been removed).

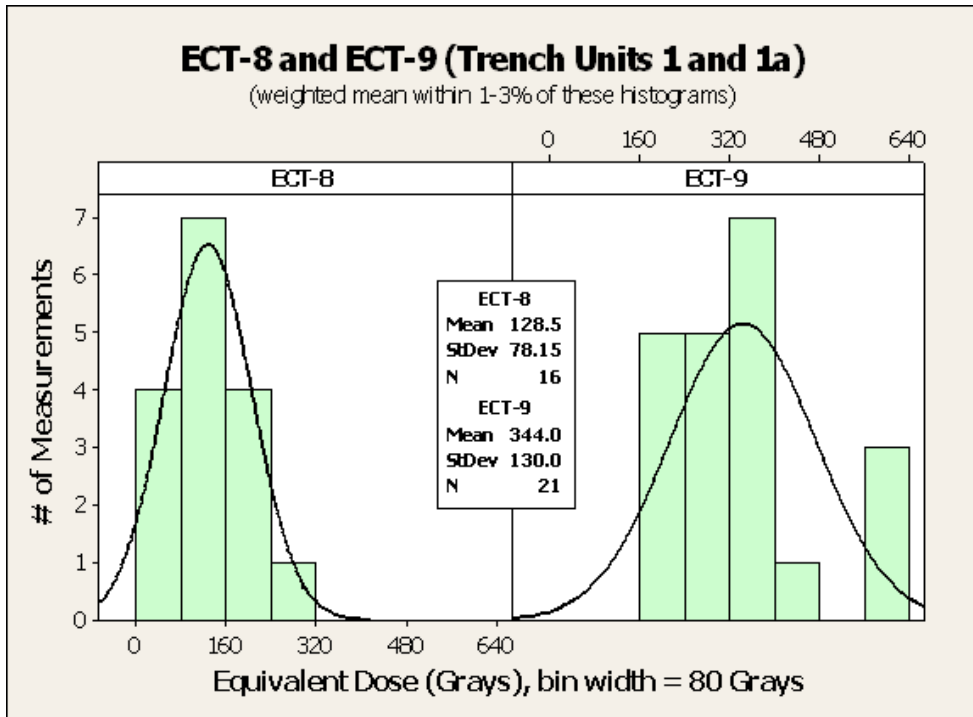


Figure 5. Multiple histograms for the lower trench units (no outliers have been removed).

**Attachment A:**

**General Concepts of Luminescence Dating:**

Most minerals react to ionizing radiation by essentially gaining energy at the electron level, which accumulates through time if that energy is not released (as light) by some outside stimuli (sunlight or intense heat over 200°C). Thus, sediment grains can record their exposure history to ionizing radiation, which can then be “read” in the laboratory and used as a clock. This procedure is referred to as luminescence geochronology (Aitken, 1998), the goal of which is to establish the timing of the burial of mineral grains in sedimentary deposits. If the mineral grains were transported at night, in turbid fluvial conditions or in those deposits generally considered to be deposited in massive, sudden discharge events (i.e. debris flows, colluvium, etc.) however, luminescence dating may produce depositional ages that are too old because the luminescence clock was not reset to “zero” just prior to burial.

Luminescence dating is based on solid-state dosimetric properties of natural mineral grains. Minerals react to ionizing radiation, which is generated by radioactive isotopes found in minor quantities in most terrestrial sediments and by cosmic radiation. Specifically, ionizing radiation creates charge pairs/carriers (e<sup>-</sup>, h<sup>+</sup>) in mineral crystals. The charge carriers are mobile within the crystals, but can become localized, or trapped, at lattice defects and held there over geologically significant time scales. Over time, the number of segregated, or trapped, charge carriers builds up in a way that can be described by a saturating exponential function.

Exposure to heat, light, or high pressures can release charge carriers from trapping sites and permit recombination, during which light is emitted from the mineral grains. This detrapping resets the system within the mineral grains. In terrestrial environments exposure to sunlight during sediment transport resets the clock and it is also why a

**Appendix E. Report from USGS Luminescence Dating Laboratory**  
luminescence age is considered a burial age. In the laboratory, sediment is stimulated to emit light, which is measured. The sediment is stimulated by exposure to light of specific wavelengths (optically stimulated luminescence, OSL), or heat (thermoluminescence, TL), in proscribed manners. The intensity of emitted light measured in the laboratory is proportional to the trapped charge population, which is proportional to the total absorbed radiation dose ( $D_e$ ) that the sedimentary deposit experienced, and that relation is proportional to the time elapsed since burial.

The simplest form of the OSL age equation is:

$$t_{OSL} = \frac{D_e}{D'}$$

where

$$t_{OSL} = \text{age}$$

$$D_e = \text{total absorbed radiation dose,}$$

$$D' = \text{natural environmental dose rate.}$$

The accuracy of OSL ages is primarily dependent on the intensity and duration of the sediment grains' exposure to sunlight during transport, often referred to as "resetting" or "bleaching". Traditionally, sediments deposited from fluvial systems have been among the most challenging to date using OSL methods because the grains were not fully bleached prior to burial. Bleaching problems arise from the light filtering effects of water, particularly water turbid with high suspended-sediment concentrations, and from transport at night. A review of studies that used OSL to date fluvial sediments can be found in Wallinga (2002). Unfortunately, many of these studies met with mixed results, yet luminescence dating has important potential because fluvial deposits often lack the foreign objects (charcoal, potsherds, living trees) that are essential for alternative dating methods (e.g. Friedman and others, 2005).

## **Appendix E. Report from USGS Luminescence Dating Laboratory**

Fortunately, modern luminescence dating equipment and experimental procedures show promise. For example geochronological measurements can be made on small collections of grains, termed single aliquots, or even single grains. This in turn permits hundreds or even thousands of absorbed doses to be determined for individual field samples. These data sets or dose distributions can then be visualized and statistically interrogated. Numerous studies have now documented that “incomplete resetting” or “partial bleaching” manifests itself as positive asymmetry in a sample’s dose distribution ( Murray and others, 1995; Olley and others, 1998; Lepper and others, 2000). In these cases, standard measures of central tendency (mean, standard deviation) do not represent the true depositional age of the sediment. At least two analytical tools have been developed that address this issue and attempt to objectively determine a representative dose, including the "zero age model" (Galbraith and others, 1999) and the "leading edge method" (Lepper and McKeever, 2002).

## Appendix E. Report from USGS Luminescence Dating Laboratory

### Attachment B:

Particle Size analysis was performed on nine soil samples from trench sites around Park City, Utah.

Samples were submitted as bulk. Because most samples contained small sand - sized clumps, light agitation with a rubber mortar and pestle was performed to aid in disaggregation of the samples as needed.

Prior to analysis, all samples were treated with 30% H<sub>2</sub>O<sub>2</sub> to remove organic matter. **Sample ECT-L9 was also treated with 15% HCl to remove secondary carbonate.**

Sodium hexametaphosphate was added to all samples and the samples were shaken on a shaker table for four hours to ensure deflocculation of the clays.

Particle size was determined using a Malvern Mastersizer-S long bed laser analyzer. The sample was introduced into an aqueous medium and pumped through the laser analyzer for grain size measurements.

After analysis was completed, no sample was retrieved per submitter's instructions. However, remaining un-treated sample has been returned to submitter.

LABORATORY	TEST	WT (g)	% SAND	% SILT	% CLAY	TEXTURAL CLASSIFICATION
GRL -	ECT-1	0.50	10.80	49.54	39.66	Clayey Silt
-	ECT-2	0.53	9.89	54.84	35.27	Clayey Silt
-	ECT-3	0.60	19.42	50.43	30.15	Clayey Silt
-	ECT-4	0.56	16.91	51.13	31.96	Clayey Silt
-	ECT-5	0.53	15.44	53.45	31.12	Clayey Silt
-	ECT-6	0.64	14.94	54.82	30.24	Clayey Silt
-	ECT-7	0.45	12.57	54.61	32.82	Clayey Silt
-	ECT-9	0.46	48.68	35.85	15.47	Silty Sand
-	ECT-8	0.84	67.06	18.56	14.38	Silty Sand

---

Sample weight reported on oven dry basis (105 °C). Sample weight and particle size distribution exclusive of organic matter.  
<2000µm material

Tested by Malvern Long Bed Laser Particle Size Analyzer and reported as volume percentage.

## Appendix E. Report from USGS Luminescence Dating Laboratory

**NAME:** Shannon Mahan  
**LOCATION:** Henefer Utah

SEDIMENTOLOGY LABORATORY - USGS - ESP  
Particle Size Analysis Report –  
**Wentworth Grade Scale**  
Malvern Particle Size Analyzer

### <2000µ. MINERAL MATERIAL SIZE DISTRIBUTION - PER FRACTION & CUMULATIVE PERCENT

[Size Separates are Expressed In Microns]

MICRONS		GRL -	ECT-1	GRL -	ECT-2	GRL -	ECT-3	GRL -	ECT-4	GRL -	ECT-5	GRL -	ECT-6	GRL -	ECT-L7	GRL -	ECT-L8	GRL -	ECT-L9
2000	1680	0.00	0.00	0.00	0.00	0.00	0.00	0.00	0.00	0.00	0.00	0.00	0.00	0.00	0.00	9.17	9.17	0.00	0.00
1680	1414	0.00	0.00	0.00	0.00	0.00	0.00	0.00	0.00	0.00	0.00	0.00	0.00	0.00	0.00	9.50	18.67	0.00	0.00
1414	1189	0.00	0.00	0.00	0.00	0.00	0.00	0.00	0.00	0.00	0.00	0.00	0.00	0.00	0.00	11.68	30.35	0.00	0.00
1189	1000	0.00	0.00	0.00	0.00	0.00	0.00	0.00	0.00	0.00	0.00	0.00	0.00	0.00	0.00	9.60	39.95	0.00	0.00
1000	841	0.00	0.00	0.00	0.00	0.00	0.00	0.00	0.00	0.00	0.00	0.00	0.00	0.00	0.00	6.71	46.66	0.00	0.00
841	707	0.00	0.00	0.00	0.00	0.00	0.00	0.00	0.00	0.00	0.00	0.00	0.00	0.00	0.00	4.03	50.69	0.00	0.00
707	595	0.00	0.00	0.00	0.00	0.00	0.00	0.00	0.00	0.00	0.00	0.00	0.00	0.00	0.00	2.07	52.76	0.00	0.00
595	500	0.00	0.00	0.00	0.00	0.00	0.00	0.00	0.00	0.00	0.00	0.00	0.00	0.00	0.00	0.91	53.67	0.00	0.00
500	420	0.00	0.00	0.00	0.00	0.00	0.00	0.00	0.00	0.00	0.00	0.00	0.00	0.00	0.00	0.32	53.99	0.12	0.12
420	354	0.00	0.00	0.00	0.00	0.00	0.00	0.00	0.00	0.00	0.00	0.00	0.00	0.00	0.00	0.11	54.10	1.37	1.48
354	297	0.00	0.00	0.00	0.00	0.67	0.67	0.46	0.46	0.31	0.31	0.31	0.31	0.31	0.31	0.24	54.34	3.11	4.59
297	250	0.06	0.07	0.00	0.00	1.38	2.05	0.99	1.44	0.65	0.96	0.61	0.93	0.54	0.84	0.56	54.90	4.23	8.82
250	210	0.42	0.49	0.03	0.03	1.79	3.84	1.30	2.74	0.98	1.94	0.90	1.83	0.76	1.60	0.94	55.84	4.94	13.76
210	177	0.71	1.20	0.22	0.25	1.79	5.63	1.33	4.07	1.08	3.02	0.97	2.79	0.78	2.38	1.20	57.04	5.08	18.84
177	149	1.02	2.22	0.60	0.85	1.69	7.32	1.33	5.40	1.16	4.18	1.02	3.81	0.80	3.18	1.40	58.44	5.15	23.98
149	125	1.29	3.52	0.93	1.78	1.68	9.00	1.45	6.85	1.33	5.51	1.18	4.99	0.93	4.12	1.57	60.01	5.23	29.22
125	105	1.49	5.01	1.26	3.04	1.86	10.86	1.72	8.57	1.65	7.17	1.54	6.53	1.24	5.36	1.67	61.68	5.15	34.36
105	88	1.72	6.72	1.75	4.79	2.33	13.19	2.25	10.82	2.21	9.38	2.16	8.69	1.80	7.16	1.81	63.49	5.12	39.48
88	74	1.95	8.67	2.33	7.12	2.92	16.11	2.85	13.66	2.83	12.21	2.88	11.56	2.46	9.62	1.84	65.33	4.88	44.36
74	63	2.13	10.80	2.78	9.89	3.31	19.42	3.24	16.91	3.24	15.44	3.38	14.94	2.95	12.57	1.73	67.06	4.32	48.68
63	53	2.68	13.48	3.61	13.50	4.12	23.54	4.03	20.93	4.03	19.47	4.27	19.21	3.81	16.38	1.82	68.88	4.34	53.02
53	44	3.34	16.82	4.46	17.96	4.72	28.26	4.75	25.68	4.75	24.22	5.08	24.29	4.63	21.01	1.86	70.74	4.23	57.25
44	37	3.44	20.27	4.46	22.42	4.35	32.61	4.43	30.12	4.57	28.79	4.90	29.19	4.55	25.56	1.59	72.33	3.49	60.73
37	31.2	3.57	23.83	4.45	26.87	4.16	36.77	4.18	34.29	4.33	33.12	4.63	33.82	4.46	30.02	1.41	73.74	3.00	63.73
31.2	26.3	3.61	27.44	4.24	31.10	3.93	40.70	3.95	38.24	4.09	37.21	4.33	38.15	4.21	34.23	1.26	75.00	2.62	66.35
26.3	22.1	3.52	30.97	4.02	35.13	3.69	44.39	3.71	41.95	3.88	41.08	4.06	42.20	3.97	38.20	1.15	76.15	2.32	68.67
22.1	18.6	3.32	34.29	3.68	38.81	3.32	47.71	3.35	45.30	3.54	44.62	3.65	45.85	3.62	41.82	1.04	77.19	2.04	70.71
18.6	15.6	3.21	37.50	3.46	42.26	3.06	50.76	3.09	48.39	3.31	47.93	3.37	49.22	3.39	45.20	0.98	78.17	1.88	72.58

Appendix E. Report from USGS Luminescence Dating Laboratory

15.6	13.1	3.03	40.53	3.18	45.44	2.77	53.54	2.81	51.20	3.03	50.96	3.04	52.26	3.10	48.31	0.94	79.11	1.73	74.31
13.1	11	2.92	43.46	2.99	48.43	2.58	56.12	2.62	53.82	2.84	53.81	2.82	55.08	2.92	51.23	0.92	80.03	1.64	75.96
11	9.3	2.75	46.21	2.76	51.19	2.36	58.48	2.41	56.23	2.61	56.41	2.56	57.64	2.69	53.92	0.89	80.92	1.52	77.48
9.3	7.8	2.87	49.07	2.83	54.03	2.40	60.88	2.46	58.69	2.65	59.06	2.59	60.23	2.76	56.68	0.95	81.87	1.55	79.03
7.8	6.6	2.73	51.80	2.65	56.68	2.24	63.12	2.31	60.99	2.46	61.52	2.40	62.63	2.59	59.27	0.91	82.78	1.43	80.46
6.6	5.5	2.98	54.78	2.86	59.54	2.40	65.52	2.49	63.48	2.63	64.14	2.55	65.18	2.80	62.06	1.00	83.78	1.49	81.95
5.5	4.6	2.91	57.69	2.74	62.28	2.29	67.81	2.40	65.88	2.51	66.65	2.42	67.60	2.69	64.76	0.97	84.75	1.38	83.33
4.6	3.9	2.65	60.34	2.45	64.73	2.04	69.85	2.16	68.04	2.24	68.89	2.15	69.76	2.42	67.18	0.87	85.62	1.20	84.53
3.9	3.3	2.61	62.95	2.39	67.12	1.98	71.83	2.11	70.15	2.17	71.06	2.08	71.84	2.36	69.54	0.85	86.47	1.12	85.65
3.3	2.8	2.49	65.44	2.24	69.36	1.85	73.69	1.99	72.13	2.04	73.09	1.95	73.79	2.23	71.77	0.79	87.26	1.01	86.66
2.8	2.3	2.86	68.30	2.53	71.89	2.09	75.77	2.25	74.38	2.30	75.39	2.19	75.98	2.52	74.29	0.89	88.15	1.10	87.76
2.3	1.95	2.31	70.61	2.01	73.90	1.64	77.41	1.78	76.16	1.81	77.20	1.73	77.72	1.99	76.27	0.70	88.85	0.84	88.60
1.95	1.64	2.34	72.96	2.01	75.91	1.63	79.04	1.77	77.92	1.79	78.99	1.72	79.44	1.97	78.24	0.69	89.54	0.80	89.40
1.64	1.38	2.27	75.23	1.94	77.85	1.55	80.59	1.67	79.60	1.69	80.69	1.64	81.08	1.86	80.11	0.65	90.19	0.73	90.13
1.38	1.16	2.21	77.43	1.87	79.73	1.48	82.06	1.59	81.19	1.61	82.30	1.58	82.66	1.77	81.87	0.62	90.81	0.68	90.80
1.16	0.98	2.05	79.48	1.75	81.48	1.37	83.44	1.47	82.66	1.48	83.78	1.46	84.12	1.62	83.49	0.59	91.40	0.62	91.42
0.98	0.82	2.07	81.56	1.80	83.28	1.40	84.84	1.49	84.15	1.50	85.28	1.49	85.61	1.62	85.11	0.61	92.01	0.63	92.04
0.82	0.69	1.93	83.48	1.72	85.00	1.33	86.17	1.40	85.56	1.42	86.70	1.41	87.02	1.50	86.61	0.59	92.60	0.59	92.64
0.69	0.58	1.89	85.37	1.75	86.74	1.37	87.53	1.43	86.99	1.45	88.15	1.43	88.45	1.51	88.12	0.64	93.24	0.62	93.26
0.58	0.49	1.84	87.21	1.76	88.51	1.40	88.93	1.46	88.45	1.48	89.62	1.45	89.89	1.52	89.64	0.68	93.92	0.65	93.91
	<0.49	12.80	100.00	11.49	100.00	11.07	100.00	11.55	100.00	10.38	100.00	10.11	100.00	10.36	100.00	6.08	100.00	6.09	100.00

## Appendix E. Report from USGS Luminescence Dating Laboratory

**Table 1. Gamma spectrometry analysis, cosmic and total dose rate, equivalent dose and age for ECT OSL samples.**

Sample #	K%	Th (ppm)	U (ppm)	Water (%) <sup>a</sup>	Cosmic dose rate (Gy/ka) <sup>b</sup>	Total dose rate (Gy/ka) <sup>c</sup>	De (Gy) <sup>d</sup>	N <sup>e</sup>	Age (ka) <sup>f</sup>
ECT-L5	2.27 ± 0.11	12.5 ± 0.33	3.58 ± 0.13	5 (48)	0.26 ± 0.02	3.59 ± 0.07	18.6 ± 1.22	22 (30)	5.17 ± 0.35 <sup>e</sup>
ECT-L6	3.23 ± 0.06	12.1 ± 0.33	3.30 ± 0.12	13 (57)	0.27 ± 0.02	4.28 ± 0.07	24.6 ± 1.15	29 (35)	5.75 ± 0.28 <sup>e</sup>
ECT-L4	2.15 ± 0.07	12.5 ± 0.32	3.47 ± 0.12	9 (74)	0.26 ± 0.02	3.31 ± 0.06	44.3 ± 1.94	24 (28)	13.4 ± 1.06 <sup>e</sup>
ECT-L7	1.62 ± 0.14	11.3 ± 0.27	2.54 ± 0.11	10 (54)	0.26 ± 0.02	2.78 ± 0.06	40.9 ± 3.11	27 (35)	14.7 ± 0.73 <sup>e</sup>
ECT-L3	1.82 ± 0.12	12.0 ± 0.27	3.23 ± 0.12	9 (68)	0.25 ± 0.02	2.98 ± 0.05	92.6 ± 2.18	30 (37)	31.1 ± 2.14 <sup>e</sup>
ECT-L2	1.50 ± 0.05	11.3 ± 0.29	3.16 ± 0.11	13 (58)	0.23 ± 0.02	2.65 ± 0.05	96.0 ± 6.21	8 (20)	36.2 ± 2.49 <sup>f</sup>
ECT-L1	1.36 ± 0.06	10.8 ± 0.27	2.55 ± 0.10	15 (51)	0.21 ± 0.02	2.50 ± 0.04	94.2 ± 2.36	15 (15)	37.7 ± 2.86 <sup>f</sup>
ECT-L8	1.56 ± 0.14	11.1 ± 0.23	2.38 ± 0.11	7 (51)	0.24 ± 0.02	2.67 ± 0.05	>127 ± 5.02	16 (29)	>47.6 ± 4.04 <sup>c</sup>
ECT-L9	1.68 ± 0.09	11.0 ± 0.24	2.80 ± 0.10	7 (34)	0.24 ± 0.02	2.84 ± 0.05	>334 ± 8.34	21 (24)	>118 ± 5.66 <sup>c</sup>

<sup>a</sup>Moisture value used in calculation of age (usually 45% of total saturation, except ECT-9 which was 60%). Figures in parentheses indicate the complete sample saturation %.

<sup>b</sup>Analyses obtained using laboratory Gamma spectrometry (low resolution NaI).

<sup>c</sup>Cosmic doses and attenuation with depth were calculated using the methods of Prescott and Stephens (1982) and Prescott and Hutton (1994). See text for details.

<sup>d</sup>Number of replicated equivalent dose (De) estimates used to calculate the mean. Figures in parentheses indicate total number of measurements made including failed runs with unusable data.

<sup>e</sup>Dose rate and age for fine-grained 90-125 µm quartz sand. Linear and exponential fit used on age, errors to one sigma.

<sup>f</sup>Dose rate and age for fine-grained 90-250 µm quartz sand. Exponential fit used on age, errors to one sigma.

**Appendix F.**  
**Examination of Bulk Soil and AMS Radiocarbon Analysis of Material**  
**From Trench Across the Main Canyon Fault, Utah**  
**By**  
**Kathryn Puseman**  
**With assistance from R. A. Varney**  
**Paleo Research Institute**  
**Golden, Colorado**

EXAMINATION OF BULK SOIL AND AMS RADIOCARBON ANALYSIS OF MATERIAL FROM  
EAST CANYON TRENCH, UTAH

By

Kathryn Puseman

With Assistance from  
R. A. Varney

Paleo Research Institute  
Golden, Colorado

Paleo Research Institute Technical Report 06-95

Prepared For

Bureau of Reclamation  
Reclamation Service Center  
Denver, Colorado

February 2007

## INTRODUCTION

A total of eight bulk soil samples from the East Canyon Trench in Summit County, Utah, were floated to recover organic fragments suitable for radiocarbon analysis. These samples were recovered from trenches along the East Canyon fault, a northeast-trending range-front fault generally bounding the northern side of the intermontane valley between East Canyon and Croyden in the Wasatch Range (Black and Hecker 1999). Botanic components and detrital charcoal were identified, and potentially radiocarbon datable material was separated. One sample of charred organic material was processed for AMS radiocarbon analysis.

## METHODS

### Macrofloral

The bulk samples were floated using a modification of the procedures outlined by Matthews (1979). Each sample was added to approximately 3 gallons of water. The sample was stirred until a strong vortex formed, which was allowed to slow before pouring the light fraction through a 150 micron mesh sieve. Additional water was added and the process repeated until all visible macrofloral material was removed from the sample (a minimum of five times). The material that remained in the bottom (heavy fraction) was poured through a 0.5-mm mesh screen. The floated portions were allowed to dry.

The light fractions were weighed, then passed through a series of graduated screens (US Standard Sieves with 4-mm, 2-mm, 1-mm, 0.5-mm and 0.25-mm openings to separate charcoal debris and to initially sort the remains. The contents of each screen were then examined. Charcoal pieces larger than 1-mm in diameter were broken to expose a fresh cross section and examined under a binocular microscope at a magnification of 70x. The remaining light fraction in the 4-mm, 2-mm, 1-mm, 0.5-mm, and 0.25-mm sieves was scanned under a binocular stereo microscope at a magnification of 10x, with some identifications requiring magnifications of up to 70x. The material that passed through the 0.25-mm screen was not examined. The coarse or heavy fractions also were screened and examined for the presence of botanic remains. Remains from both the light and heavy fractions were recorded as charred and/or uncharred, whole and/or fragments. Individual detrital charcoal/wood samples also were broken to expose a fresh cross-section and examined under a binocular microscope at a magnification of 70x.

Macrofloral remains, including charcoal, were identified using manuals (Core, et al. 1976; Martin and Barkley 1961; Panshin and Zeeuw 1980; Petrides and Petrides 1992) and by comparison with modern and archaeological references. The term "seed" is used to represent seeds, achenes, caryopses, and other disseminules. Because charcoal and possibly other botanic remains were to be sent for radiocarbon dating, clean laboratory conditions were used during flotation and identification to avoid contamination. All instruments were washed between samples, and samples were protected from contact with modern charcoal.

## **Radiocarbon Dating**

Wood and charcoal samples submitted for radiocarbon dating are weighed prior to selecting subsamples for pre-treatment. The remainder of each sample is permanently curated at Paleo Research. The subsample selected for pre-treatment is first subjected to hot (at least 110 °C), 6N hydrochloric acid (HCl), with rinses to neutral between each HCl treatment, until the supernatant is clear. This removes iron compounds and calcium carbonates that would hamper removal of humate compounds later. Next the samples are subjected to 5% potassium hydroxide (KOH) to remove humates. Once again, the samples are rinsed to neutral and re-acidified with pH 2 HCl between each KOH step. This step is repeated until the supernatant is clear, signaling removal of all humates. After humate removal, each sample is made slightly acidic and left that way for the next step. Charcoal samples (but not wood samples) are subjected to a concentrated, hot nitric acid bath, which removes all modern and recent organics. This treatment is not used on unburned or partially burned wood samples because it oxidizes the submitted sample of unknown age.

Each submitted sample is then freeze-dried using a vacuum system, freezing out all moisture at -98 °C. Each individual sample is combined with cupric oxide (CuO) and elemental silver (Ag<sup>0</sup>) in a quartz tube, then flame sealed under vacuum.

Standards and laboratory background samples also are treated in the same manner as the wood and charcoal samples of unknown age. A radiocarbon “dead” EUA wood blank from Alaska that is more than 70,000 years old (currently beyond the detection capabilities of AMS) is treated using the same chemical processing as the samples of unknown age in order to calibrate the laboratory correction factor. Standards of known age, such as Two Creeks wood that dates to 11,400 RCYBP and others from the Third International Radiocarbon Intercomparison (TIRI), are also processed simultaneously to establish the laboratory correction factor. Each wood standard is run in a quantity similar to the submitted samples of unknown age and sealed in a quartz tube after the requisite pre-treatment. Once all the wood standards, blanks, and submitted samples of unknown age are prepared and sealed in their individual quartz tubes, they are combusted at 820 °C, soaked for an extended period of time at that temperature, and then slowly allowed to cool to enable the chemical reaction that extracts carbon dioxide (CO<sub>2</sub>) gas.

Following this last step, all samples of unknown age, the wood standards, and the laboratory backgrounds are sent to the Keck Carbon Cycle AMS Facility at the University of California, Irvine, where the CO<sub>2</sub> gas is processed into graphite. The graphite in these samples is then placed in the target and subjected to a cesium ion beam, which produces the numbers that are converted into the radiocarbon date presented in the data section. Dates are presented as conventional radiocarbon ages, as well as calibrated ages using Intcalc05 curves on Oxcal v.3.10.

## **FTIR (Fourier Transform Infrared Spectrometry)**

Infrared (IR) spectrometry has been experiencing a renaissance for identifying organic substances during the past few decades. Today it is considered one of the more powerful tools in organic and analytical chemistry.

Fourier Transform infrared spectrometry (FTIR) is performed using a Nicolet 6700 optical bench with an ATR and a zinc selenoid crystal for examining organic remains. Sediments are measured using a silicon crystal. The sample is placed in the path of a specially encoded infrared beam. The infrared beam passes through the sample and produces a signal called an "interferogram." The interferogram contains information about the frequencies of infrared that are absorbed and the strength of the absorptions, which is determined by the sample's chemical make-up. A computer reads the interferogram and uses Fourier transformation to decode the intensity information for each frequency (wave numbers) and presents a spectrum.

One of the primary advantages to the FTIR is that it measures all wave lengths simultaneously. It has a relatively high signal-to-noise ratio and a short measurement time. Each peak in the spectrum represents either a chemical bond or a functional group. Samples containing many compounds are more difficult to identify – and many archaeological samples are complex mixtures. Mixtures sometimes have many absorption bands, which overlap, yielding only broad envelopes of adsorption and few distinctive features. Each spectrum collected from a sample is considered to serve as a chemical fingerprint. Comparison of this spectrum with a set of standard spectra, as well as a reference library that is continually being expanded, provides information critical to identifying the unknown material. Carbohydrates, lipids, proteins, etc. all are associated with specific wave number bands (Isaksson 2000:36-39). Identifying geologic materials, such as asphaltum, is simpler than working with the combinations of materials often found in archaeological samples.

## DISCUSSION

The East Canyon fault is located between East Canyon and Croyden in the Wasatch Range, northeast Utah. Local vegetation in this area is dominated by sagebrush (*Artemisia*) and grasses (Poaceae). Eight samples from Trenches 5, 8, and 9 were analyzed for organic material that could be submitted for AMS radiocarbon analysis.

Sample ECT-C1 was recovered from Unit 5d - lower (Table 1). The only organic material present in this sample were a few uncharred rootlets from modern plants (Table 2). A moderate amount of possible asphaltum spheres were noted, as well as two pieces of coal. Natural asphaltum in eastern Utah is called gilsonite or uintahite.

Sample ECT-C2 from Unit 5d - upper yielded numerous possible asphaltum spheres and one piece of coal. One uncharred Boraginaceae seed (Table 3), a few Poaceae leaf/stem fragments, and a few uncharred rootlets represent modern plants. No charred organic material suitable for AMS radiocarbon analysis was present.

Sample ECT-C3 was collected from the lower portion of Unit 5e. This sample yielded six small fragments of charcoal too small for identification weighing less than 0.001 g. One piece of unidentified root charcoal weighing less than 0.001 g also was present. These charcoal fragments were too small for AMS radiocarbon dating. In addition, the sample contained a few uncharred rootlets from modern plants, a few possible asphaltum spheres, a piece of coal, and a rodent tooth fragment.

Four pieces of charcoal too small for identification and weighing less than 0.001 g were present in sample ECT-C4 from the upper portion of Unit 5e. One piece of charred PET fruity tissue weighing less than 0.001 g also was present. The term PET (processed edible tissue) was originated by Nancy Stenholm (1994) and refers to softer tissue types, such as starchy parenchymoid or fruity epitheloid tissues. PET fruity tissues resemble sugar-laden fruit or berry tissue without the seeds, as well as tissue from succulent plant parts such as cactus pads. A few uncharred roots and rootlets represent modern plants. Non-floral remains include a moderate amount of possible asphaltum spheres, a coal fragment, and one piece of rodent tooth enamel.

Samples ECT-C7 and ECT-C8 also were recovered from Unit 5. Sample ECT-C7 contained numerous possible asphaltum spheres, as well as a few uncharred roots and rootlets from modern plants.

Eight charred, vitrified monocot/herbaceous dicot stem fragments were present in sample ECT-C8. Vitrified material has a shiny, glassy appearance due to fusion by heat. These stem fragments weighed 0.018 g and were processed for AMS radiocarbon analysis. A conventional AMS radiocarbon date of  $10280 \pm 25$  RC yr. BP (PRI-06-95-C8) was returned for the charred stem fragments, with a two-sigma calibrated date of 12160-11970 CAL yr. BP (Table 4, Figure 1). In addition, the sample yielded a moderate amount of possible asphaltum spheres and a few uncharred rootlets from modern plants.

Sample ECT-C5 from Unit 8 yielded several fragments of charcoal weighing less than 0.001 g. These charcoal fragments were too small for identification and too small for AMS radiocarbon dating. A few possible asphaltum spheres and a few uncharred roots and rootlets from modern plants also were present.

Sample ECT-C6 was collected from Unit 9. Organic remains in this sample consist of a moderate amount of uncharred rootlets from modern plants. Non-floral remains include a moderate amount of possible asphaltum spheres, two small fragments of coal, and one insect chitin fragment.

Fourier Transform infrared spectrometry (FTIR) was performed on the possible asphaltum spheres from sample ECT-C6. The spectrum obtained from this sample was compared to spectra from street asphalt, California asphalt, and historic coal. No gilsonite currently is available for comparison. The spectrum from sample ECT-C6 compared most favorably with that from asphalt collected in the street (Figure 2). Asphalt in Colorado is made using natural asphalt obtained from Wyoming, the Colorado Basin in western Colorado, Kansas, Texas, Oklahoma, and others (personal communication, Tom Clayton, Colorado Asphalt Pavement Association, February 13, 2007).

## **SUMMARY AND CONCLUSIONS**

Flotation of bulk samples from East Canyon Trench in northeast Utah resulted in recovery of very few charred organic remains. Charcoal was present in three of the samples; however, these charcoal fragments were too small for dating. Sample ECT-C8 yielded charred monocot/herbaceous dicot stem fragments in sufficient quantities for AMS radiocarbon dating.

These charred stem fragments yielded a conventional AMS radiocarbon date of  $10280 \pm 25$  RC yr. BP (PRI-06-95-C8). All of the samples yielded varying amounts of possible asphaltum spheres that might represent a natural asphalt in northeast Utah called gilsonite. Initial FTIR analysis of this material from sample ECT-C6 compared most favorably with street asphalt. Further comparisons will be made when a sample or spectrum of gilsonite is available.

TABLE 1  
 PROVENIENCE DATA FOR SAMPLES FROM EAST CANYON TRENCH, UTAH

Sample No.	Trench Unit No.	Context/Significance; Morphologic/Sedimentary Constraints	Analysis
ECT-C1	5d (lower)	Pre-event 1 sed	Float/Charcoal ID
ECT-C2	5d (upper)	Pre-event 1 sed/soil	Float/Charcoal ID
ECT-C3	5e (lower)	Event 1 sed/wedge; Sedimentation appears continuous throughout Unit 5	Float/Charcoal ID
ECT-C4	5e (upper)	Sed/soil buried by MRE; Faulted, minimal overlying sediment/soils	Float/Charcoal ID
ECT-C7	5	Sed/soil buried by MRE; Faulted, minimal overlying sediment/soils	Float/Charcoal ID
ECT-C8	5	Sed/soil buried by MRE; Faulted, minimal overlying sediment/soils	Float/Charcoal ID AMS <sup>14</sup> C analysis
ECT-C5	8	Post-MRE sediments; Minimal soil development	Float/Charcoal ID
ECT-C6	9	Post-MRE sediments; Minimal soil development	Float/Charcoal ID

TABLE 2  
MACROFLORAL REMAINS IN SAMPLES FROM EAST CANYON TRENCH, UTAH

Sample No.	Identification	Part	Charred		Uncharred		Weights/ Comments
			W	F	W	F	
C-1	Liters Floated						2.60 L
Unit 5d (Lower)	Light Fraction Weight						0.67 g
	FLORAL REMAINS:						
	Rootlets					X	Few
	NON-FLORAL REMAINS:						
	cf. Asphaltum - spheroid Coal Rock/Gravel				X	2 X	Moderate 0.040 g Moderate
C-2	Liters Floated						2.40 L
Unit 5d (Upper)	Light Fraction Weight						0.79 g
	FLORAL REMAINS:						
	Boraginaceae	Seed			1		
	Poaceae	Leaf/stem				X	Few
	Rootlets					X	Few
	NON-FLORAL REMAINS:						
cf. Asphaltum - spheroid Coal Rock/Gravel					X 1 X	Numerous 0.019 g Moderate	
C-3	Liters Floated						2.40 L
Unit 5e (Lower)	Light Fraction Weight						0.31 g
	FLORAL REMAINS:						
	Rootlets					X	Few
	CHARCOAL/WOOD:						
	Unidentifiable - small	Charcoal		6			<0.001 g
	Unidentified root	Charcoal		1			<0.001 g
	NON-FLORAL REMAINS:						
	cf. Asphaltum - spheroid Coal Rock/Gravel Rodent tooth				X	1 X 1	Few 0.008 g Moderate

TABLE 2 (Continued)

Sample No.	Identification	Part	Charred		Uncharred		Weights/ Comments
			W	F	W	F	
C-4	Liters Floated						2.40 L
Unit 5e (Upper)	Light Fraction Weight						2.51 g
	FLORAL REMAINS:						
	PET Fruity Roots Rootlets	Tissue		1		X X	<0.001 g Few Few
	CHARCOAL/WOOD:						
	Unidentifiable - small	Charcoal		4			<0.001 g
	NON-FLORAL REMAINS:						
	cf. Asphaltum - spheroid Coal Rock/Gravel Rodent tooth enamel				X	1 X 1	Moderate 0.002 g Moderate
C-7	Liters Floated						2.10 L
Unit 5	Light Fraction Weight						0.71 g
	FLORAL REMAINS:						
	Roots Rootlets					X X	Few Few
	NON-FLORAL REMAINS:						
	cf. Asphaltum - spheroid Rock/Gravel					X X	Numerous Few
C-8 Feature Unit 5	Liters Floated						2.60 L
	Light Fraction Weight						0.29 g
	FLORAL REMAINS:						
	Monocot/Herbaceous dicot - vitrified ** Rootlets	Stem		8		X	0.018 g Few
	NON-FLORAL REMAINS:						
cf. Asphaltum - spheroid Rock/Gravel					X X	Moderate Few	

TABLE 2 (Continued)

Sample No.	Identification	Part	Charred		Uncharred		Weights/ Comments	
			W	F	W	F		
C-5	Liters Floated						2.75 L	
Feature Unit 8	Light Fraction Weight						2.00 g	
	FLORAL REMAINS:							
	Root					1	Moderate	
	Rootlets					X		
	CHARCOAL/WOOD:							
	Unidentifiable - small	Charcoal		14			<0.001 g	
NON-FLORAL REMAINS:								
cf. Asphaltum - spheroid						X	Few	
	Rock/Gravel					X	Few	
C-6	Liters Floated						2.40 L	
Unit 9	Light Fraction Weight						2.01 g	
	FLORAL REMAINS:							
	Rootlets					X	Moderate	
	NON-FLORAL REMAINS:							
	cf. Asphaltum - spheroid						X	Moderate
	Coal						2	0.01 g
Insect	Chitin					1		
	Rock/Gravel					X	Few	

W = Whole  
 F = Fragment  
 X = Presence noted in sample  
 L = Liters  
 g = grams  
 \* = Estimated frequency  
 \*\* = Submitted for AMS radiocarbon dating

TABLE 3  
INDEX OF MACROFLORAL REMAINS RECOVERED FROM EAST CANYON TRENCH, UTAH

Scientific Name	Common Name
FLORAL REMAINS:	
Boraginaceae	Borage family
Monocot/Herbaceous dicot	A member of the Monocotyledonae class of Angiosperms, which include grasses, sedges, lilies and palms/A non-woody member of the Magnoliopsida class of Angiosperms, which is characterized by embryos with two cotyledons
Poaceae	Grass family
PET fruity tissue	Fruity epitheloid tissues; resemble sugar-laden fruit or berry tissue without the seeds, or succulent plant tissue such as cactus pads

TABLE 4  
RADIOCARBON RESULTS FROM EAST CANYON TRENCH, UTAH

Sample No.	Sample Identification	AMS <sup>14</sup> C Date*	1-sigma Calibrated Date (68.2%)	2-sigma Calibrated Date (95.4%)	δ <sup>13</sup> C (‰)
ECT-C8	Monocot/Herbaceous dicot stem - vitrified	10280 ± 25 RC yr. BP	12095-11995 CAL yr. BP	12160-11970 CAL yr. BP	-22.4

\* Reported in radiocarbon years at 1 standard deviation measurement precision (68.2%), corrected for δ<sup>13</sup>C

## REFERENCES CITED

- Black, B.D. and S. Hecker  
1999 Fault Number 2354b, East Canyon Fault. Electronic document,  
<http://earthquakes.usgs.gov/regional/qfaults>, accessed February 13, 2007. U.S.  
Geological Survey Website.
- Core, H. A., W. A. Cote and A. C. Day  
1976 *Wood Structure and Identification*. Syracuse University Press, Syracuse, New  
York.
- Isaksson, Sven  
2000 *Food and Rank in Early Medieval Time*. Archaeological Research Laboratory,  
Stockholm University, Stockholm.
- Martin, Alexander C. and William D. Barkley  
1961 *Seed Identification Manual*. University of California, Berkeley, California.
- Matthews, Meredith H.  
1979 Soil Sample Analysis of 5MT2148: Dominguez Ruin, Dolores, Colorado.  
Appendix B. In *The Dominguez Ruin: A McElmo Phase Pueblo in Southwestern  
Colorado*, edited by A. D. Reed. Bureau of Land Management Cultural Resource Series.  
vol. 7. Bureau of Land Management, Denver, Colorado.
- Panshin, A. J. and Carl de Zeeuw  
1980 *Textbook of Wood Technology*. McGraw-Hill Book, Co., New York, New York.
- Petrides, George A. and Olivia Petrides  
1992 *A Field Guide to Western Trees*. The Peterson Field Guide Series. Houghton  
Mifflin Co., Boston.
- Stenholm, Nancy A.  
1994 Paleoethnobotanical Analysis of Archaeological Samples Recovered in the Fort  
Rock Basin. In *Archaeological Researches in the Northern Great Basin: Fort Rock  
Archaeology since Cressman*, edited by C. M. Aikens and D. L. Jenkins, pp. 531-560.  
University of Oregon Anthropological Papers 50. Department of Anthropology and State  
Museum of Anthropology, University of Oregon, Eugene, Oregon.

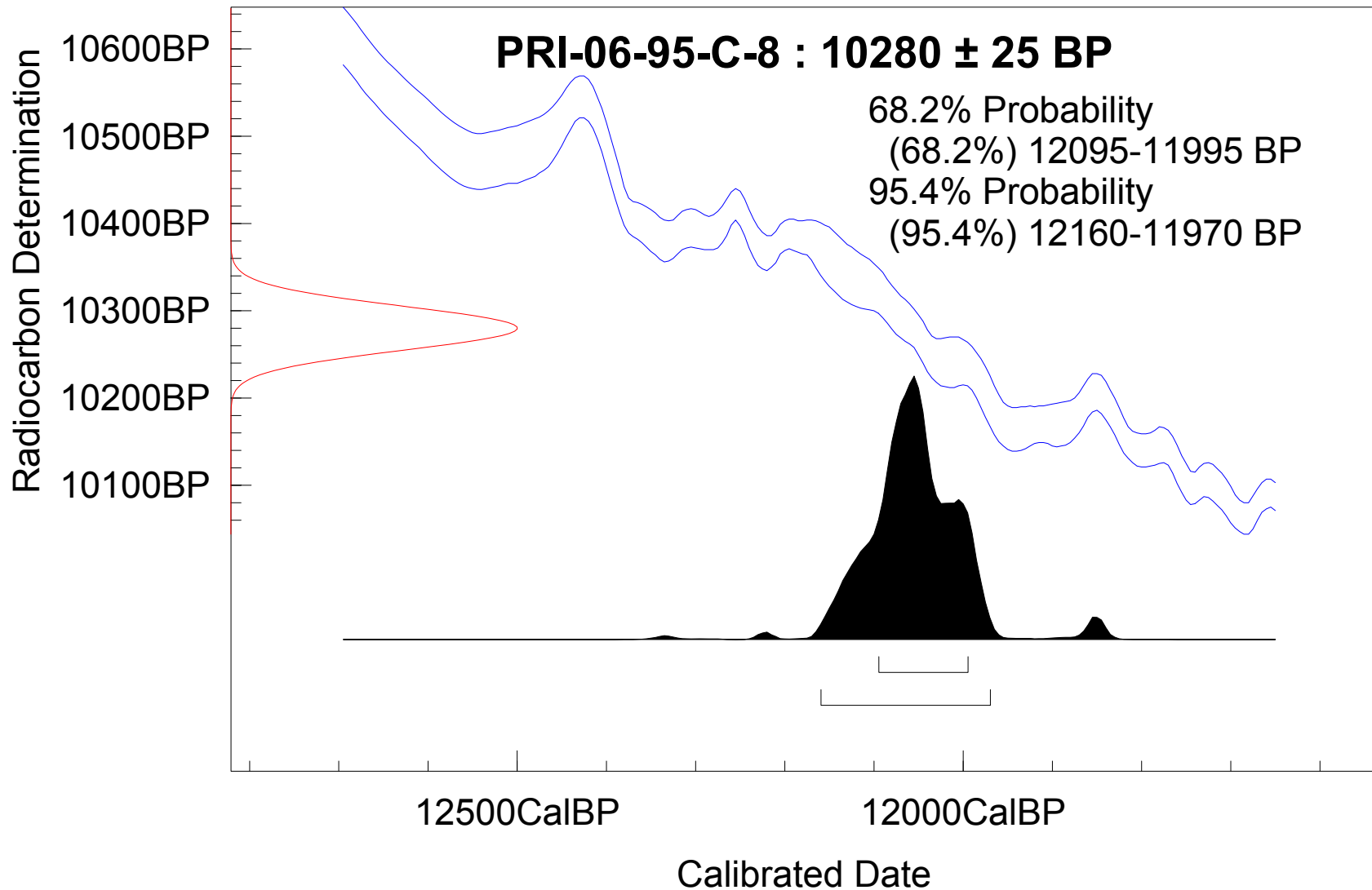


FIGURE 1. AMS RADIOCARBON RESULTS FROM EAST CANYON TRENCH, UTAH.

**Appendix G.**  
**Analyses on Asphaltum Samples From Trench Across Main Canyon**  
**Fault, Summit County, Utah**

This appendix includes the following reports on asphaltum samples from the trench across the Main Canyon fault:

**Report G-1.**

**Geochemical Analysis of an Asphaltum Sample, Summit County, Utah**

**By**

**B.M. Jarvie and D.M. Jarvie**

**Humble Instruments & Services, Inc.**

**Humble Geochemical Services Division**

**Humble, Texas**

**Report G-2.**

**FTIR Spectrum Analyses for Asphaltum in Sample ECT-C6**

**By**

**Paleo Research Institute**

**Golden, Colorado**

**Report G-1.**  
**Geochemical Analysis of an Asphaltum Sample, Summit County, Utah**  
**By**  
**B.M. Jarvie and D.M. Jarvie**  
**Humble Instruments & Services, Inc.**  
**Humble Geochemical Services Division**  
**Humble, Texas**



## ***Humble Geochemical Services***

Division of Humble Instruments & Services, Inc.  
218 Higgins Street Humble, Texas 77338  
P.O. Box 789 Humble, Texas 77347

**Telephone:** 281-540-6050 **Fax:** 281-540-2864

---

# Geochemical Analysis of an Asphaltum Sample, Summit County, Utah

Prepared for U.S. Bureau of Reclamation

Prepared by B.M. Jarvie & D.M. Jarvie

Project 07-4355

Humble Geochemical Services Division  
Humble Instruments & Services, Inc.

February, 2007

## Interpretative Summary

Whole Extract Gas Chromatography (GC) and Gas Chromatography-Mass Spectrometry (GC-MS) has been performed on a sample (#ECT-C7) identified as asphaltum spheroids from a backhoe trench outcrop locality in Summit County, Utah. The sample was submitted for analysis by the U.S. Bureau of Reclamation and is noted as being found in Holocene aged alluvium at a depth of 0.7 meters. The sample provided for analysis was crushed in a mortar under solvent to rapidly extract the asphaltum and the recovered product was very light yellow in color. The limited amounts of extract precluded quantification and subsequent fractional liquid chromatographic separation techniques could not be applied.

To address the origin of this asphaltum sample, the extract was initially analyzed by GC to examine its hydrocarbon fingerprint (all data documented in the attachments to this report). The whole extract gas chromatographic fingerprint shows relatively abundant hydrocarbon components, along with low molecular weight aromatics and some unidentified peaks. Most of the major peaks are identified by abbreviation and consist predominantly of normal alkanes such as n-C<sub>13</sub>, which is the predominant peak in the gas chromatogram. The alkane envelope is generally unimodal and extends from n-C<sub>13</sub> to n-C<sub>29</sub>. Attenuation of lower molecular weight components is attributable to weathering effects associated with this outcrop sample. Branched chain isoprenoids are also abundant in the asphaltum extract. The distribution of these isoprenoid biomarkers, such as pristane and phytane, can be used to assess source rock kerogen type and depositional environment. These ratios (Pr/Ph = 1.24) are generally indicative of an origin from low sulfur marine shale source rocks containing predominant Type II marine algal organic matter deposited under oxic to sub-oxic conditions, however, they are not entirely unique and other source rock types (e.g. lacustrine) can also have similar ratios.

The relatively wide distribution of alkanes indicates minimal secondary alteration effects on the extract from processes such as biodegradation. Further, this pattern is not typical of processed petroleum products, such as diesel, which tend to have narrow boiling point ranges due to fractional distillation during processing. Catalytic hydrocracking during processing also typically produces a complex and wide range of branched chained components that have rather diagnostic fingerprints. These features also appear to be missing from the asphaltum sample, although it contains abundant isoprenoids in a pattern common to naturally occurring crude oils. Low molecular weight aromatic compounds, such as toluene and xylenes are present in this extract and several unidentified peaks elsewhere in the chromatogram also likely represent aromatic or other functionalized hydrocarbon compounds (eg. the major peak just past n-C<sub>28</sub>).

With preliminary GC analysis suggesting that the asphaltum was not a processed hydrocarbon sample, but likely represented a natural crude oil seep, further GC-MS biomarker analyses were undertaken. The patterns commonly found in saturated hydrocarbons, such as the steranes and hopanes, were analyzed in the whole extract using a single ion monitoring GC-MS program. The amounts of steranes and hopanes are considered low (judging from the moderately high signal/noise ratio) and they appear to possibly have some cross-over contamination from unidentified compounds. However, the patterns present are typical of natural crude oils and further support the interpretative conclusion that this asphaltum does not represent a processed hydrocarbon sample.

Steranes are dominated by the C<sub>27</sub> regular sterane series of compounds, with relatively low abundances of the diasteranes. This pattern is typical of many marine carbonate sourced crude oils commonly associated with Cretaceous aged source rocks, but is also found in some lacustrine source rocks, such as the saline facies oil shales in the Green River

Formation. Some sterane maturity ratios, such as the  $C_{29} 20S/(S+R)$ , appear to be near their thermal endpoint values of  $\sim 0.5$ , suggesting a peak oil window maturity. However, all sterane maturity ratios are not consistent due to relatively poor data quality. In general, the overall pattern within the sterane chromatograms is consistent with the asphaltum originating from thermally mature natural crude oil seep.

Hopane distributions show approximately equal abundances of tricyclic terpanes and pentacyclic hopanes. The hopanes are dominated by  $C_{30}$  hopane, with lesser amounts of the  $C_{29}$  norhopane. The biomarker gammacerane appears to be present in these sample, which is used to infer anoxic depositional conditions and is commonly found in lacustrine source rocks, such as the Tertiary Green River Formation. The  $Ts/Tm$  hopane maturity ratio shows depleted amounts of  $Tm$  indicating a peak oil window thermal maturity. This assessment is corroborated by  $C_{32} S/(S+R)$  terpane ratios that appear to have reached their thermal endpoints.

In summary, based on whole extract GC and GC-MS analyses the asphaltum sample collected from Summit County, Utah appears to be some type of a natural crude oil seep. The geochemical analyses are certainly not unequivocal, due to the generally insoluble nature of the asphaltum and low yields of extract recovered. However, the molecular fingerprints from the asphaltum show distributions of hydrocarbons, including alkanes, that are typical of natural crude oils and unlike processed hydrocarbon samples. Biomarker patterns in the steranes and hopanes also show distributions of compounds typical for natural crude oils of peak oil window maturity and further indicate that the asphaltum is not contamination from processed hydrocarbons nor associated with bitumen seepage from a low maturity source rock (eg. gilsonite type deposits located elsewhere in Utah). Although the extract from the asphaltum shows no indications of extensive secondary alteration by biodegradation, attenuation of low molecular weight compounds has undoubtedly occurred as a consequence of near-surface exposure. Such devolatilization may also explain the relatively insoluble nature of the asphaltum, although further quantitative experimentation and other analytical techniques, such as thermal extract gas chromatography (TE-GC) and/or pyrolysis gas chromatography (Py-GC) would need to be applied to address this aspect in more detail.

## **Experimental Methods**

### ***Extraction***

Samples were extracted using carbon disulfide as a solvent. The samples were crushed in a mortar and pestle under solvent, filtered to remove and residual solid material and evaporated to a an ~1 ml aliquot size.

### ***Whole Fluid Chromatography***

Gas chromatography may be completed on whole extract or oil samples as well as on the saturate or aromatic fractions. Gas chromatography is performed using HP 6890 Series GC System with high-resolution column (50 m, PONA phase, 0.2 mm i.d., 0.5  $\mu$ m film). A 2  $\mu$ l aliquot of diluted sample is injected into the 300°C split inlet set at a 50/1 split ratio. The GC is temperature programmed from 35°C (20 min. hold) to 300°C at 8°C/min. and then to 325°C at 0.5°C/min. with a final hold time of 30 min. Light hydrocarbons, isoprenoids and normal paraffins are identified when they are present in the sample.

### ***Biomarkers***

Samples are prepared by performing liquid chromatography (LC) on oil or extracts samples to isolate saturate and aromatic fractions. Saturate fractions are diluted with 5  $\mu$ l and aromatic fractions/whole extracts/whole oils with 10  $\mu$ l of carbon disulfide per mg of fraction.  $\beta$ -cholane and *o*-terphenyl-d14 are used as saturate and aromatic internal standards, respectively. Samples are analyzed on an HP6890GC / 5973MSD system equipped with a high-resolution column (60 m, DB-1 phase, 0.2 mm i.d., 0.2  $\mu$ m film). The GC is temperature programmed from 80°C (2 min. hold) to 320°C at 3.5°C/min. with a final hold time of 20 min. There is a 7.5 min. solvent delay on acquisition and selected ion monitoring (SIM) is the standard method for analysis. Reports of peaks and standard geochemical parameters are included for both the saturate and aromatic fractions.

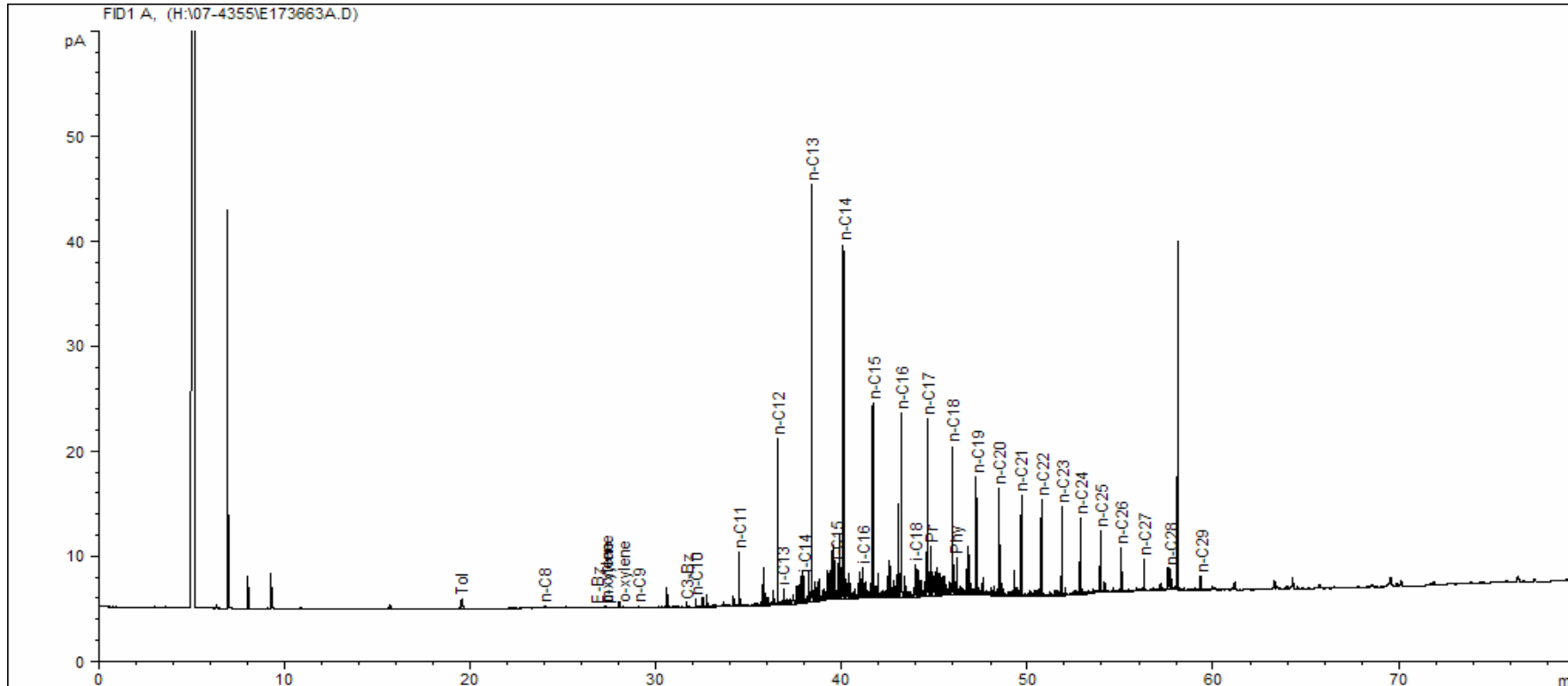


# Humble Geochemical Services

Division of Humble Instruments & Services, Inc.

218 Higgins Street Humble, TX 77338  
P. O. Box 789 Humble, TX 77347  
Telephone: 281-540 6050 Fax: 281-540 2864

Client: **United States Department of Energy** Formation: **API:**  
Client ID: **ECT-C7** Basin:  
HGS ID: **07-4355-173663** Country:  
Type: **asphaltum spheroids** County, State: **Summit Co., UT**  
Well:  
Depth:  
Field:







# Humble Geochemical Services

Division of Humble Instruments & Services, Inc.

218 Higgins Street Humble, TX 77338  
P. O. Box 789 Humble, TX 77347  
Telephone: 281-540 6050 Fax: 281-540 2864

Client: United States Department of the Interior  
Client ID: ECT-C7 API:  
HGS ID: 07-4355-173663 County,State: Summit Co., UT  
Type: asphaltum spheroids  
Well:  
Depth:  
Field:  
Formation:  
Basin:  
Country:

## Gas Chromatography Integration Results

Peak Label	Compound Name	R.Time (min.)	Peak Height	Peak Area
i-C4	iso-butane	0.00	0	0
n-C4	butane	0.00	0	0
i-C5	iso-pentane	0.00	0	0
n-C5	pentane	0.00	0	0
22-DMB	2,2-dimethylbutane	0.00	0	0
CP	cyclopentane	0.00	0	0
23-DMB	2,3-dimethylbutane	0.00	0	0
2-MP	2-methylpentane	0.00	0	0
3-MP	3-methylpentane	0.00	0	0
I-Std.	Internal Standard	0.00	0	0
n-C6	hexane	0.00	0	0
22-DMP	2,2-dimethylpentane	0.00	0	0
MCP	methylcyclopentane	0.00	0	0
24-DMP	methylcyclopentane	0.00	0	0
223-TMB	2,2,3-trimethylbutane	0.00	0	0
Bz	benzene	0.00	0	0
33-DMP	3,3-dimethylpentane	0.00	0	0
CH	cyclohexane	0.00	0	0
2-MH	2-methylhexane	0.00	0	0
23-DMP	2,3-dimethylpentane	0.00	0	0
11-DMCP	1,1-dimethylcyclopentane	0.00	0	0
3-MH	3-methylhexane	0.00	0	0
c-13-DMCP	cis-1,3-dimethylcyclopentane	0.00	0	0
t-13-DMCP	trans-1,3-dimethylcyclopentane	0.00	0	0
3-EP	3-ethylpentane	0.00	0	0
t-12-DMCP	trans-1,2-dimethylcyclopentane	0.00	0	0
n-C7	heptane	0.00	0	0
MCH	methylcyclohexane	0.00	0	0
ECP	ethylcyclopentane	0.00	0	0
Tol	toluene	19.54	1	6
n-C8	octane	24.04	0	1
E-Bz	ethylbenzene	26.89	0	0
m-xylene	meta-xylene	27.29	0	0
p-xylene	para-xylene	27.34	0	0
o-xylene	ortho-xylene	28.23	0	0
n-C9	nonane	29.10	0	0
C3-Bz	propylbenzene	31.67	0	0
n-C10	decane	32.14	1	1
n-C11	undecane	34.52	5	8
n-C12	dodecane	36.56	16	23
i-C13	C13 isoprenoid	36.87	2	3
i-C14	C14 isoprenoid	37.97	3	5
n-C13	tridecane	38.40	40	59
i-C15	farnesane (C15 isoprenoid)	39.78	3	5
n-C14	tetradecane	40.10	34	51
i-C16	C16 isoprenoid	41.16	3	7
n-C15	pentadecane	41.70	19	28
n-C16	hexadecane	43.20	18	29
i-C18	norpristane (C18 isoprenoid)	43.96	3	6
n-C17	heptadecane	44.63	17	31
Pr	pristane (C19 isoprenoid)	44.78	5	9
n-C18	octadecane	45.98	14	23
Phy	phytane (C20 isoprenoid)	46.18	4	7
n-C19	nonadecane	47.26	11	18
n-C20	eicosane	48.49	10	15
n-C21	heneicosane	49.66	10	14
n-C22	docosane	50.79	9	14
n-C23	tricosane	51.86	8	13
n-C24	tetracosane	52.90	7	11
n-C25	pentacosane	53.93	6	10
n-C26	hexacosane	55.05	4	8
n-C27	heptacosane	56.31	3	7
n-C28	octacosane	57.72	2	5
n-C29	nonacosane	59.33	1	5
n-C30	triacontane	0.00	0	0
n-C31	hentriacontane	0.00	0	0
n-C32	dotriacontane	0.00	0	0
n-C33	tritriacontane	0.00	0	0
n-C34	tetratriacontane	0.00	0	0
n-C35	pentatriacontane	0.00	0	0
n-C36	hexatriacontane	0.00	0	0
n-C37	heptatriacontane	0.00	0	0
n-C38	octatriacontane	0.00	0	0
n-C39	nonatriacontane	0.00	0	0
n-C40	tetracontane	0.00	0	0
n-C41	hentetracontane	0.00	0	0
n-C42	dotetracontane	0.00	0	0
n-C43	tritetracontane	0.00	0	0
b-CAROTANE	beta-carotane	0.00	0	0
n-C44	tetratetracontane	0.00	0	0
n-C45	pentatetracontane	0.00	0	0
n-C46	hexatetracontane	0.00	0	0



# Humble Geochemical Services

Division of Humble Instruments & Services, Inc.

218 Higgins Street Humble, TX 77338  
 P. O. Box 789 Humble, TX 77347  
 Telephone: 281-540 6050 Fax: 281-540 2864

Client: **United States Department of the Interior**  
 Client ID: **ECT-C7** API:  
 HGS ID: **07-4355-173663** County, State: **Summit Co., UT**  
 Type: **asphaltum spheroids**  
 Well:  
 Depth:  
 Field:  
 Formation:  
 Basin:  
 Country:

<b>Gas Chromatography Interpretive Ratios</b>			
<b>Interpretive Ratios</b>		<b>Interpretive Ratios</b>	
<b>Ratios by Area</b>		<b>Mango Ratios<sup>2</sup></b>	
Pristane / Phytane	1.24	P1	not available
Prisane / nC17	0.29	P2	not available
Phytane / nC18	0.32	P3	not available
nC18 / (nC18 + nC19)	0.55	5N1	not available
nC17 / (nC17 + nC27)	0.82	6N1	not available
Carbon Preference Index	1.18	N2	not available
<b>Totals by Weight %</b>		<b>Invariant Ratios</b>	
Normal Alkanes	not available	K1	not available
Isoalkanes	not available	K2	not available
Branched Alkanes	not available	<b>Ring Preference Ratios</b>	
Cycloalkanes	not available	5N1 / 6N1	not available
Aromatics	not available	P3 / N2	not available
<b>Halpern Ratios<sup>1</sup></b>		<b>Thompson Ratios<sup>3</sup></b>	
Tr1	#DIV/0!	Bz / nC6	#DIV/0!
Tr2	#DIV/0!	Tol / nC7	#DIV/0!
Tr3	#DIV/0!	(nC6 + nC7) / (CH + MCH)	#DIV/0!
Tr4	#DIV/0!	Isoheptane Value	#DIV/0!
Tr5	#DIV/0!	nC7 / MCH	#DIV/0!
Tr6	not available	CH / MCP	#DIV/0!
Tr7	#DIV/0!	nC7 / 2-MH	#DIV/0!
Tr8	#DIV/0!	nC6 / 2,2-DMB	#DIV/0!
C1	#DIV/0!	Heptane Value	#DIV/0!
C2	#DIV/0!		
C3	#DIV/0!		
C4	#DIV/0!		
C5	#DIV/0!		

<sup>1</sup> Halpern, H.I., 1995. APPG Bull.: v.79, p801-815

<sup>2</sup> Mango, F.D., 1994. GCS: V.58, p.895-901

<sup>3</sup> Thompson, K.F.M., 1983. GCA: v.47, p303-316



# Humble Geochemical

Division of Humble Instruments & Services, Inc.

218 Higgins Street Humble, TX 77338  
 P. O. Box 789 Humble, TX 77347  
 Telephone: 281-540 6050 Fax: 281-540

**Client:** United States Department of the Interior  
**Client ID:** ECT-C7  
**HGS ID:** 07-4355-173663  
**Well:**  
**Depth:**  
**Field:**  
**Lease:**  
**Formation:**  
**Basin:**  
**County, State:** Summit Co., UT  
**Country:**

Bulk Properties	
API (°)	
S (%)	
Saturate (%)	
Aromatics (%)	
Resin (%)	
Asphaltene (%)	
$\delta^{13}C$ Sat (‰)	
$\delta^{13}C$ Aro (‰)	
$\delta^{13}C$ Res (‰)	
$\delta^{13}C$ Asp (‰)	
$\delta^{13}C$ Oil (‰)	

Whole Oil/Extract GC	
CPI	
Pristane/n-C17	
Phytane/n-C18	
Pristane/Phytane	

**C<sub>27</sub>-C<sub>28</sub>-C<sub>29</sub>  
αβ Steranes**

**Tricyclic,  
Pentacyclic  
Terpanes &  
Steranes**

Saturate Biomarker Interpretive Ratios			
Interpretive Ratios	By Area	By Height	
<u>Terpanes (m/z 191)</u>			
C19t/C23t	0.36	0.30	
C22t/C21t	0.55	0.41	
C22t/C24t	1.18	0.87	
C24t/C23t	0.36	0.36	
C26t/C25t	0.84	0.79	
C24Tet/C23t	0.21	0.19	
C24Tet/C26t	0.81	0.74	
C23t/C30H	0.63	0.68	
C24Tet/C30H	0.14	0.13	
C28BNH/C30H	0.00	0.00	
25-Nor/C30H	0.00	0.00	
C29H/C30H	0.63	0.59	
C30DiaH/C30H	0.18	0.20	
Ole/C30H	0.06	0.15	
C30Ts/C30H	0.08	0.10	
Gam/C30H	0.08	0.13	
Gam/C31HR	0.27	0.49	
C35HS/C34HS	#DIV/0!	#DIV/0!	
C35 Homohopane Index	0.00	0.00	
Ts/(Ts+Tm)	0.57	0.58	
C29Ts/(C29Ts+C29H)	0.31	0.30	
Mor/C30H	0.10	0.13	
C32 S/(S+R)	0.63	0.60	
<u>Steranes (m/z 217)</u>			
% C27 ααα 20R	32.3	38.4	
% C28 ααα 20R	21.4	16.6	
% C29 ααα 20R	46.3	44.9	
C27 Dia/(Dia+Reg)	0.27	0.38	
(C21+C22)/(C27+C28+C29)	0.13	0.20	
C29 αββ/(ααα+αββ)	0.38	0.45	
C29 ααα 20S/20R	0.72	0.48	
C29 ααα 20S/(S+R)	0.42	0.33	
<u>αββ- Steranes (m/z 218)</u>			
% C27 αββ 20(R+S)	54.6	50.6	
% C28 αββ 20(R+S)	16.1	18.5	
% C29 αββ 20(R+S)	29.3	30.9	
C29/C27 αββ Sterane Ratio	0.54	0.61	
Tricyclic/Pentacyclic Terpanes	0.52	0.55	
Steranes/Terpanes	0.23	0.19	
% Tricyclic Terpanes	27.6	29.9	
% Pentacyclic Terpanes	53.5	53.9	
% Steranes	18.8	16.1	



# Humble Geochemical Services

Division of Humble Instruments & Services, Inc.

218 Higgins Street Humble, TX 77338  
P. O. Box 789 Humble, TX 77347  
Telephone: 281-540 6050 Fax: 281-540 2864

Client: **United States Department of the Interior**  
Client ID: **ECT-C7**  
HGS ID: **07-4355-173663**  
Well:  
Depth:  
Field:  
Lease  
Formation:

Basin:  
County,State: **Summit Co., UT**  
Country:

Saturate Biomarker Integration Results (Steranes)							
Ion	Peak Label	Compound Name	R.Time (min.)	Peak Area	ppm (A.)	Peak Height	ppm (Ht.)
217	S21	C21 sterane	47.24	4739	#DIV/0!	1659	#DIV/0!
217	S22	C22 sterane	49.93	1063	#DIV/0!	483	#DIV/0!
217	27Dbas	C27 ba 20S diacholestane	57.17	1827	#DIV/0!	708	#DIV/0!
217	27DbasR	C27 ba 20R diacholestane	57.92	990	#DIV/0!	438	#DIV/0!
217	28DbasSA	C28 ba 20S diasterane a	0.00	0	#DIV/0!	0	#DIV/0!
217	28DbasSB	C28 ba 20S diasterane b	0.00	0	#DIV/0!	0	#DIV/0!
217	28DbasRA	C28 ba 20R diasterane a	0.00	0	#DIV/0!	0	#DIV/0!
217	28DbasRB	C28 ba 20R diasterane b	0.00	0	#DIV/0!	0	#DIV/0!
217	27aaS	C27 aa 20S cholestane	60.29	4008	#DIV/0!	807	#DIV/0!
217	27bbR	C27 bb 20R cholestane	60.49	13175	#DIV/0!	2881	#DIV/0!
217	27bbS	C27 bb 20S cholestane	60.60	3794	#DIV/0!	1035	#DIV/0!
217	27aaR	C27 aa 20R cholestane	61.25	3508	#DIV/0!	1029	#DIV/0!
217	28aaS	C28 aa 20S ergostane	62.33	590	#DIV/0!	338	#DIV/0!
217	28bbR	C28 bb 20R ergostane	62.59	1938	#DIV/0!	371	#DIV/0!
217	28bbS	C28 bb 20S ergostane	62.75	2294	#DIV/0!	613	#DIV/0!
217	28aaR	C28 aa 20R ergostane	63.34	2325	#DIV/0!	445	#DIV/0!
217	29aaS	C29 aa 20S stigmastane	63.93	3612	#DIV/0!	583	#DIV/0!
217	29bbR	C29 bb 20R stigmastane	64.23	2881	#DIV/0!	775	#DIV/0!
217	29bbS	C29 bb 20S stigmastane	64.32	2521	#DIV/0!	711	#DIV/0!
217	29aaR	C29 aa 20R stigmastane	65.05	5029	#DIV/0!	1203	#DIV/0!
218	27bbR	C27 bb 20R cholestane	60.50	6925	#DIV/0!	1840	#DIV/0!
218	27bbS	C27 bb 20S cholestane	60.60	3706	#DIV/0!	1050	#DIV/0!
218	28bbR	C28 bb 20R ergostane	62.61	1490	#DIV/0!	422	#DIV/0!
218	28bbS	C28 bb 20S ergostane	62.76	1648	#DIV/0!	632	#DIV/0!
218	29bbR	C29 bb 20R stigmastane	64.23	3051	#DIV/0!	874	#DIV/0!
218	29bbS	C29 bb 20S stigmastane	64.33	2649	#DIV/0!	890	#DIV/0!
259	27Dbas	C27 ba 20S diacholestane	57.17	1340	#DIV/0!	450	#DIV/0!
259	27DbasR	C27 ba 20R diacholestane	57.92	850	#DIV/0!	282	#DIV/0!
259	28DbasSA	C28 ba 20S diaergostane a	0.00	0	#DIV/0!	0	#DIV/0!
259	28DbasSB	C28 ba 20S diaergostane b	0.00	0	#DIV/0!	0	#DIV/0!
259	28DbasRA	C28 ba 20R diaergostane a	0.00	0	#DIV/0!	0	#DIV/0!
259	28DbasRB	C28 ba 20R diaergostane b	0.00	0	#DIV/0!	0	#DIV/0!
259	29Dbas	C29 ba 20S diastigmastane	60.50	5211	#DIV/0!	1589	#DIV/0!
259	29DbasR	C29 ba 20R diastigmastane	61.83	424	#DIV/0!	195	#DIV/0!
259	30TP1	C30 Terpane	65.93	8348	#DIV/0!	2035	#DIV/0!
259	30TP2	C30 Terpane	66.01	2664	#DIV/0!	881	#DIV/0!
217	b-Cholane	5b-cholane (inter. STD)	0.00	0	#DIV/0!	0	#DIV/0!
218	b-Cholane	5b-cholane (inter. STD)	0.00	0	#DIV/0!	0	#DIV/0!



# Humble Geochemical Services

Division of Humble Instruments & Services, Inc.

218 Higgins Street Humble, TX 77338  
P. O. Box 789 Humble, TX 77347  
Telephone: 281-540 6050 Fax: 281-540 2864

Client: **United States Department of the Interior** Basin:  
 Client ID: **ECT-C7** County,State: **Summit Co., UT**  
 HGS ID: **07-4355-173663** Country:  
 Well:  
 Depth:  
 Field:  
 Lease  
 Formation:

Saturate Biomarker Integration Results (Terpanes)							
Ion	Peak Label	Compound Name	R.Time (min.)	Peak Area	ppm (A.)	Peak Height	ppm (Ht.)
125	BCRT	b-carotane					
191	C19t	C19 tricyclic diterpane	40.27	6812	#DIV/0!	1967	#DIV/0!
191	C20t	C20 tricyclic diterpane	42.54	9039	#DIV/0!	3053	#DIV/0!
191	C21t	C21 tricyclic diterpane	44.86	14875	#DIV/0!	5011	#DIV/0!
191	C22t	C22 tricyclic terpane	46.99	8142	#DIV/0!	2064	#DIV/0!
191	C23t	C23 tricyclic terpane	49.40	18896	#DIV/0!	6633	#DIV/0!
191	C24t	C24 tricyclic terpane	50.72	6893	#DIV/0!	2363	#DIV/0!
191	C25tS	C25 tricyclic terpane (S)	53.28	2916	#DIV/0!	1115	#DIV/0!
191	C25tR	C25 tricyclic terpane (R)	53.36	3032	#DIV/0!	988	#DIV/0!
191	C24T	C24 tetracyclic terpane (TET)	54.88	4027	#DIV/0!	1232	#DIV/0!
191	C26tS	C26 tricyclic terpane (S)	55.16	2546	#DIV/0!	857	#DIV/0!
191	C26tR	C26 tricyclic terpane (R)	55.33	2447	#DIV/0!	810	#DIV/0!
191	C28tS	C28 extended tricyclic terpane (S)	0.00	0	#DIV/0!	0	#DIV/0!
191	C28tR	C28 extended tricyclic terpane (R)	0.00	0	#DIV/0!	0	#DIV/0!
191	C29tS	C29 extended tricyclic terpane (S)	0.00	0	#DIV/0!	0	#DIV/0!
191	C29tR	C29 extended tricyclic terpane (R)	0.00	0	#DIV/0!	0	#DIV/0!
191	C30tS	C30 extended tricyclic terpane (S)	0.00	0	#DIV/0!	0	#DIV/0!
191	C30tR	C30 extended tricyclic terpane (R)	0.00	0	#DIV/0!	0	#DIV/0!
191	Ts	Ts 18a(H)-trisnorhopane	61.66	8041	#DIV/0!	2563	#DIV/0!
191	Tm	Tm 17a(H)-trisnorhopane	62.42	6139	#DIV/0!	1893	#DIV/0!
191	C28BNH	C28 17a18a21b(H)-bisnorhopane	0.00	0	#DIV/0!	0	#DIV/0!
191	Nor25H	C29 Nor-25-hopane	0.00	0	#DIV/0!	0	#DIV/0!
191	C29H	C29 Tm 17a(H)21b(H)-norhopane	65.06	18652	#DIV/0!	5671	#DIV/0!
191	C29Ts	C29 Ts 18a(H)-norhopane	65.17	8518	#DIV/0!	2429	#DIV/0!
191	C30DiaH	C30 17a(H)-diahopane	65.50	5387	#DIV/0!	1901	#DIV/0!
191	Normor	C29 normoretane	65.93	15061	#DIV/0!	3548	#DIV/0!
191	a-Ole	a-oleanane	66.49	1156	#DIV/0!	856	#DIV/0!
191	b-Ole	b-oleanane	66.51	609	#DIV/0!	572	#DIV/0!
191	C30H	C30 17a(H)-hopane	66.65	29766	#DIV/0!	9688	#DIV/0!
191	C30Ts	17a(H)-30-nor-29-homohopane	67.02	2451	#DIV/0!	968	#DIV/0!
191	Mor	C30 moretane	67.34	3012	#DIV/0!	1212	#DIV/0!
191	C31HS	C31 22S 17a(H) homohopane	68.47	11493	#DIV/0!	3408	#DIV/0!
191	C31HR	C31 22R 17a(H) homohopane	68.68	8566	#DIV/0!	2540	#DIV/0!
191	Gam	gammacerane	68.97	2285	#DIV/0!	1248	#DIV/0!
191	C32HS	C32 22S 17a(H) bishomohopane	69.89	12293	#DIV/0!	3073	#DIV/0!
191	C32HR	C32 22R 17a(H) bishomohopane	70.18	7255	#DIV/0!	2077	#DIV/0!
191	C33HS	C33 22S 17a(H) trishomohopane	71.55	7856	#DIV/0!	1934	#DIV/0!
191	C33HR	C33 22R 17a(H) trishomohopane	72.01	5579	#DIV/0!	1471	#DIV/0!
191	C34HS	C34 22S 17a(H) extended hopane	0.00	0	#DIV/0!	0	#DIV/0!
191	C34HR	C34 22R 17a(H) extended hopane	0.00	0	#DIV/0!	0	#DIV/0!
191	C35HS	C35 22S 17a(H) extended hopane	0.00	0	#DIV/0!	0	#DIV/0!
191	C35HR	C35 22R 17a(H) extended hopane	0.00	0	#DIV/0!	0	#DIV/0!



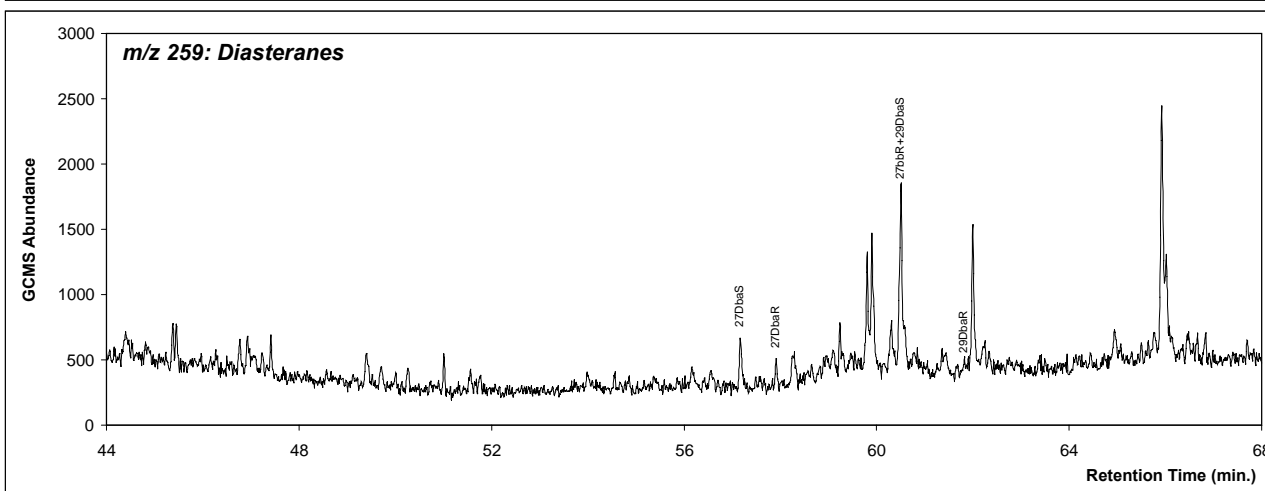
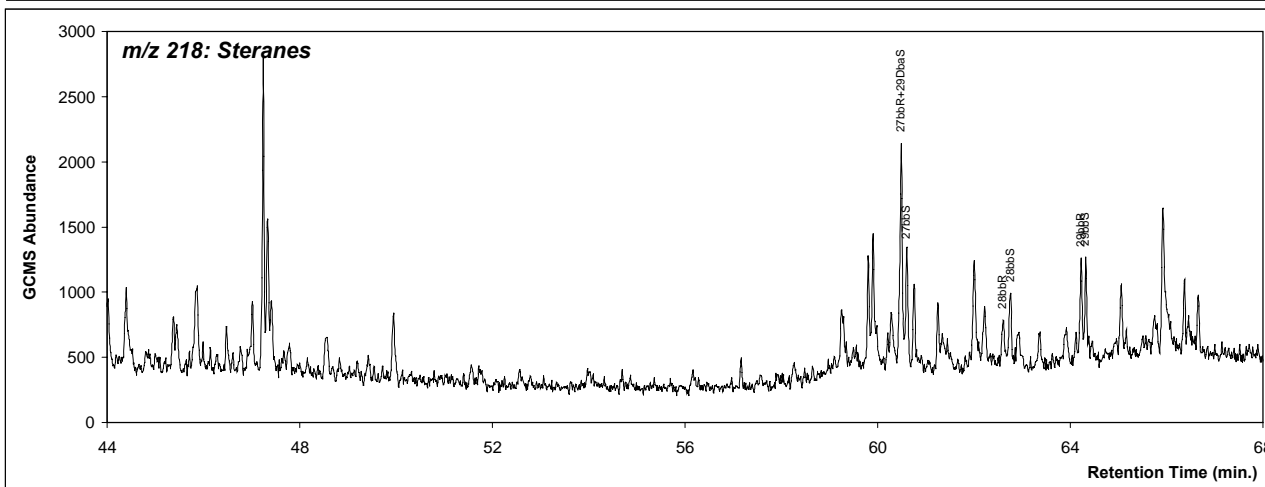
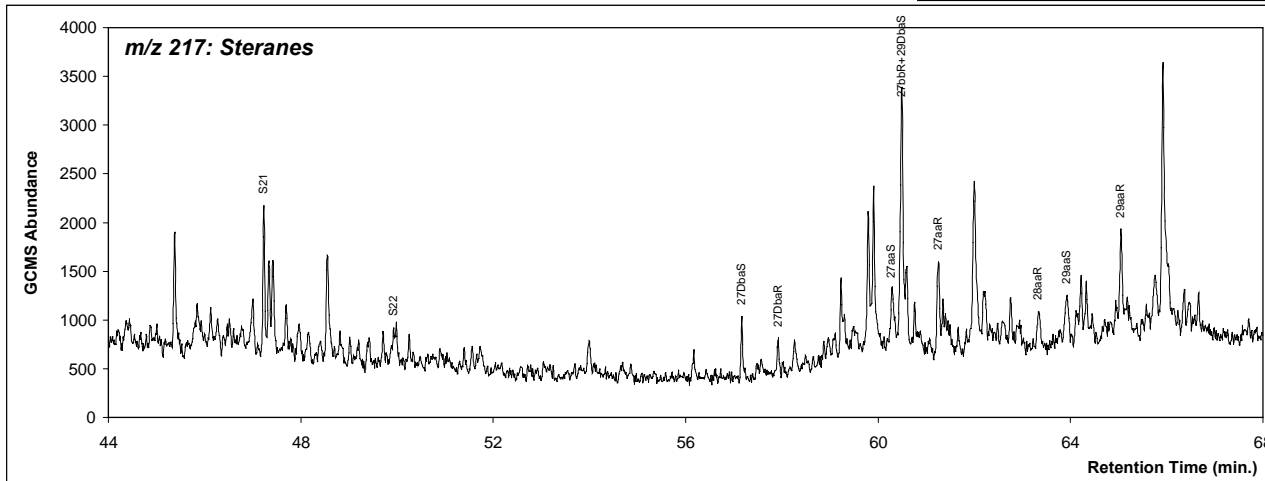
# Humble Geochemical Services

Division of Humble Instruments & Services, Inc.

218 Higgins Street Humble, TX 77338  
P. O. Box 789 Humble, TX 77347  
Telephone: 281-540 6050 Fax: 281-540 2864

Client: **United States Department** Client ID: **ECT-C7**  
HGS ID: **07-4355-173663**

## Key Saturate GC-MS Ion Chromatograms





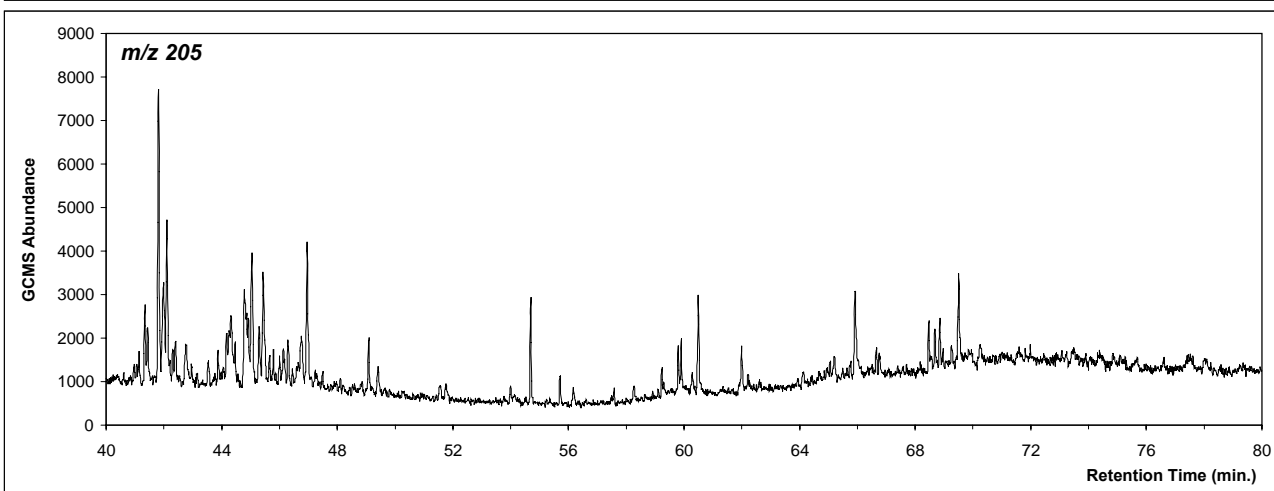
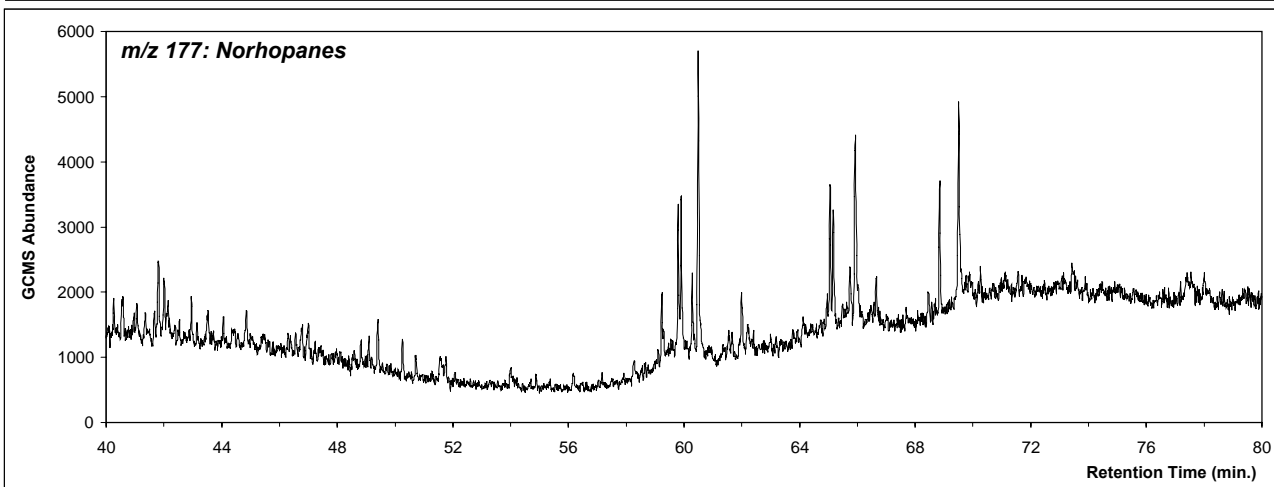
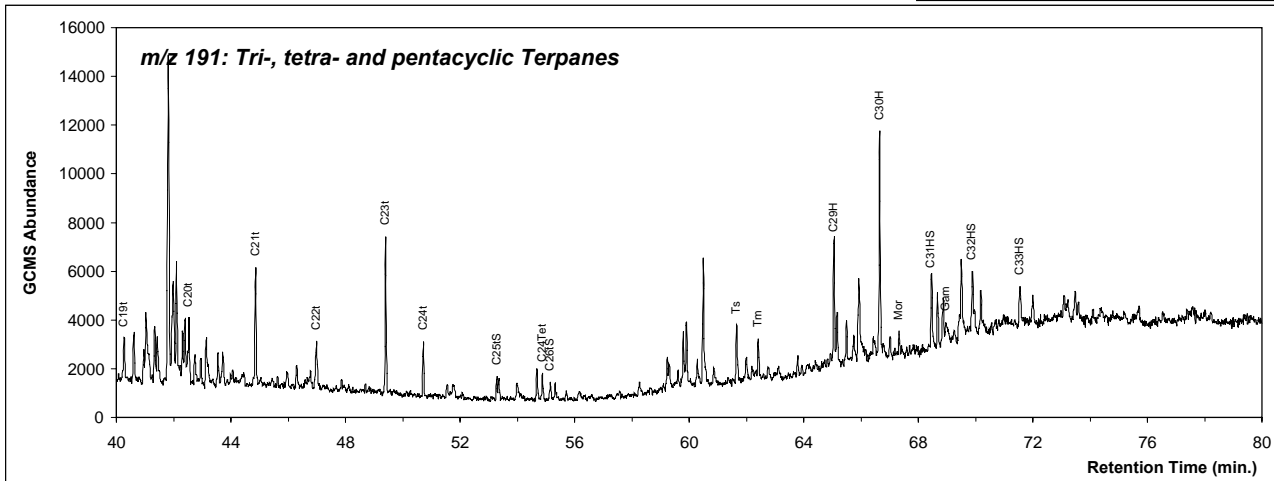
# Humble Geochemical Services

Division of Humble Instruments & Services, Inc.

218 Higgins Street Humble, TX 77338  
P. O. Box 789 Humble, TX 77347  
Telephone: 281-540 6050 Fax: 281-540 2864

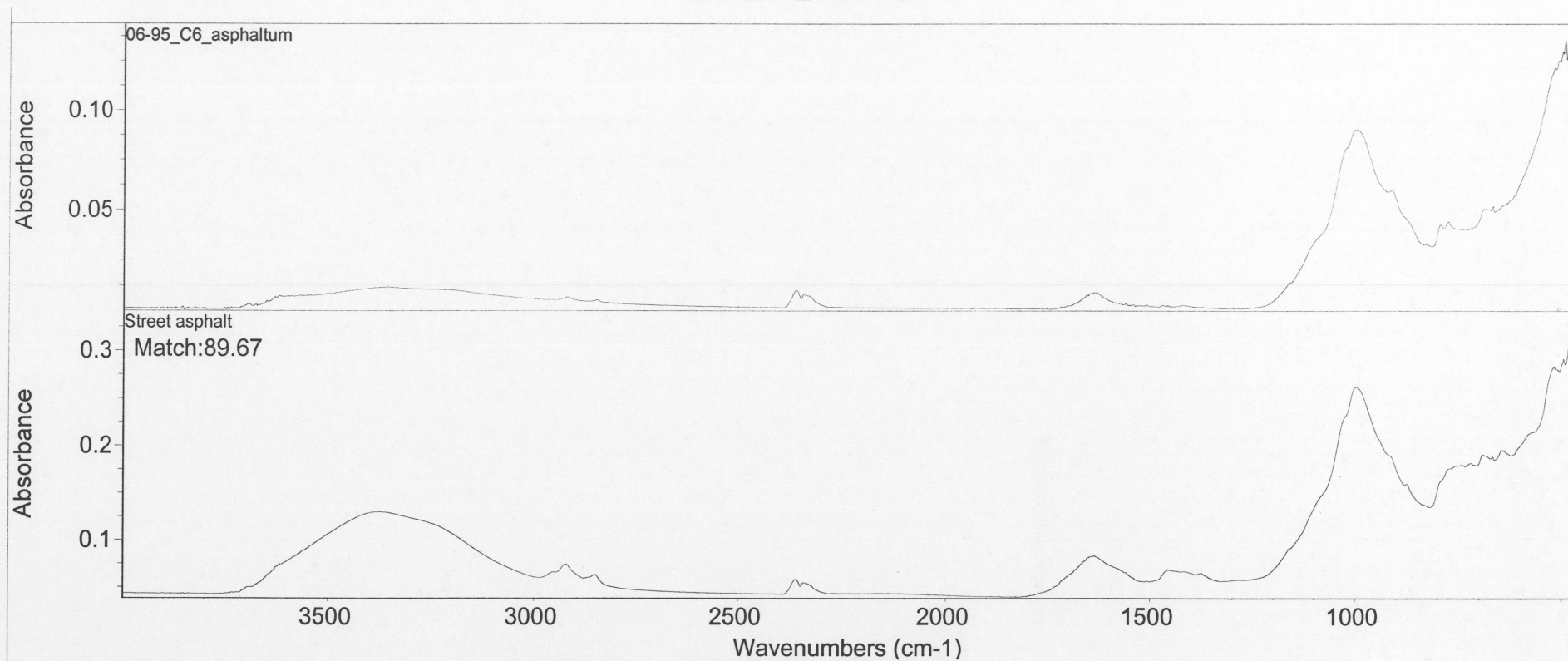
Client: **United States Department** Client ID: **ECT-C7**  
HGS ID: **07-4355-173663**

## Key Saturate GC-MS Ion Chromatograms



**Report G-2.**  
**FTIR Spectrum Analyses for Asphaltum in Sample ECT-C6**  
**By**  
**Paleo Research Institute**  
**Golden, Colorado**

06-95\_C6\_asphaltum



Number of sample scans: 64  
 Number of background scans: 64  
 Resolution: 4.000  
 Sample gain: 4.0  
 Mirror velocity: 0.6329  
 Aperture: 17.00

Spectrum: 06-95\_C6\_asphaltum

Region: 3495.26-651.85

Search type: Correlation

Hit List:

Index	Match	Compound name	Library
1	89.67	Street asphalt	Minerals

Tue Feb 20 14:58:07 2007 (GMT-07:00)

FIND PEAKS:

Spectrum: 06-95\_C6\_asphaltum

Region: 4000.00000 400.00000

Absolute threshold: 0.021

Sensitivity: 60

Peak list:

Position:	479.76328	Intensity:	0.144
Position:	493.48004	Intensity:	0.135
Position:	669.26569	Intensity:	0.0520
Position:	777.10791	Intensity:	0.0440
Position:	997.82703	Intensity:	0.0902

Figure 2. FTIR spectrum for possible asphaltum in sample ECT-C6, East Canyon Trench.

**Appendix H.**  
**Review of Trench Across the Main Canyon Fault, Utah, of October**  
**2006**  
**By**  
**James P. McCalpin**  
**GEO-HAZ Consulting, Inc.**  
**Crestone, Colorado**

## REVIEW OF EAST CANYON TRENCH, UTAH, OF OCT. 2006; v2

By: James P. McCalpin  
Date: 13 Dec 2006

At the request of the Seismotectonic Section of the US Bureau of Reclamation, Denver, CO, I attended a 1-day review of a trench across a strand of the East Canyon (Utah) fault zone on Wednesday, Oct. 25, 2006.

The purpose of the trench review was twofold:

- 1) to verify that the fault had indeed moved in the late Quaternary, and
- 2) to determine whether or not there was evidence for sudden vs gradual offset (colluvial wedges?).

Prior to the review, USBR had provided me with some previous work and current maps and trench location photographs. After the trench was excavated and the walls were cleaned, USBR provided the following preliminary observations: *“So far, it appears that the trench does expose a fault, which juxtaposes very weathered, red-colored alluvium on the NE side against grey-brown pebbly alluvium and clay on the SW side. The clay, appears to be a ponded unit on the upslope side of the scarp, which was subsequently buried by younger alluvium/colluvium. Overlying the clay are silty and pebbly alluvial/colluvial units, partly in a fault-bounded depression, some of which appear to be derived locally from flanking scarps on either side of the depression. One possible explanation for what we have seen to date includes two distinct surface-faulting events here, both of which are late Quaternary. It is not immediately obvious how young the MRE may be, the surface has been plowed, but the surface soils that might overlie fault-related units are not particularly well-developed.”*

### **1) Verify that the fault had indeed moved in the late Quaternary**

The key evidence for late Quaternary faulting is found at the main fault zone between stations 7 and 7.5 (Fig. 1). Unfaulted units include a surface colluvium (unit 10) and its weak A/C soil, and a thicker alluvium-slopewash deposit (unit 8; however, see later comments on age of faulting). The minimal degree of soil formation in these 2 unfaulted deposits suggests that only ca. 10 ka has elapsed since the MRE. The youngest clearly faulted unit (the cumulic? buried A horizon developed on unit 5e) contains dark gray disseminated carbon. Preservation of this type of organic material is unusual in buried soils older than late Quaternary.

Therefore, if units 8-10 are unfaulted and units 5e and older are faulted, the MRE almost certainly occurred during the late Quaternary. Dating samples C5 and L5 (from unit 8) and C4 and L4 (from the buried A horizon) bracket the MRE event horizon, and will confirm whether the MRE is late Quaternary.



## Suggestions for Unit Numbering

The current unit numbering scheme used in the USBR description of map units and in annotated photomosaics is the field numbering scheme. This field scheme has several internal contradictions, such as unit 4 being correlated to the lower part of unit 5e, whereas it's number (4) indicates it is older than all of unit 5. Likewise, the event horizon for the PE falls at the contact between units 5d and 5e, whereas the event horizon for the MRE falls at the contact between units 5e and 8. Normally, letter subscripts are used only to subdivide a major unit into nearly-contemporaneous units of slightly different texture. In contrast, major breaks in time or in style of deposition are represented by jumps in the units numbers; the longer the time break, the larger the jump in unit numbers. Thus, it is not appropriate to have an event horizon separate units with the same number and only a different letter subscript.

I would renumber the units in a more standard fashion, to let the unit numbering scheme tell the reader explicitly the sequence of events deduced from the trench, and where the major time breaks are. In such a scheme, the "unconformity/erosion" times marked on USBRs preliminary correlation of trench units would mark major jumps in the unit numbering sequence. One way to do this is to have the numbers jump from one decade (0-9) to the next higher decade (10-19), etc. This shows the reader the significance of the time break between units.

## 2) Determine whether or not there was evidence for sudden vs gradual offset (colluvial wedges?).

To distinguish between sudden versus gradual offset on the main fault zone, we have to consider if the geometry of trench deposits matches the expected physical evidence from those 2 deformation styles. During the trench review, I tried to list the salient geometric evidence from the trench wall and how it supported one of 4 faulting hypotheses:

Table 2. Four hypotheses for the type of faulting in the East Canyon trench.

	EPISODIC FAULTING	GRADUAL CREEP
UNIT 8 is younger than MRE	Hypothesis 1 <sup>1</sup> Unit 5e is clearly truncated, but unit 8 is not Small amount of scarp colluvium Fault slightly bends at 5e/8 contact	Hypothesis 3 <sup>3</sup> No scarp colluvium 5e cleanly truncated Unit 8 not bent (maybe insufficient time since MRE)
Unit 8 is older than MRE	Hypothesis 2 <sup>2</sup> No unit 8 on footwall No colluvium younger than unit 8 No shear fabric in unit 8	Hypothesis 4 <sup>4</sup> No scarp colluvium Unit 8 not bent

Green means trench evidence supports hypothesis

Red means trench evidence contradicts hypothesis

<sup>1</sup> unit 5e is cleanly truncated, not smeared out as it would be with creep; there is no shear fabric in unit 8 against contact with unit 5c; buried free face (unit 8/5c contact) is nearly as steep as underlying fault

<sup>2</sup> Unit 8 does not exist on the footwall; there is no thickened colluvium or other sediments on the hanging wall overlying unit 8; the contact of 5c against 8 does not have shear fabric

<sup>3</sup> There is little scarp-derived colluvium in the hanging wall; unit 5e is cleanly truncated by the fault, but creep should have smeared it out and stretched it; soil 5eAb should be present on a degraded free face, if formed by creep

<sup>4</sup> There is little scarp-derived colluvium in the hanging wall; unit 5e is cleanly truncated by the fault, but creep should have smeared it out and stretched it; unit 8 does not appear deformed in any way by creep

According to Table 2, hypothesis 2 is very unlikely. The gradual creep hypotheses (3 and 4) do have some lines of support, although in each case, there are possible alternative explanations for the absence of scarp-derived colluvium and for the presence of plastic deformation, even if deformation had been episodic. Hypothesis 1 seems to have the most positive evidence.

## PALEOSEISMIC CHRONOLOGY OF THE TRENCH

The USBR interpretation of the trench includes an MRE younger than unit 8/ older than unit 5e, and a PE older than unit 5e/ younger than unit 5d (Fig. 4). In this interpretation, unit 5e was deposited as “tectonic colluvial wedge and pond-paludal deposits after the PE.

During the trench review, I tried to reconstruct the sequence of deposition and soil formation after the deposition of unit 5e. The existence of the antithetic fault that displaces unit 5e at station 9.5 caused me somewhat of a problem, however. I observed that the strong buried A horizon developed atop unit 5e was not continuously present at the top of 5e, but only existed between the main fault and antithetic fault. In contrast, the soil B horizon appears to be present everywhere in unit 5e. That would make sense, if the soil B horizon had already developed before the A horizon, then the antithetic fault had displaced the top of unit 5e downward to create a small graben, which then retained enough moisture to differentially develop an A horizon in the graben.

However, if movement on the antithetic fault was required to explain the limited spatial extent of the buried A horizon, in which faulting event did the antithetic fault move? It could not be the MRE, because the MRE postdates the buried A horizon. However, it could not be the PE either, because the PE predates the deposition of unit

5e. I tried to make a simple retrodeformation sequence to explain the observed geometry (Fig. 3). This sequence requires that movement on the antithetic fault occur after the B horizon had developed on unit 5e but before the cumulic A horizon had developed.

This sequence has a contradiction, in that there is no deposition in the graben after movement on the antithetic scarp forms the graben. In other words, no deposits such as 5e or 8 were deposited after this supposed event. Given the sedimentologic setting of this scarp, that is rather unlikely. It would require that movement on the antithetic fault was not accompanied by any movement on the main fault.

So, perhaps the limited spatial extent of the cumulic A horizon can be explained another way. In the USBR drawing "revised trench schematic.tif" of Dec. 4, 2006, the hand-written text says "organic A near fault, grades laterally to AB in clay." There is no explanation given why this lateral soil horizon transition should have occurred. This may become apparent when the full retrodeformation sequence is drawn, after the C14 and OSL dates are processed.